Universidade de Aveiro Departamento de Química
2016/2017

Mariam Achraf
Mohamed Bahie El Din El Kholany

Separação enantiosseletiva de compostos quirais usando sistemas aquosos bifásicos e sistemas de duas fases sólida-líquida

Enantioselective separation of chiral compounds using aqueous biphasic systems and solid-liquid biphasic system

Universidade de Aveiro Departamento de Química
2016/2017

Mariam Achraf
Mohamed Bahie El Din El Kholany

Separação enantiosseletiva de compostos quirais usando sistemas aquosos bifásicos e sistemas de duas fases sólida-líquida

Enantioselective separation of chiral compounds using aqueous biphasic systems and solid-liquid biphasic system

Dissertação apresentada à Universidade de Aveiro para cumprimento dos requisitos necessários à obtenção do grau de Mestre em Biotecnologia, ramo Industrial e Ambiental, realizada sob a orientação científica do Professor Doutor João Manuel da Costa e Araújo Pereira Coutinho, Professor Catedrático do Departamento de Química, CICECO, da Universidade de Aveiro e coorientação da Doutora Sónia Patrícia Marques Ventura, Equiparada a Investigadora Auxiliar do Departamento de Química da Universidade de Aveiro.

This work was partly funded by the FCT project SAICTPAC/0040/2015.

O júri

Presidente

Doutora Ana Maria Rebelo Barreto Xavier

Professora Auxiliar do Departamento de Química da Universidade de Aveiro

Doutor Óscar Rodríguez Figueiras

Investigador Programa Ramón y Cajal do Departamento de Química da Universidade de Santiago

Professor Doutor João Manuel da Costa e Araújo Pereira Coutinho

Professor Catedrático do Departamento de Química da Universidade de Aveiro

Acknowledgments

Agradecimentos

Gostaria de começar por manifestar o meu sincero agradecimento a todos os que me ajudaram ao longo deste percurso.

Ao meu orientador, Professor Doutor João Coutinho, pela oportunidade que me proporcionou para trabalhar neste excelente grupo, numa área tão desafiante e pela qual desenvolvi um enorme gosto, e por todo o apoio que me deu ao longo da tese. Queria também agradecer à minha coorientadora, Doutora Sónia Ventura, por toda a ajuda e valiosas palavras dadas ao longo da realização do trabalho. À Francisca e à Tânia, pela motivação que me deram ao longo do ano, pela paciência e por tudo o que me ensinaram, um muito obrigada cheio de carinho. Gostaria de agradecer ao PATh e a todos os seus elementos por tudo o que me ensinaram e por toda a animação.

À minha mãe, à minha irmã, aos meus avós, ao meu tio. À minha família, minha claque desde o início do meu percurso, e conselheiros constantes. Mãe, o maior, mais gigantesco obrigada por todo o carinho nos momentos mais difíceis, pelo incansável apoio, por tudo.

A todos os meus amigos, os que me viram crescer na Murtosa, os que viveram comigo Aveiro. Eles, que nunca me deixaram, que partilharam comigo as melhores memórias e ampararam todas as minhas quedas. Obrigada, do fundo do coração, por me ajudarem a percorrer este caminho!

palavras-chave Separação enantiomérica, sistemas aquosos bifásicos, excesso enantiomérico, ácido mandélico, líquidos iónicos, líquidos iónicos quirais, sistemas de duas fases sólida-líquida

Resumo

Tipicamente, apenas um dos enantiómeros é responsável pelo efeito pretendido de um fármaco, sendo que o outro pode levar a respostas menos potentes ou até mesmo indesejadas. As entidades reguladoras praticam políticas restritas em relação à comercialização de fármacos como misturas racémicas. Assim, a indústria farmacêutica tem enfrentado desafios relacionados com o desenvolvimento de métodos para produção de fármacos oticamente puros. No entanto, e considerando a dificuldade acrescida na produção de enantiómeros puros por síntese direta, a síntese de misturas racémicas seguida da sua purificação surge como uma alternativa mais barata, simples e flexível.

Os sistemas aquosos bifásicos (SABs) e os sistemas de duas fases sólida-líquida (SDFSL) são técnicas alternativas mais biocompatíveis que têm sido utilizados como técnicas de separação enantiosseletiva de fármacos e/ou aminoácidos com enantiosseletividades bastante promissoras. Para além disso, apresentam benefícios de custo, rapidez, simplicidade e versatilidade de operação e possibilidade de aumento de escala.

Este trabalho foca-se no desenvolvimento de SABs e SDFSL constituídos por seletores quirais que possam atuar simultaneamente como solvente. Numa primeira abordagem o objetivo foi desenvolver novos SABs quirais, mais biocompatíveis, simples e eficientes. Para tal, SABs constituídos por açúcares, aminoácidos e líquidos iónicos quirais foram aplicados na resolução enantiomérica de ácido mandélico racémico. O sistema mais promissor, composto por $[C_1Qui][C_1SO_4]$ + K_3PO_4, obteve um excesso enantiomérico de -33.4%. Numa segunda abordagem, foi possível criar uma alternativa mais simples e mais eficiente recorrendo a SDFSL. Com estes sistemas, foi obtido o valor mais elevado de excesso enantiomérico deste trabalho, de 49.0%, através da precipitação enantiosseletiva do R-ácido mandélico por interação com $[N_{4444}]$[D-Phe].

Keywords Enantioseparation, aqueous biphasic systems, enantiomeric excess, mandelic acid, ionic liquids, chiral ionic liquids, solid-liquid biphasic system

Abstract

Conventionally, only one of the enantiomers is responsible for the intended effect of a drug, whilst the other may lead to a less potent or even undesired response. Regulation entities are very strict regarding the commercialization of racemic drugs. Thus, pharmaceutical industry has been facing challenges related to the creation of methods to produce optically active drugs. However, considering the increased difficulty in the production of pure enantiomers by direct synthesis, the synthesis of racemic mixtures followed by their purification appears as a cheaper, simpler and more flexible alternative.

Aqueous biphasic systems (ABS) and solid-liquid biphasic system (SLBS) are more biocompatible alternatives that have been used to separate racemic drugs and amino acids with promising enantioselectivities. Furthermore, these are cost-effective, quick, simple and operationally flexible.

This work intended to develop ABS and SLBS using chiral selectors that can simultaneously act as solvents. In a first attempt, chiral ABS of better biocompatibility, simplicity and efficiency were developed. For that purpose, ABS constituted by sugars, amino acids and chiral ionic liquids (CILs) were applied for chiral resolution of racemic mandelic acid (MA). The most promising ABS was a system composed of $[C_1Qui][C_1SO_4]$ + K_3PO_4 which yielded the maximum enantiomeric excess of -33.4%. In a second approach, it was possible to create a simpler and more efficient technique resorting to SLBS. The enantiomeric excess value of 49.0% was achieved, by the enantioselective precipitation of the *R*-MA caused by interactions with $[N_{4444}]$[D-Phe].

Contents

List of acronyms and abbreviations

A	Selectivity
α-CHMA	α-Cyclohexylmandelic acid
β-CD	*β*-Cyclodextrin
ABS	Aqueous biphasic systems
AMBS	Aqueous micellar biphasic systems
ATPF	Aqueous two-phase flotation
Asp	Asparagine
BSA	Bovine serum albumin
CIL	Chiral ionic liquid
CM-*β*-CD	Carboxymethyl-*β*-cyclodextrin
CPMK	(4-Chlorophenyl)-(pyridin-2-yl)methanone
e.e.%	Enantiomeric excess
EE	Extraction efficiency
ELLE	Enantioselective liquid-liquid extraction
FLU	Flurbiprofen
HP-*β*-CD	Hydroxypropyl-*β*-cyclodextrin
HPLC	High-performance liquid chromatography
IL	Ionic liquid
Ile	Isoleucine
KYN	Kynurenine
LLE	Liquid-liquid extraction
L-IPTA	L-(+)-tartaric acid diisopropyl ester
MA	Mandelic acid
ME-*β*-CD	Methyl-*β*-cyclodextrin
OFLX	Ofloxacin
PEG	Polyethylene glycols
Phe	Phenylalanine
PPG	Polypropylene glycol
PSA	Phenylsuccinic acid
SBE-*β*-CD	Sulfobutyl ether-*β*-cyclodextrin

Ser	Serine
SLBS	Solid-liquid biphasic systems
THF	Tetrahydrofuran
Thr	Threonine
Trp	Tryptophan
Tyr	Tyrosine
TL	Tie-line
TLL	Tie-line length
TPA	Three-point attachment
ZPC	Zopiclone
(S)-CPMA	(S)-(4-Chlorophenyl)-(pyridin-2-yl)methanol
$[C_1Qui][C_1SO_4]$	1-Methyl quininium methylsulfate
$[C_1C_1C_1Pro]I$	*N*,*N*-Dimethyl-L-proline methyl ester iodide
$[C_1C_1C_1Pro][C_1SO_4]$	*N*,*N*-Dimethyl-L-proline methyl ester methylsulfate
$[C_1C_1C_1Val]I$	*N*,*N*,*N*-Trimethyl-L-valinolium iodide
$[C_1C_1C_1Val][C_1SO_4]$	*N*,*N*,*N*-Trimethyl-L-valinolium methylsulfate
$[C_2C_1im]$ $[C_4F_9SO_3]$	1-Ethyl-3-methylimidazolium perfluorobutanesulfonate
$[C_2C_1py][C_4F_9SO_3]$	1-Ethyl-3-methylpyridinium perfluorobutanesulfonate
$[C_2C_2C_2Pro]Br$	*N*,*N*-Diethyl-L-proline ethyl ester bromide
$[C_4mim][BF_4]$	1-Butyl-3-methylimidazolium tetrafluoroborate
$[C_4mim][CF_3SO_3]$	1-Butyl-3-methylimidazolium trifluoromethanesulfonate
$[C_4mim][N(CN)_2]$	1-Butyl-3-methylimidazolium dicyanamide
[Ch][*β*-Ala]	Cholinium *β*-alaninate
[Ch][Abt]	Cholinium abietate
[Ch][D-Gal]	Cholinium D-galactouronate
[Ch][D-Phe]	(2-Hydroxyethyl)trimethylammonium D-phenylalaninate
[Ch][Gly]	Cholinium glycinate
[Ch][L-Ala]	(2-Hydroxyethyl)trimethylammonium L-alaninate
[Ch][L-Asc]	Cholinium L-ascorbate
[Ch][L-Phe]	(2-Hydroxyethyl)trimethylammonium L-phenylalaninate
[Ch][Leu]	Cholinium leucinate
[Ch][Lys]	Cholinium lysinate

[Ch][Phe]	Cholinium phenylalaninate
[Ch][Qui]	Cholinium D-quinate
[Ch][Ser]	Cholinium serinate
[Ch][Val]	Cholinium valinate
$[N_{4444}]_2$[L-Glu]	Di(tetrabutylammonium) L-glutamate
$[N_{4444}]$[D-Phe]	Tetrabutylammonium D-phenylalaninate
$[N_{4444}]$[L-Phe]	Tetrabutylammonium L-phenylalaninate
$[P_{4444}]$Br	Tetrabutylphosphonium, bromide

List of figures

List of tables

1. General Introduction

Like the two hands of a person, a molecule is chiral if not superimposable to its mirror image (Figure 1). Enantiomers share the same physical and chemical properties, with the exception that they rotate the plane of polarized light in opposite directions to the same degree.[1] However, biological systems can discriminate between the two enantiomers of a molecule, having different physiological responses. In the case of a drug, it is common that only one of the isomers exerts the desired therapeutic effect. For most racemic drugs, the pharmaceutical activity is essentially inherent to one of the enantiomers (the eutomer), while the other is often inert, nefarious or responsible for unpredictable and undesired side effects (the distomer).[2,3]

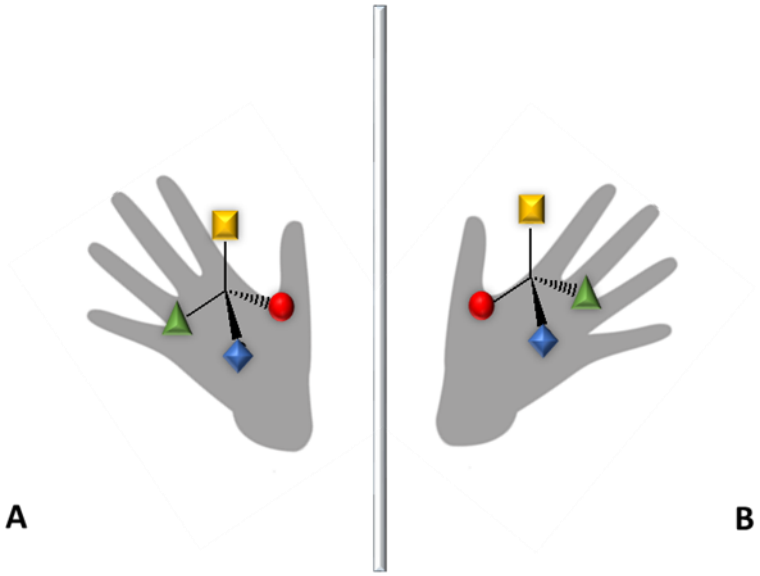

Figure 1. *Generic representation of a chiral structure with two non-superimposable forms (■≠▲≠●≠♦) as an analogy to two hands. Adapted from* [1].

In 1886, Piutti reported one of the first cases associated with the distinct biological effects of enantiomers, in particular the taste of asparagine enantiomers. The L-isomer is tasteless, while the D-isomer has a sweet taste.[4] Almost a century later, in the late 1950s and early 1960s, the "thalidomide scandal" occurred. Thalidomide was available as a racemic mixture in the market, where the (R)-isomer exhibits the desired effects and the (S)-isomer is teratogenic and induces birth defects. Since thalidomide was widely prescribed to heal nausea in pregnant women, over 10,000 embryos were affected.[2,5] Several chiral drugs have been investigated ever since, as indicated in some reviews.[6,7]

Under this scenario, attention was drawn to the stereochemistry of drugs and the regulation entities around the world[8,9] are nowadays stricter. In the beginning of the 2000's, more than 70% of new chiral drugs were commercialized in their enantiopure form,[2] due to the more selective pharmacodynamics profile, the reduction in complex drug interactions and patients exposure to weaker doses of the drug. However, selling a drug in its racemic form forces the pharmaceutical companies to provide detailed toxicological and pharmacological data for each enantiomer and the respective racemate.

In this context, it is necessary to find new methods to produce enantiopure drugs. There are two main approaches aimed at obtaining enantiopure compounds (Figure 2): the asymmetric synthesis and the separation of racemates.[2] Asymmetric synthesis, which was object of a Noble Prize in 2001,[10] comprises both non-enzymatic and enzymatic methods. It is the most powerful approach to obtain enantiopure compounds. Nevertheless, asymmetric synthesis generally requires highly enantiopure raw materials and or highly stereospecific catalysts that make it expensive and limited by the number of reactions needed to obtain highly enantiopure compounds. The separation of enantiomers from a racemate consists of a simpler, more flexible and cheaper alternative to asymmetric synthesis.

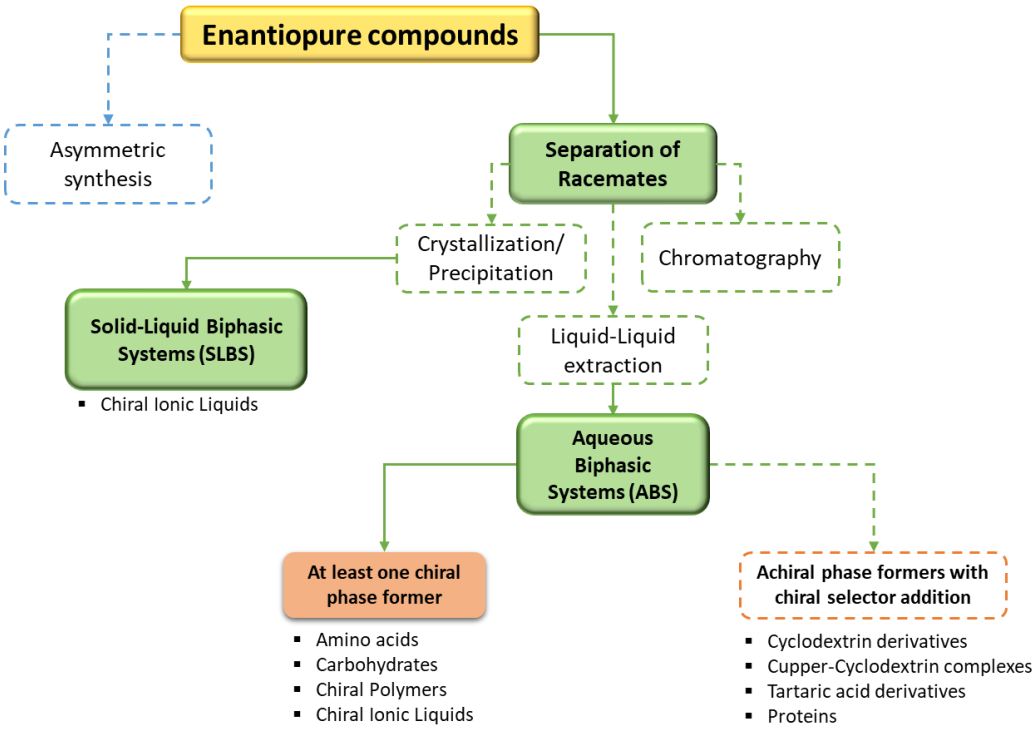

Figure 2. *Most common methods for producing enantiopure compounds (dashed lines) and alternative methods resorting to chiral aqueous biphasic systems and solid-liquid biphasic systems (full lines).*

Racemic synthesis followed by enantiomer separation is a propitious strategy for the production of enantiopure compounds. In general, the time-to-market for this approach is significantly shorter than for asymmetric catalysis.[11] The separation of pure enantiomers from a racemic mixture can be performed by several techniques, with chromatography and crystallization being the most common, as summarized in Figure 2.

Crystallization has on its basis the formation of diastereomeric salts or conglomerates of distinct solubilities. On the other hand, chromatography lies on the formation of diastereomers by derivatization (indirect) or diastereomeric complexes with a chiral selector (direct) allowing the enantiomers separation in a chromatographic column.[12,13] Overall, crystallization has operational simplicity, cost efficiency and can be easily coupled to other techniques. As an example, Köllges et al. proposed and optimized a continuous crystallization process resorting to a mill to separate conglomerate forming enantiomers achieving a 100% purity yield.[14] However, only 5 to 10% of the racemic mixtures form conglomerates, being thus limited to a certain number of chiral compounds. Moreover, it normally requires an additional step of enantiomeric enrichment to overcome the low yields obtained.[13,15]

In turn, chromatographic techniques are quick and applicable to a large number of racemates. Moreover, they are flexible due to the number of chiral stationary phases and chiral columns currently available and the racemates that they can resolve.[16] For instance, Wang et al. evaluated the enantioseparation for several compounds through HPLC using newly synthesized chiral stationary phases.[17] With a maximum separation factor of 5.83, they have proved the great potential of the novel stationary phases. However, chromatography has its industrial application limited by the high costs associated with the enantioselective columns and the low loading capacities.[18]

Enantioselective liquid-liquid extraction (ELLE) is cost-effective, quick, simple and versatile to operate and easy to scale up.[11] Aqueous biphasic systems (ABS), a particular type of LLE, add extra degrees of versatility and biocompatibility to conventional ELLE.[19] Although its application to resolve racemates remains scarcely studied, ABS are promising routes for chiral resolution. Enantiomeric precipitation shows to be another route of enhanced simple execution and reasonably low cost, if compared to ABS. By using solid-liquid biphasic systems (SLBS) with tunable solvents, the applicability of classic crystallization/precipitation techniques can be extended.

1.1. Scopes and objectives

In this work, the main focus is to develop robust and simple enantioseparation platforms based on ELLE, in particular chiral ABS, and on SLBS (Figure 3). Thus, the core objective of this thesis is to extend and investigate the applicability of chiral ABS and SLBS to separate racemic compounds as efficient and biocompatible alternatives to the most common techniques.

It is intended to develop enantioselective ABS in which the chiral selector is simultaneously one of the phase-forming components, thus creating a highly performant, yet of simple implementation, separation platform.

Given the promising status of ionic liquids (ILs) when applied in ABS,[19] mainly due to their "*designer solvent*" character, this thesis aims at enlarging the range of ABS based on ILs for chiral resolution purposes. By enantiomers' partition studies for each ABS class, their chiral resolution will be evaluated. This will allow the proper selection of the phase formers yielding the most promising enantioseparations. Thus, a complete screening of different ABS will be done covering three classes:

i) IL/carbohydrate-based ABS;

ii) IL/amino acid-based ABS

iii) CIL/salt-based ABS (where chirality can be present on the IL cation, anion or both).

The IL role in these ABS is that of only a solvent (class ***i*** and ***ii***, where the chiral selectors are carbohydrates and amino acids) and simultaneously of solvent and chiral selector (class ***iii***).

Considering the useful role of ILs in the precipitation or crystallization of several compounds,[20–22] including drugs,[23,24] SLBS composed of chiral ILs (CILs) aqueous solutions will be developed. This technique is used to promote the enantioselective precipitation of only one enantiomer in a racemic mixture due to cooperative interactions with the CILs. When compared to ABS, this class of systems is of simpler nature since it allows the isolation of the target enantiomer in a single step.

Mandelic acid (MA) was selected as the model racemic compound to perform this work due to its wide industrial application. In cosmetics, MA is used in several skin care products due to its antibacterial and facial skin renovating activities.[25,26] The interest on resolving MA racemates is to obtain *R*-MA, which is an intermediate used as a precursor

for semisynthetic penicillin and cephalosporin and many other pharmaceuticals, and a good resolving agent.[27].

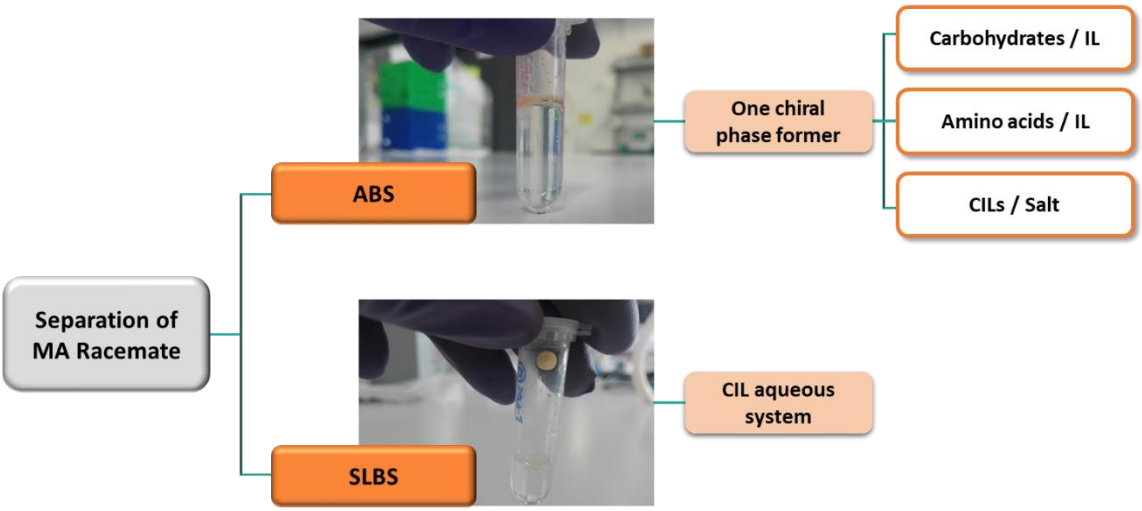

Figure 3. *Thesis overview.*

2. Separation of enantiomers using ELLE

2.1. Literature review

As mentioned above, the scalability, reduced costs and easy operation of ELLE makes it an attractive alternative for enantiomers separation when compared to the most common techniques. ELLE requires two immiscible phases, normally an aqueous and an organic phase. By combining solvent extraction with chiral recognition, ELLE needs one chiral selector (or more), otherwise enantiomeric separation does not take place. The introduction of a chiral selector and its partition between the two phases of an ELLE system controls the partition of the enantiomers. The chiral recognition is commonly monophasic, with the addition of only one chiral selector (Figure 4A). The chiral selectors most frequently used are crown ether-based,[28,29] metal complexes and metalloids,[30–32] cyclodextrin derivatives [33,34] and tartaric acid-based chiral selectors.[35] Biphasic recognition, where two chiral selectors with opposite partition tendencies are introduced in the ELLE system, has been proposed to overcome limitations related with the poor enantioselectivities achieved (Figure 4B). Cyclodextrin derivatives, highly soluble in the aqueous phase, and tartaric acid derivatives, exhibiting high affinity towards the organic phase, are the most popular pair of chiral selectors.[36–39] The principle of enantiomeric recognition for enantioselective complexation follows the three-point attachment (TPA) model – Figure 4C,[40] by which three simultaneous intermolecular interactions, like ion pairing, hydrogen bonding, π-π interactions, dipole-dipole and van der Waals, between the chiral-host and the chiral-guest take place, as shown in Figure 4C. In addition to the advantages already indicated, the enantiomeric excesses attained are very promising.[28–34,36–39] For instance, it is possible to achieve up to 99% of enantiomeric excess for chiral amino acids using a LLE system formed by water/dichloromethane + lipophilic salen-cobalt(III) complex as the chiral selector.[32] Nevertheless, ELLE uses large amounts of volatile organic solvents[41] and often requires additional steps to recover the resolved enantiomer. Owing to environmental issues related with the use of these organic solvents, that ignore the principles of Green Chemistry,[42] there is an intense search for more biocompatible techniques.[11–13]

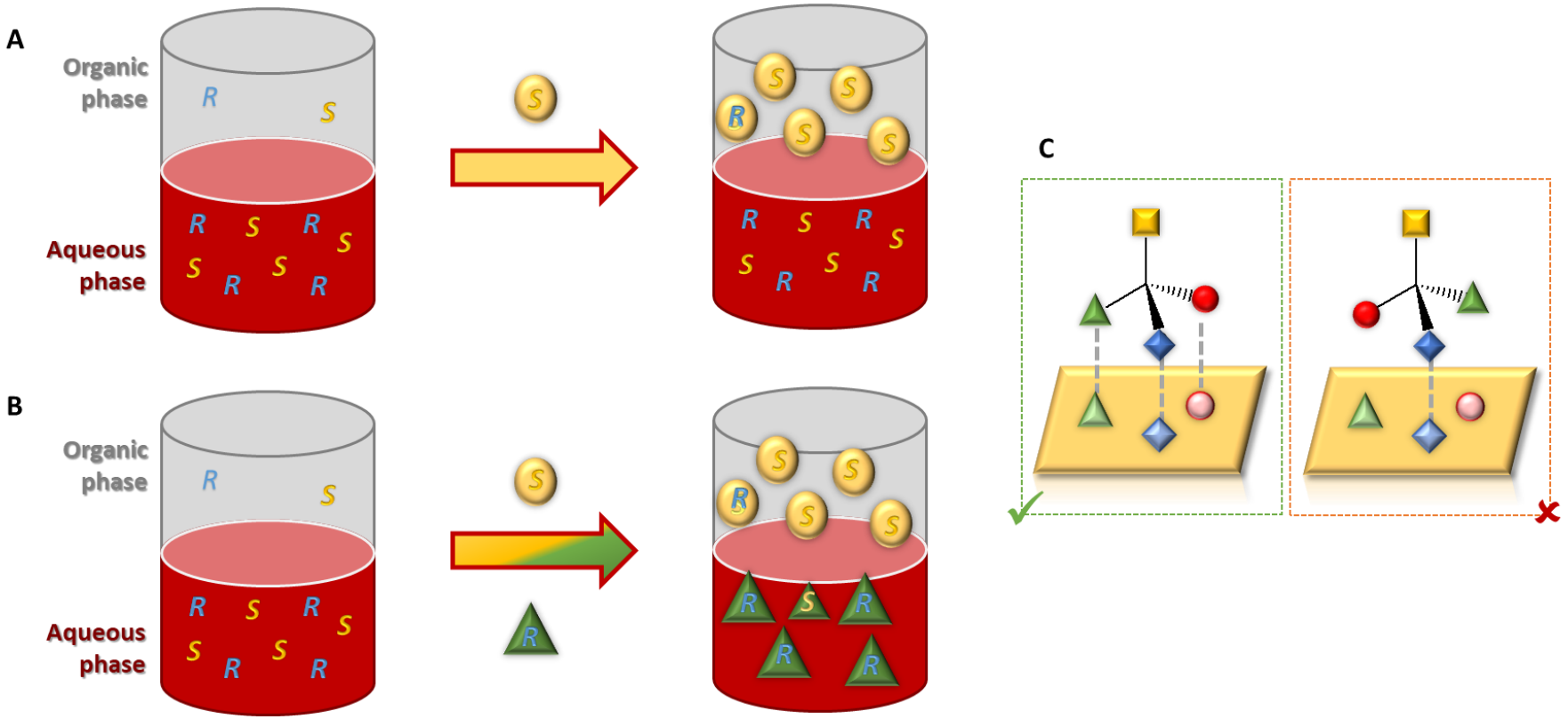

Figure 4. *Schematic representation of enantiomeric recognition using LLE systems and the molecular-level mechanisms justifying it: A) recognition with one chiral selector; B) recognition with two chiral selectors; C) TPA model.*

2.1.1. Chiral Aqueous Biphasic Systems

ABS are a specific type of LLE system that do not use toxic or volatile organic solvents. They are based on two water-rich phases, which form by mixing two incompatible water-soluble solutes above certain concentrations. One of the aqueous phases is enriched in one of the solutes, while the coexisting phase is mainly formed by the remaining one.[43] Although pairs of two polymers and of a polymer and a salt are the most used, multiple combinations appeared in the last decades.[19] Some examples involve the use of polar organic solvents,[44,45] surfactants, carbohydrates,[46] amino acids[47] and ILs.[19] ABS retain the benefits of traditional LLE (cost-effectiveness, quickness, simple operation, easy scale-up and recyclability) while adding the advantages of biocompatibility and tunability.[19,48,49] From the extraction of small compounds (alkaloids,[50] phenolic compounds[51] and amino acids[52]) and more sensitive biomolecules (proteins,[53,54] antibodies[55,56] and nucleic acids[57]) from natural matrices, to drugs from pharmaceutical wastes or wastewaters,[58,59] ABS were shown to be highly performant and selective if well selected. All the advantages given to ABS bring new opportunities considering the development of new/adapted enantioseparation techniques. It is in this context that this section is presented. It focuses on two aspects, the first being the description of the liquid-liquid equilibria data available for ABS formed by chiral compounds as phase formers and the second, the summary of specific cases where the chiral resolution of racemates resorting to ABS has been attempted.

2.1.2.1. Liquid-liquid equilibria data for ABS formed by chiral compounds

Since the extraction/separation of any compound with ABS follows its affinity between the two phases, the liquid-liquid equilibria must be described and the impact of several operational parameters upon the extraction understood (temperature, pH, mixture composition and phases volume ratio). A complete description on how to determine the solubility curves, to apply the mathematical descriptions for correlation of the experimental data and to fully characterize the phase diagrams was recently reviewed by Freire *et al*.[19] Briefly, the phase diagram allows the definition of the ternary compositions able to form the biphasic system and the composition of each individual phase (tie-lines, TLs). A schematic representation of a phase diagram is provided in

Figure 5. The solubility curve is the boundary between the biphasic (above) and the monophasic (below) zones. The TL for a given biphasic mixture composition represents the line that links the two *nodes* that represent the top and bottom phase compositions. The difference in the properties of the phases compositions increases with the tie-line length (TLL), which is the Euclidean distance between the two nodes. Different mixture points chosen along the same TL allow obtaining systems with the same composition at the coexisting phases, just differing in the volume ratio of the phases. Finally, the critical point represents the biphasic mixture composition with the two aqueous phases possessing equal compositions.

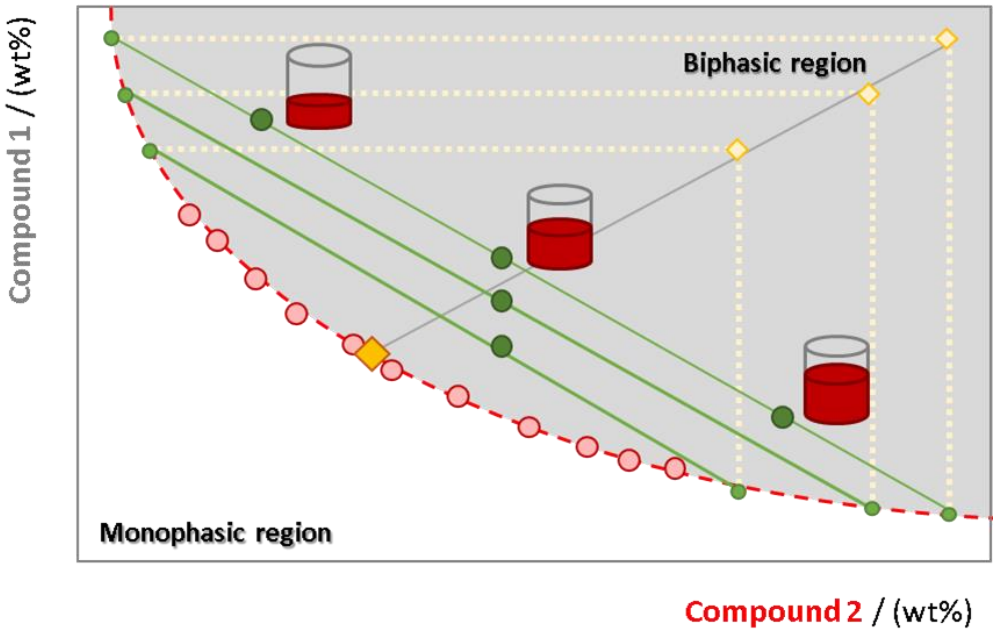

Figure 5. *Schematic representation of a hypothetic ternary phase diagram fully characterized: solubility curve experimental data* (●), *fitting of the experimental data* (dashed red line), *mixture points and corresponding nodes* (●), *TLs* (full green line) *and critical point* (◆).

Among the huge variety of compounds prone to form ABS, some can present chirality, thus being adequate for enantioseparation applications. These can be carbohydrates, amino acids, chiral polymers and chiral ILs, combined with other achiral compounds (salts, polymers, organic solvents and ILs) – Figure 6.

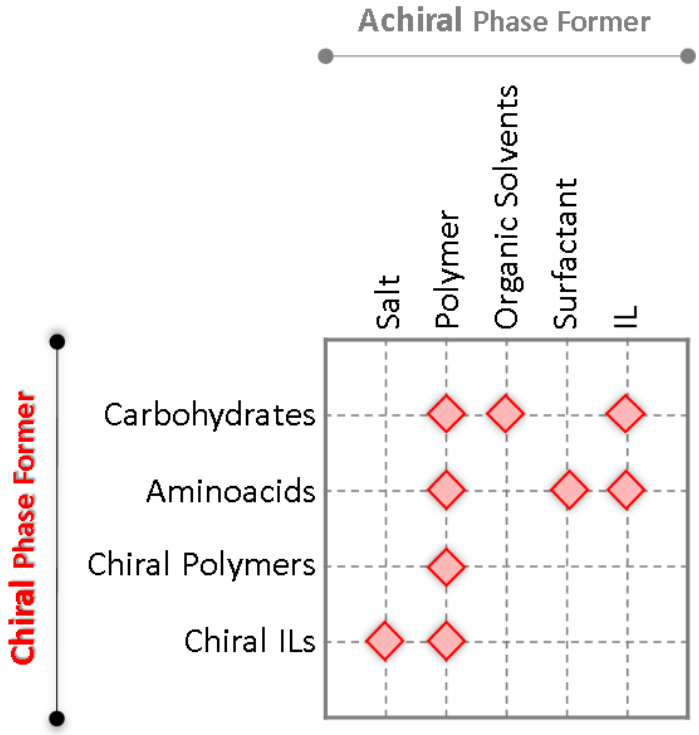

Figure 6. *Schematic representation of the pairs of compounds described in literature as phase formers to prepare chiral ABS for enantioseparation.*[60–66,44,67–80]

2.1.2.1.1. Carbohydrates

Carbohydrates are chiral molecules that, due its non-charged nature, biocompatibility and natural origin have been adopted in the development of greener ABS. The use of ABS composed of chiral carbohydrates for the resolution of racemic mixtures has been neglected (only two works were described until now, which will be further discussed in ***section 2.1.2.2.***[68,72] Still, there is a considerable number of works describing the liquid-liquid equilibrium of these systems that is important for the design of enantioseparation applications. Carbohydrates were used with polymers[81], organic solvents[68,72,82–85] and ILs[46,86,87] to form ABS, as summarized in Table 1. The ability of fourteen carbohydrates to form ABS with different water soluble polymers was proposed by Sadeghi et al.[81] Polyethylene glycols (PEGs) of different molecular weight were not able to form ABS due to their preferential interactions with the carbohydrates. Meanwhile, polypropylene glycol (PPG) 400 $gmol^{-1}$ and PPG 725 $gmol^{-1}$ (PPG 400 and PPG 725), which are more hydrophobic than PEGs, were able to form ABS. From the data described in literature, the tendency of the carbohydrates to form ABS with PPG 400

obeys to the following temperature-independent decreasing order: raffinose > lactose > maltitol ≥ maltose > sucrose > galactose > sorbitol > glucose > fructose > arabinose > xylitol > mannose > xylose > ribose. Three main tendencies were assessed by the authors: ***i)*** hexoses (glucose, fructose, galactose and mannose) have better performance than pentoses (xylose, ribose and arabinose) forming ABS; ***ii)*** trisaccharides (raffinose) are stronger than disaccharides (sucrose, maltose and lactose) and monosaccharides forming ABS; and ***iii)*** polyols (maltitol, sorbitol, xylitol) are stronger than their respective saccharides (maltose, glucose, xylose). Due to the high viscosity that polymer-rich phases display, other options like polar organic solvents were also evaluated in the ABS formation. The four works available studied combinations of saccharides + acetonitrile,[83] polyols + acetonitrile,[84] saccharides + tetrahydrofuran[82] and polyols + tetrahydrofuran.[85] Cardoso et al. investigated ABS formed by acetonitrile and saccharides (D-(+)-glucose, D-(+)-mannose, D-(+)-galactose, D-(+)-xylose, L-(+)-arabinose, and D-(-)-fructose, sucrose and D-(+)-maltose)[83] and polyols (glycerol, erythritol, xylitol, sorbitol and maltitol).[84] The liquid-liquid demixing aptitude decreases as follows: D-(+)-galactose > D-(+)-mannose > D-(+)-glucose > D-(+)-xylose > D-(-)-fructose >L-(+)-arabinose[83] for saccharides and maltitol > sorbitol > xylitol > erythritol > glycerol for polyols.[84] Changing the acetonitrile by tetrahydrofuran, slight inversions in this behaviour were found,[82] while the polyols kept the same ability to induce phase separation.[85] These tendencies, although being slightly distinct in PPG400-based ABS,[81] correlate well with the number of carbons and hydration ability of the carbohydrates.

ILs represent another option to overcome the high viscosity of polymeric-based ABS. As extensively described in literature, ILs are considered as "*designer solvents"*, as it is possible to pair multiple cations and anions to define and tune their main properties, allowing their design as task-specific solvents. Wu and co-authors delivered the first report on the combined use of ILs and carbohydrates for ABS formation. Using the IL 1-butyl-3-methylimidazolium tetrafluoroborate ($[C_4mim][BF_4]$) four saccharides were screened, being their ability to form ABS described as follows: sucrose > glucose > xylose > fructose.[86] After establishing the poor chemical stability of $[C_4mim][BF_4]$,[88] Freire et al.[46] proposed its replacement by the 1-butyl-3-methylimidazolium trifluoromethanesulfonate ($[C_4mim][CF_3SO_3]$). Moreover, the authors provided a more

complete screening of carbohydrates.[46] The phase separation ability of the carbohydrates studied (Figure 7) followed the trend: D-maltitol > D-(+)-maltose > D-sorbitol > sucrose > D-(+)-glucose ≈ D-(+)- galactose > xylitol ≈ D-(-)-fructose ≈ D-(+)-mannose > D-(-)-arabinose > L-(+)-arabinose > D-(+)-xylose. The trend is, D-(+)-maltose > sucrose > D-(+)-glucose ≈ D-(+)- galactose > D-(-)-fructose ≈ D-(+)-mannose > D-(-)-arabinose > L-(+)-arabinose > D-(+)-xylose for saccharides (Figure 7A) and D-maltitol > D-sorbitol > xylitol (Figure 7B for polyols) that, with fructose as an exception, agrees with the work by Wu et al.[86] In accordance to what was already disclosed for organic solvent-containing[82–85] and/or PPG400-based systems,[81] four aspects were highlighted: ***i)*** the number of hydroxyl groups of the sugar, where a higher number of hydroxyl groups will favour the ABS formation; ***ii)*** hexoses are better to induce the phase split than pentoses; ***iii)*** the configuration of the hydroxyl groups at the C(2) and C(4) positions demonstrated a great influence and ***iv)*** polyols are more efficient than the corresponding saccharides in the ABS formation.[46] Given the limited number of ILs with adequate properties to form ABS with carbohydrates, Freire and co-workers[87] worked on the synthesis of new fluorinated ILs, for which the same tendency towards the ABS formation was confirmed.[46]

Cyclodextrins and their derivatives are oligossacharides widely applied as chiral selectors. Recently, Wang and collaborators[68,72] proposed chiral ABS composed of *β*-cyclodextrin (*β*-CD) derivatives for the resolution of racemic phenylsuccinic acid and zoplicone. The formation of these systems was performed by their combination with organic solvents, namely acetone[68], alcohols[72] and acetonitrile.[72] While the ABS formation ability was generally poor for neutral *β*-CD derivatives – the methyl-*β*-cyclodextrin (ME-*β*-CD) and the hydroxypropyl-*β*-cyclodextrin (HP-*β*-CD) – the anionic *β*-CD derivatives – the carboxymethyl-*β*-cyclodextrin (CM-*β*-CD) and the sulfobutyl ether-*β*-cyclodextrin (SBE-*β*-CD) – were much better. This could be attributed to the formation of hydration complexes between the water molecules and the anionic *β*-CD derivatives, suppressing the formation of hydration complexes between water and the organic solvents.[68,72] Moreover, long chain alcohols and acetonitrile are the organic solvents inducing larger biphasic regions, as a result of their higher hydrophobicity.[72]

Of importance to highlight is the fact that not all of the carbohydrates overviewed in this section are specified as being used in their chiral form. But, as reported by some authors, chirality has no major effect on phase formation ability.[46,82]

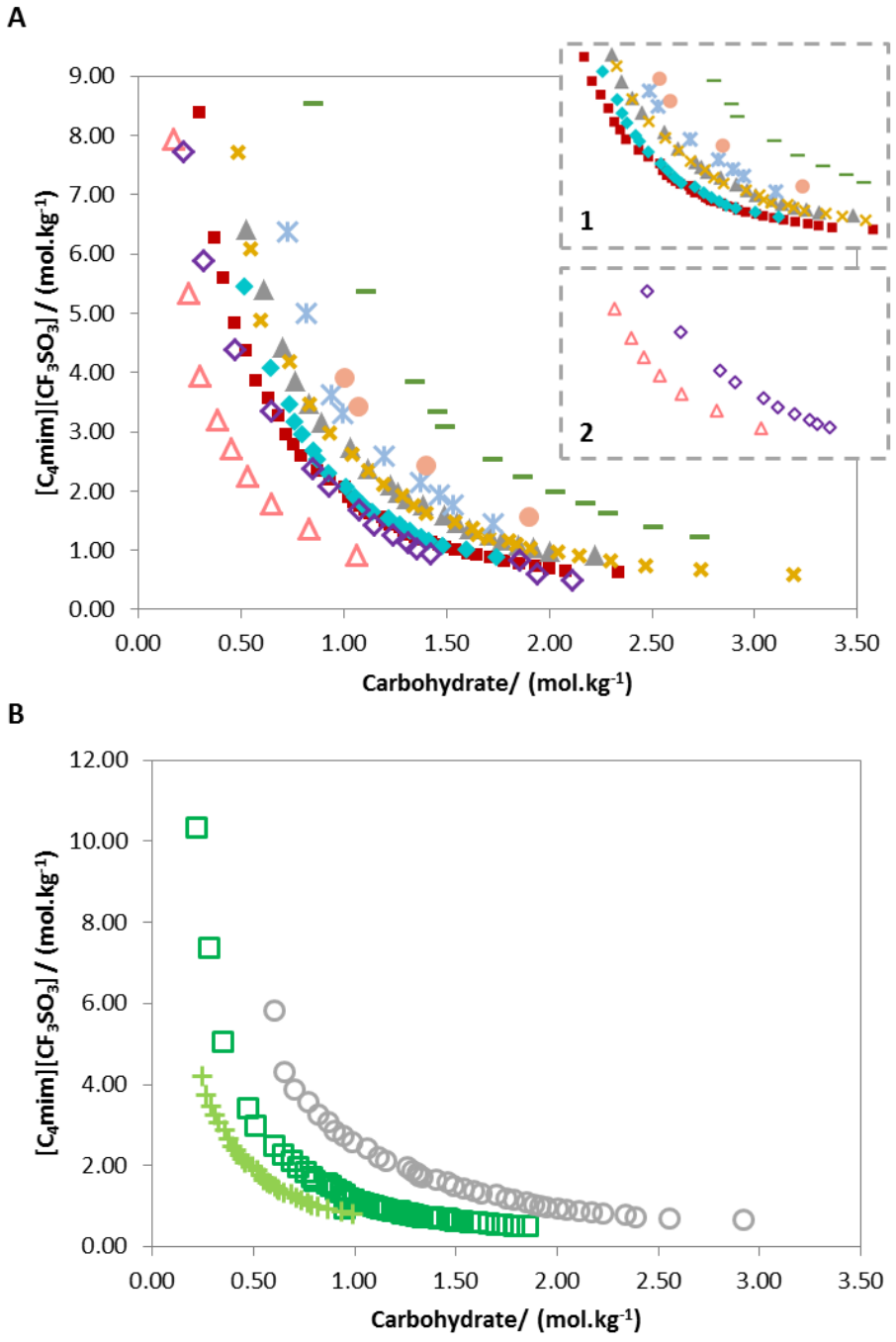

Figure 7. *Phase diagrams of the systems composed of: (A) [C₄mim][CF₃SO₃] + Saccharide + H₂O at 298 K:(■)D-(+)-glucose, (▲)D-(+)-manose, (✖)D-(-)-frutose, (◆)D-(+)-galactose, (–)D-(+)-xylose, (✱) D-(-)-arabinose, (●)L-(-)-arabinose, (△)D-(+)-maltose, (◇)Sucrose; (B) [C₄mim][CF₃SO₃] + Polyol+ H₂O at 25 (±1)ºC:(□)D-Sorbitol, (○)Xylitol, (+)D-maltitol. The insets represent the comparisons between (1) monossacharides and (2) dissacharides. Adapted from* [46].

Table 2. *Summary of carbohydrates applied as chiral phase formers in ABS.*

Carbohydrate	**Second Phase Component**
Glucose	$[C_4mim][CF_3SO_3]$[46], PPG 400[81], PPG725[81], THF[82], acetonitrile [83], $[C_4mim][BF_4]$[86], $[C_2C_1py][C_4F_9SO_3]$[87]
Xylose	$[C_4mim][CF_3SO_3]$[46], PPG 400[81], THF[82], acetonitrile [83], $[C_4mim][BF_4]$[86]
Fructose	$[C_4mim][CF_3SO_3]$[46], PPG 400[81], PPG725[81], THF[82], acetonitrile [83], $[C_4mim][BF_4]$[86], $[C_2C_1py][C_4F_9SO_3]$[87]
Arabinose	$[C_4mim][CF_3SO_3]$[46], PPG 400[81], THF[82], acetonitrile [83], $[C_2C_1py][C_4F_9SO_3]$[87]
Mannose	$[C_4mim][CF_3SO_3]$[46], PPG 400[81], THF[82], acetonitrile [83], $[C_2C_1py][C_4F_9SO_3]$[87]
Sucrose	$[C_4mim][CF_3SO_3]$[46], PPG 400[81], PPG725[81], THF[82], acetonitrile [83], $[C_4mim][BF_4]$[86], $[C_2C_1py][C_4F_9SO_3]$[87]
Maltose	$[C_4mim][CF_3SO_3]$[46], PPG 400[81], THF[82], acetonitrile [83], $[C_2C_1py][C_4F_9SO_3]$[87], $[C_2C_1im][C_4F_9SO_3]$[87]
β-CD derivatives	Ethanol[72], 1-propanol[72], 2-propanol[72], acetonitrile[72], acetone [68]
Glycerol	acetonitrile[84], THF[85]
Erythritol	acetonitrile[84], THF[85]
Xylitol	$[C_4mim][CF_3SO_3]$[46], PPG 400[81], acetonitrile[84], THF[85], $[C_2C_1py][C_4F_9SO_3]$[87]
Sorbitol	$[C_4mim][CF_3SO_3]$[46], PPG 400[81], acetonitrile[84], THF[85], $[C_2C_1py][C_4F_9SO_3]$[87]
Maltitol	$[C_4mim][CF_3SO_3]$[46], PPG 400[81], acetonitrile[84], THF[85], $[C_2C_1py][C_4F_9SO_3]$[87]
Galactose	$[C_4mim][CF_3SO_3]$[46], PPG 400[81], acetonitrile [83], $[C_2C_1py][C_4F_9SO_3]$[87]
Raffinose	PPG 400[81]
Lactose	PPG 400[81]
Ribose	PPG 400[81]

2.1.2.1.2. Amino acids

Amino acids appear in the ABS domain as phase formers for the same reasons of carbohydrates, namely their simple chemical structure and the ready availability of both enantiomers.[89] Glycine, as the only achiral amino acid, will be discarded from this

literature overview. Polymers,[90] surfactants[91] and ILs,[47,92] can be combined with amino acids to form ABS. As reported by Sadeghi et al.,[90] PPG 400 and PPG 725 are able to form ABS with amino acids, contrarily to PEG-based polymers as found for carbohydrates.[81] Serine (the most efficient for salting-out), alanine and proline (the least prone for salting-out) were the amino acids tested, as shown in Figure 8. Moreover, the ABS formation is improved by the amino acid hydrophilicity, temperatures and polymers molecular weight.

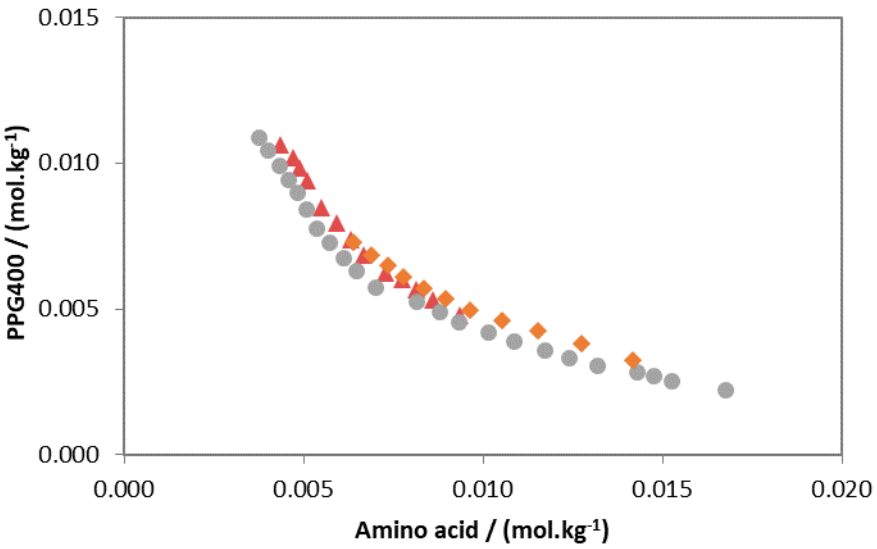

Figure 8. *Phase diagrams of the systems composed of PPG400 + Amino acid + H_2O at 298 K:(▲) Alanine, (●) Serine, (◆) Proline. Adpated from* [90].

Due to their amphiphilic nature and improved biocompatibility, surfactants have been also used to create ABS.[93–95] Although several surfactants may exhibit chirality,[96–99] thus serving as chiral selectors in enantioseparation processes, there is no report on their use as phase formers in chiral ABS. But, the achiral Triton X-100 + L-proline ABS was proposed by Chakraborty and collaborators.[91] No promising status was identified, since the system presents a limited window of conditions at which is stable (< 3 $mol.kg^{-1}$ of L-proline and 6 < pH < 8), thus requiring a hydrophobic additive.

ILs are also promising phase former pairs for amino acids, as first proposed by Zhang et al.[92] and then by Domínguez-Pérez et al.[47] L-serine and L-proline combined with the $[C_4mim][BF_4]$ were able to form ABS following the same amino acids' ranking of PPGs-based ABS.[92] However, the temperature dependency of amino acids + ILs ABS was opposite to that obtained for amino acids + PPGs systems.[90] Again,

[C_4mim][CF_3SO_3] and 1-butyl-3-methylimidazolium dicyanamide ([C_4mim][$N(CN)_2$])[47] were proposed as stable replacements to [C_4mim][BF_4].[88] Lysine and its monohydrochloride form, as well as proline, were the amino acids investigated, with lysine presenting higher aptitude to form ABS than proline. The 3 authors justified these results by the hydrophilicity of the amino acid that enlarges the biphasic region of the phase diagram, as previously described in other works.[90,92] Lysine and Lysine HCl bear an additional $–NH_2$ group in its side chain, being thus more soluble in water than proline.

Table 2. *Summary of the amino acids applied in the formation of ABS.*

Amino acid	**Second Phase Component**
Alanine	PPG400[90], PPG725[90]
Serine	[C_4mim][BF_4][92], PPG400[90], PPG725[90]
Proline	[C_4mim][BF_4][47,92], [C_4mim][CF_3SO_3][47], [C_4mim][$N(CN)_2$][47], Triton X-100[91], PPG400[90], PPG725[90]
Lysine	[C_4mim][BF_4],[47] [C_4mim][CF_3SO_3],[47] [C_4mim][$N(CN)_2$][47]

2.1.2.1.3. Chiral Polymers

Another interesting approach to develop chiral ABS is to synthesize specific polymers with both chiral selector potential and ABS formation capacity. This was proposed by Tan and his collaborators [63], who have synthesized a new thermo-sensitive polymer, poly(MAH-*β*-CD-co-NIPAAm), through the copolymerization of N-isopropylazylamide (NIPAAm) with maleic anhydride (MAH) modified *β*-CD. The phase diagram of poly(MAH-*β*-CD-co-NIPAAm) + dextran ABS was determined and further utilized for chiral separation of mandelic acid (MA) enantiomers (further discussed in ***section 2.1.2.2.***). Poly(MAH-*β*-CD-co-NIPAAm) has chiral selector potential due to the formation of a hydrophobic cavity, which hosts the chiral guests.

Table 3. *Summary of the polymers applied in the formation of chiral ABS.*

Chiral Polymer	**Second Phase Component**
Poly(MAH-*β*-CD-co-NIPAAm)	Dextran T40[63]

2.1.2.1.4. Chiral Ionic Liquids

The ILs are a class of salts with low melting temperatures, usually below 100 ºC, due to the low symmetry of the composing ions and low charge density that precludes their organization into a crystal lattice.[100] Among all the unique properties of ILs (negligible vapour pressure at atmospheric conditions, strong solvation ability for a wide variety of compounds, high thermal and chemical stability),[19] their already mentioned "*designer solvent"* character[101] stands out if they are to be used as chiral selectors. Cations and anions bearing chirality can be used as starting materials to synthesize CILs, where the chirality can be defined on the cation, anion or on both.[102] Some examples are amino acid ester-based,[103] benzimidazolium-based,[104] amino alcohol-derived,[105] nicotine-based[106] and isomannide-based [107] CILs. These are gaining much favour in processes where enantioselectivity is mandatory[102,108] and in particular for chiral ABS applications.[19] Some works have already applied CILs-based ABS in the resolution of racemates, as it will be discussed in ***section 2.1.2.2.***. Wu et al. synthesized two chiral functionalized imidazolium-based ILs with the chirality in the cation and sharing the hexafluorophosphate anion ($[PF_6]^-$), [ChiralFunct^{1}C$_1$im][PF_6] and [ChiralFunct^{2}C$_1$im][PF_6]. ABS composed of these two hydrophilic CILs and the inorganic salt Na_2SO_4 have been created with the specific goal of resolving racemates of amino acids.[76] With no major impact of the CILs' structure upon the phase formation, only very small amounts of Na_2SO_4 are necessary to reach the biphasic zone. While $[PF_6]^-$ also partially hydrolyses in aqueous medium,[88] Wu et al.[77] provided another group of task-specific CILs for the resolution of racemic mixtures of amino acids. Tropine-like ILs of increasing alkyl side chain length having the prolinate ([C$_n$tropine][Pro], with $2 \leq n \leq 8$) were synthesized and further combined with salts in the formation of ABS. The molecular scenario behind the formation of ABS is in good agreement with other IL-based ABS[19]: ***i)*** larger alkyl chains are better for ABS formation due the higher hydrophobic character of the [C$_n$tropine][Pro]; ***ii)*** the effect of the salt type was studied with K_3PO_4, K_2HPO_4 and K_2CO_3, following the Hofmeister series; and ***iii)*** the increase in temperature, analogously to what was observed for achiral ILs + amino acids,[92] is limiting the ABS formation. Several cholinium-based ILs containing either natural amino acids or other organic acids as the anion moiety were also applied. Although these have appeared to create more biocompatible IL-based ABS, some of the structures available

are chiral. So, ABS composed of CILs based on the cholinium anion, $[Ch]^+$, can be promising for enantioselective extractions. Several cholinium-amino acid-based ILs are available, namely cholinium phenylalaninate ([Ch][Phe]), cholinium leucinate ([Ch][Leu]), cholinium valinate ([Ch][Val]), cholinium lysinate ([Ch][Lys]), cholinium *β*-alaninate ([Ch][*β*-Ala]), cholinium serinate ([Ch][Ser]) and cholinium glycinate ([Ch][Gly]). [Ch][Gly] being achiral will not be considered here. Cholinium-based CILs can undergo phase separation with inorganic salts of enhanced salting-out aptitude (K_3PO_4 and K_2CO_3)[109] or with polymers (e.g. PPG400).[110] In the salt-based system, cholinium-based ILs are salted-out by the inorganic salt, while in the polymer-containing system they salt-out the PPG400. Wang et al.[109] observed that, in the presence of K_3PO_4 and K_2CO_3, the ability of the three cholinium-amino acid-based ILs to generate ABS follows the hydrogen-bond donation ability of the anions. The highest aptitude of K_3PO_4 to salt-out the CIL when compared with the K_2CO_3 follows the Hofmeister series, as also shown for [C*n*tropine][Pro]-based systems.[77] Increased temperatures again proved to diminish the potential for ABS formation as in other CILs + salts[77] and achiral ILs + amino acids[92] systems. PPG400 was used with cholinium-amino acid-based ILs[110] and the tendency to induce phase separation is the following (Figure 9): [Lys] > [Ser] ≈ [*β*-Ala]. In this work, it is shown that the molecular-level mechanisms that justify these results are different from those used in the work of Wang et al.[109] Recently, cholinium-based ILs having natural organic acids were applied in the formation of ABS of polymeric basis.[111] Among the nine ILs synthesized by the authors, four possess chirality due to the presence of a chiral anion, namely cholinium abietate ([Ch][Abt]), cholinium L-ascorbate ([Ch][L-Asc]), cholinium D-galactouronate ([Ch][D-Gal]) and cholinium D-quinate ([Ch][Qui]). While [Ch][Abt] failed to form ABS with PPG400 due to its higher hydrophobicity, the remaining acted according to the trend [Ch][D-Qui] ≃ [Ch][D-Gal] > [Ch][Asc]. In agreement with the previous works evaluated, the hydration aptitude of each acid dominates the ABS.[110] If more hydrophobic anions are better to form CIL + inorganic salts ABS, the opposite occurs in CILs + PPG400 ABS.[110,109,111]

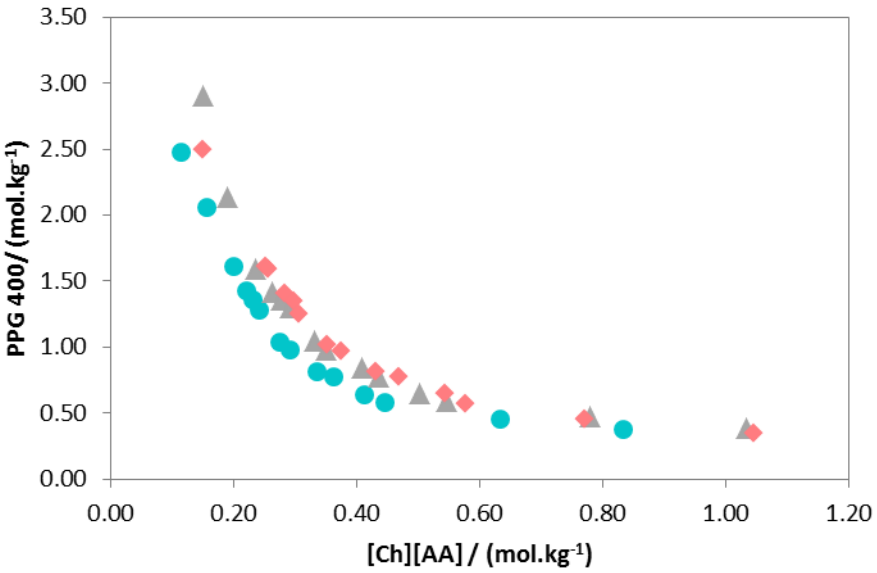

Figure 9. *Phase diagrams of the systems composed of PPG400+ [Ch][AA] + H_2O at 298 K:(●)[Ch][Lys], (▲) [Ch][Ser], (◆) [Ch][Ala]. Adpated from* [110].

Table 4. *Summary of the chiral ionic liquids applied in the formation of chiral ABS.*

Chiral Ionic Liquids	**Second Phase Component**
[ChiralFunct^{1}C$_1$im][PF_6]	Na_2SO_4[76]
[ChiralFunct^{2}C$_1$im][PF_6]	Na_2SO_4[76]
[C$_n$Tropine][Pro]	K_3PO_4[77], K_2HPO_4[77], K_2CO_3[77]
[Ch][Phe]	K_3PO_4[109], K_2CO_3[109]
[Ch][Leu]	K_3PO4[109], K_2CO_3[109]
[Ch][Val]	K_3PO_4[109], K_2CO_3[109]
[Ch][Lys]	PPG 400[110]
[Ch][*β*-Ala]	PPG 400[110]
[Ch][Ser]	PPG 400[110]
[Ch][D-Qui]	PPG 400[111]
[Ch][L-Asc]	PPG 400[111]
[Ch][D-Gal]	PPG 400[111]

Not only the chemical structure of the chiral phase former[63,64] and the temperature[60,61,63,64] are important operational parameters when enantioseparation applications are focused. Although not previously studied in the context, pH is also important as will be discussed in ***section 2.1.2.2.***

2.1.2.2. Application of chiral ABS to enantioselective separation processes

The application of ABS for enantioseparation processes was first proposed by Sellergren and Ekberg in 1985.[78] Figure 10 summarizes the incidence of works based on the type of ABS (A), type of racemate (B) and type of chiral selector (C). Few studies suggest the use of different chiral molecules (chiral ILs,[76,77] β-CD derivatives[68,72] and polymer[63]) simultaneously as phase-forming components and chiral selectors (24%, Figure 10A). These systems involve the use of a lower number of chemicals, being thus, considered simpler. Still, the most common is the addition of a small amount of a certain chiral selector to induce enantioselectivity (76% of the works reviewed, Figure 10A).[60–62,64–66,44,67,69–71,73–75,78–80] ABS with biphasic chiral recognition, *i.e.* with two distinct chiral selectors that partition to opposite phases, have also been developed, based on the premise that these may yield greater separations. [63,68,72,76,77] Most of the reported enantioselective ABS resolved drugs (71% *vs.* 29% with amino acids – Figure 10B). Over 50% of the works opted for β-CD or its derivatives as chiral selector (Figure 10C). The chemical structure of the racemates resolved is shown in Figure 11.

Throughout this section, the enantioselective separation of chiral drugs and amino acids using ABS is overviewed. Two main parameters were used in literature to evaluate the enantioselectivities attained: the selectivity (α – Eq. 1) and the enantiomeric excess (*e.e.%* – Eq. 2). The α is the ratio between the partition coefficients of the enantiomers toward one phase, meaning that certain separation occurs if $\alpha > 1$. *e.e.%* is the extent at which a mixture is enriched in one enantiomer rather than in the other, *i.e.* a mixture with an *e.e.%* of 50% is composed of 75% of one enantiomer and 25% of the other enantiomer.

$$\alpha = \frac{[R_1]/[R_2]}{[S_1]/[S_2]} = \frac{K_R}{K_S} \quad \text{(Eq. 1)} \qquad e.e.\,\% = \frac{[R_1]-[S_1]}{[R_1]+[S_1]} \times 100 \quad \text{(Eq. 2)}$$

$[R_1]$ and $[R_2]$ are the R-enantiomer concentration in phases 1 and 2, respectively. $[S_1]$ and $[S_2]$ are the S-enantiomer concentration in phases 1 and 2, respectively. K_R and K_S

are the partition coefficients of R-enantiomer and S-enantiomer, respectively, for phase 1.

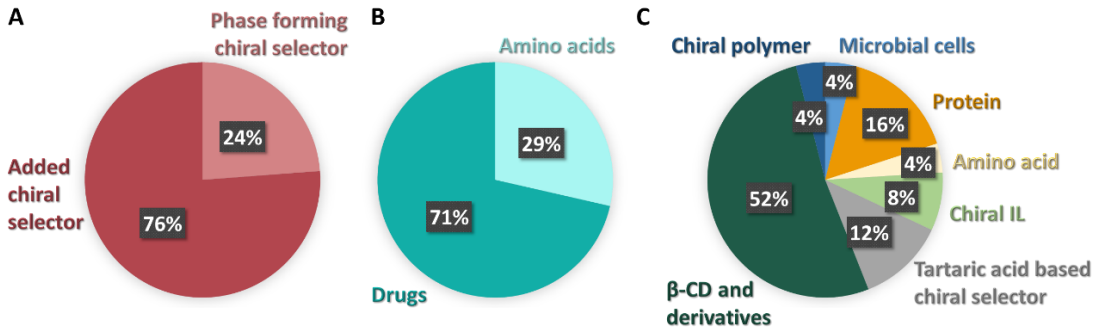

Figure 10. *Schematic representation of the data published on this field. Statistical data is organized according to (A) type of chiral recognition approach; (B) type of racemic mixture; and (C) type of chiral selector.*

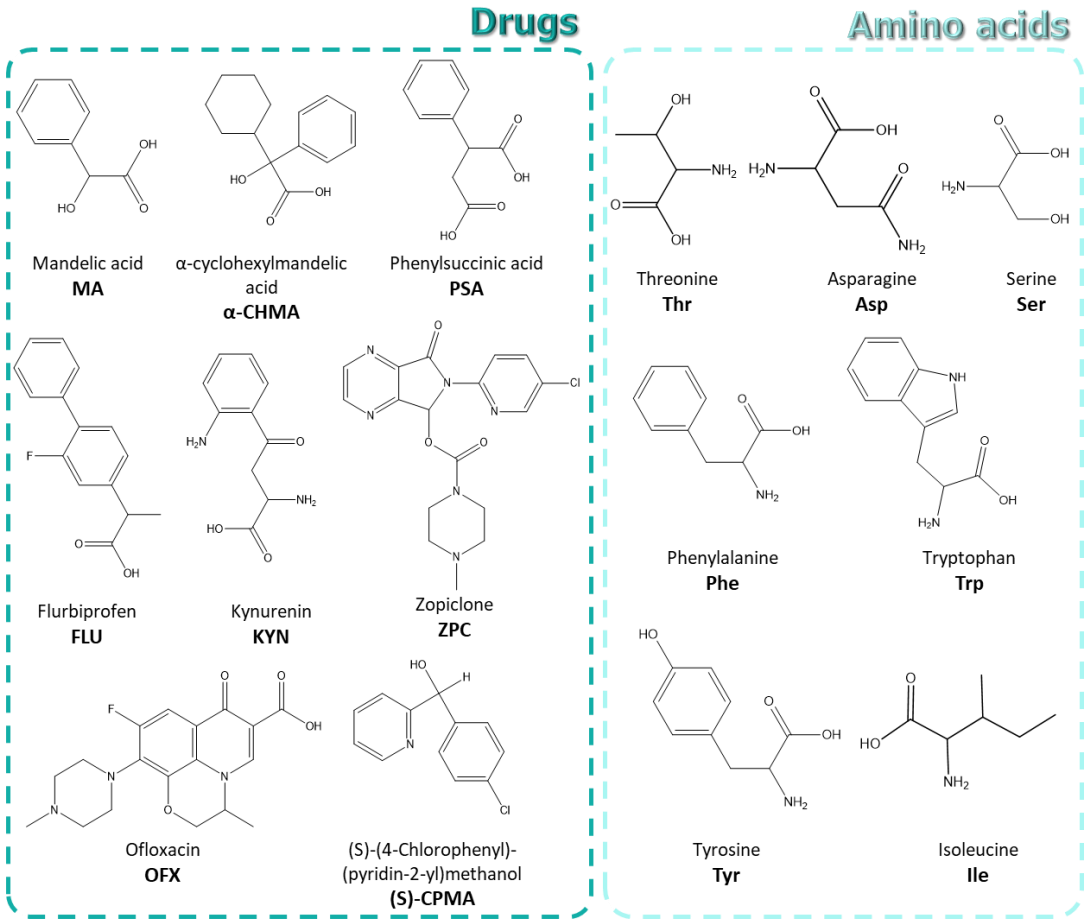

Figure 11. *Name, abbreviation and chemical structures of the drugs and amino acids evaluated so far in literature.*

2.1.2.2.1. Drugs

A considerable amount of the works overviewed dealing with racemic drugs has been devoted to the separation of mandelic acid (MA) enantiomers or their derivatives. The resolution approaches proposed cover ABS mainly composed of polymer/salt,[60,64,66,69] surfactant,[61] ethanol/salt[62] and IL/salt[65] combinations with the introduction of *β*-CD or its derivatives as chiral selectors.

PEG + salt ABS containing *β*-CD or Cu_2-*β*-CD as chiral selectors were proposed, motivated by a theoretical background involving the three-point model and the different stability and solubility between the PEG- and salt-rich phases of the inclusion complexes.[60,64] PEG + $(NH_4)_2SO_4$ + *β*-CD yielded a maximum separation factor of 2.46 for the (L)-enantiomer (30 wt% PEG 2000 + 20 wt% $(NH_4)_2SO_4$, with [*β*-CD] = 0.008 mol.L^{-1}, [MA] = 0.05 mol.L^{-1} at pH 1.0 and 30ºC).[60] Bearing one carboxylic group and one aromatic group (Figure 11), MA suffers speciation with pH. Since *β*-CD has a higher recognition ability for molecular MA than for the ionic form, systems with pH values higher than 3 hampered an efficient enantioseparation.[60] Lower temperatures in a range of 30 to 70 ºC maintain the stability of *β*-CD-MA complexes. Lower initial concentrations of *β*-CD and MA enantiomers, where no cooperation between the two diastereomeric complexes and PEG occurs, are optimal. Lower molecular weights of PEG are ideal because they are less viscous, which consequently helps the phase-separation. Li and Li resolved a racemate of α-cyclohexylmandelic acid (α-CHMA) with PEG + $Na_3C_6H_5O_7$ + Cu_2-*β*-CD ABS.[64] With preferential recognition ability for the R-CHMA, the developed system containing Cu_2-*β*-CD reached a maximum separation factor of 1.36 (pH = 8.96, T = 9 ºC and [Cu_2-*β*-CD] = 1 g) after optimization. Like MA, α-CHMA is also sensitive to pH changes due to the presence of one carboxylic group and one hydroxyl group in its structure, thus being dissociated in aqueous solution (Figure 11). Since Cu_2-*β*-CD is only stable in alkaline conditions, the pH influence on the enantioselectivity was investigated in a pH range from 8 to 12. An optimal enantioselectivity was attained at 8.96, where monovalent CHMA, for which Cu_2-*β*-CD has better chiral recognition ability and affinity, is present. With the increase in the pH, increases the concentration of divalent CHMA, which seems to be limiting the formation of inclusion complexes. Furthermore, the *"CHMA-Cu_2-β-CD"* complex formation is also influenced by changes in temperature, since the separation factor decreases while increasing temperature from 9 to 60 ºC. The poorer stability of the two diastereomeric complexes and enhanced CHMA ionization at

higher temperatures contribute to this scenario. Finally, increasing Cu_2-*β*-CD concentrations, up to 1 g *per* ca. 20 g of ABS, remarkably boosted the separation factor.

To overcome the problems presented by ABS of polymeric basis, other ABS were proposed, namely aqueous micellar biphasic systems (AMBS), ethanol/salt-based ABS,[62] and IL/salt ABS.[61,65] AMBS are specific types of ABS that use surfactants and their capacity to form micelles/aggregates, and their aptitude to undergo two-phase separation in aqueous solution by temperature manipulation. AMBS based on Triton X-114 with Cu_2-*β*-CD as chiral selector for the enantioseparation of racemic MA led, under optimal conditions (8 wt% triton X-114 + [Cu_2-*β*-CD] = 10 mmol L^{-1} + [MA] = 5 mmol L^{-1} at pH = 12 and T = 55 ºC) to an *e.e.%* of 67.91%, the highest value ever reported in literature (*cf.* Table 5).[61] As mentioned before, Cu_2-*β*-CD is stable only in alkaline pH and it was observed that *e.e.%* values increased with pH up to 12. Again, the highest recognition ability of Cu_2-*β*-CD for ionic MA is clear.[64] The concentration of Cu_2-*β*-CD and, mainly temperature, were the main operational factors affecting the MA chiral recognition. Both *R*-MA and *S*-MA form complexes with Cu_2-*β*-CD, being the higher maximization of the *e.e.%* detected at 10 mmol L^{-1} of chiral selector. In what concerns the effect of temperature, it seemed that a temperature of 55 ºC favoured enantioseparation due to the better stability of "*Cu_2-β-CD-(S)-MA*" complexes than that of the "*Cu_2-β-CD-(R)-MA"*.

It was also proposed an ABS for the separation of racemic MA and α-CHMA composed of polar alcohols and salts, K_2HPO_4 and $(NH_4)_2SO_4$, with sulfonated *β*-CD (Sf-*β*-CD) with different degrees of substitution as the chiral selector.[62] These ABS, particularly these made of ethanol + $(NH_4)_2SO_4$, were only able to chiral recognition of MA. The degree of substitution of the chiral selector, the system composition, the alcohol type, the MA concentration, temperature and pH were the conditions evaluated. *β*-CD sulfonated with 80 wt% of H_2SO_4 yielded the best results among all Sf-*β*-CD tested (sulfonated with 90 wt% or 70 % of H_2SO_4). The optimal system was defined as being composed of 30 wt% of ethanol + 15 wt% of $(NH_4)_2SO_4$ + [Sf-*β*-CD] = 20 mmol.L^{-1}, with [MA] = 0.5 mmol.L^{-1} at T = 50 ºC and pH = 2.0. For the optimum system, one α of 1.69 and *e.e.%* of 16.3% were obtained, however, these values for MA are lower than the ones obtained in PEG 2000 + $(NH_4)_2SO_4$ (α = 2.46 – see Table 5 for comparison).

IL-based ABS were suggested by Chen *et al.* for the chiral separation of α-CHMA enantiomers. Hydroxypropyl-*β*-cyclodextrin (HP-*β*-CD) was introduced as chiral selector in an ABS formed by ILs and $(NH_4)_2SO_4$. Among the three ILs tested, $[C_4mim][BF_4]$ was the most promising, yielding a maximum separation factor of 1.59 (17.09 wt% $[C_4mim][BF_4]$) + 14.05 wt% $(NH_4)_2SO_4$ at T = 5ºC and pH = 4.36, [HP-*β*-CD] = 0.21 g).[65] HP-*β*-CD, which has a preferential affinity to the enantiomer S, was reported as being mainly located in the salt-rich phase, which promoted the CHMA partition for that phase. While temperature was shown to have a clear trend on the impact upon enantioseparation, the remaining parameters investigated (pH, amount of IL, amount of salt and HP-*β*-CD) were characterized by maximum peak values. The authors argued that, between 5 and 50 ºC, the higher temperatures limited the enantioseparation of the ABS that promoted the CHMA partition towards the $[C_4mim][BF_4]$-rich phase. Moreover, as for other works reported for MA enantiomers,[60] HP-*β*-CD has better recognition for the molecular form, thus acidic pH would be favourable for enantioseparation. They reported that while pH between 1.5 and 4.36 improves enantioselectivity, it then decays as the pH is further increased up to 7. The authors attributed this behaviour to the higher affinity for the $[C_4mim][BF_4]$-rich phase exhibited by the molecular MA present at acidic pH. Giving the results obtained in the two works aimed at resolving enantiomers of CHMA,[64,65] IL-based ABS revealed boosted performances (α = 1.59 *versus* α = 1.36 reported for polymer/salt ABS,[64] while the alcohol/salt ABS[62] were unable to recognize chiral CHMA).

Tan and his collaborators[63] proposed an ABS for the enantiomeric resolution of MA using a polymer as both phase former and chiral selector to minimize the number of chemicals in the process. The chiral and thermo-sensitive polymer, poly(MAH-*β*-CD-co-NIPAAm), was synthesized by the copolymerization of N-isopropylazylamide (NIPAAm) with *β*-cyclodextrin (*β*-CD) modified maleic anhydride (MAH).[63] This presented preferential recognition for the (S)-enantiomer. In combination with dextran T40, the ABS with this newly synthesized chiral polymer yielded a maximum separation factor of 1.27 under the optimum conditions (10 wt% poly(MAH-*β*-CD-co-NIPAAm) + 10 wt% dextran T40 + [MA] = 0.010 $mol.L^{-1}$ at T = 5ºC and pH = 2.04). Acidic pH, in particular a pH of 2, increased the separation factor due to the better recognition ability for the molecular MA as revealed in other works using CD derivatives as chiral

selectors.[60] Given the thermosensitive nature of poly(MAH-*β*-CD-co-NIPAAm), the temperature was identified as being an important parameter on the enantioseparation process proposed. Actually, temperatures higher than the optimal value of 10 ºC were suggested to be responsible for the poorer MA enantiomers recognition. On the other hand, the poly(MAH-*β*-CD-co-NIPAAm) was designed to be easily recycled and reused, as schematized in Figure 12. Although revealing the lower separation factors among the ABS studied (*cf.* Table 5),[60,61,64,65] this approach is more appealing regarding the environmental and economic impacts, not only due to its simpler nature, but also due to its proved reuse of the phases components.

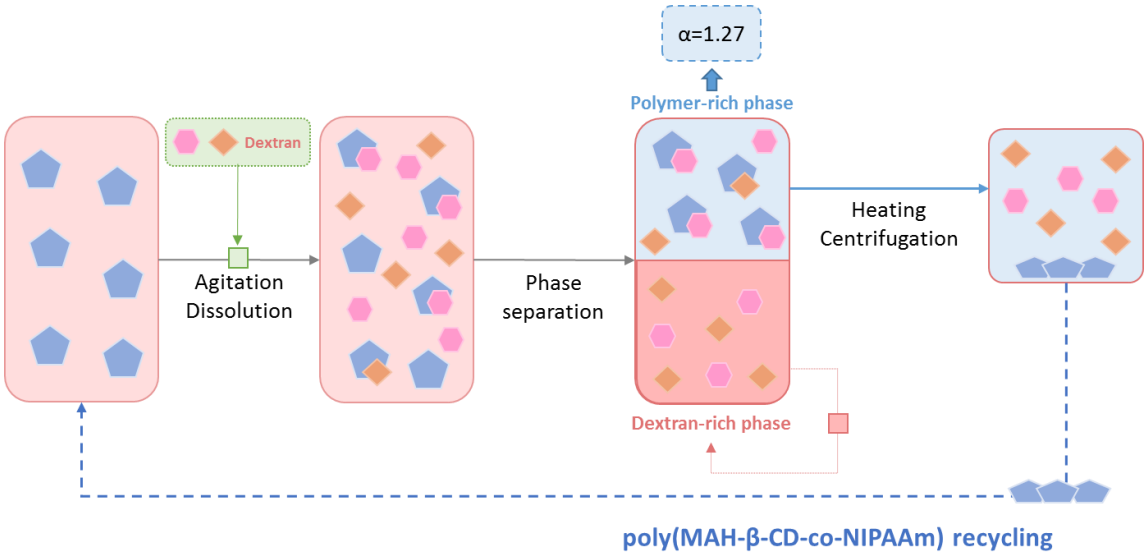

Figure 12. *Schematic diagram of a chiral separation of MA enantiomers using a chiral ABS containing a thermo-sensitive polymer, as both phase former and chiral selector. Poly(MAH-β-CD-co-NIPAAm)* ⬟*, (S)-MA* ⬢*, (R)-M A* ◆*. Adapted from* [63].

Phenylsuccinic acid (PSA) enantiomers have also been resolved using chiral ABS. This molecule is important as antitumoral agent. Systems containing ethanol and ammonium sulphate, $(NH_4)_2SO_4$, and HP-*β*-CD (hydrophilic chiral selector) were employed. The separation factor reached 1.42, under optimized conditions (18.85 wt% $(NH_4)_2SO_4$ +27.50 wt% ethanol + [HP-*β*-CD] = 0.08 mol.L^{-1}, with [PSA] = 1.0 mmol.L^{-1} at T = 6 ºC and pH = 2.5) in a single step.[44] PSA enantiomers are binary acids, with their anionic form ratio changing with pH. Therefore, separation factors are pH dependent. As the pH increased from 2.5 to 8 the separation factor to the ethanol-rich

phase drastically decreased, since the medium was more enriched in double charged anionic PSA rather than in the single charged or neutral forms. This is due to the HP-β-CD greater affinity to form enantiomer-selector complexes with molecular PSA, rather than with the ionic form. High concentrations of HP-β-CD (from 0 to 0.12 mol.L^{-1}) are an advantageous condition for the enantioseparation, with a maximum α occurring at 0.08 mol.L^{-1} of HP-β-CD. Concentrations of the chiral selector higher than this value were defined as almost deleterious to enantioseparation. The authors suggested that probably the excess of HP-β-CD promoted the S-PSA partition towards the salt-rich phase. Meanwhile, the separation factor decreased with increasing concentration of PSA. In summary, the authors argued that a balance between high and low concentrations of HP-β-CD and PSA, respectively, lead to the success of PSA enantiomers resolution. Finally, the temperature showed a favourable effect for chiral separation efficiency if decreased from 20 to 5 ºC.

Aqueous two-phase flotation (ATPF) is a specific type of ABS that combines the principles of ABS formation and solvent sublation.[112] Racemic PSA was resolved with an aqueous two-phase flotation system formed by combinations of either alcohols + $(NH_4)_2SO_4$ or PEG + $(NH_4)_2SO_4$ with HP-β-CD, where the air bubbles direct both the inclusion complexes and free PSA enantiomers to the interface for further partitioning.[66] The alcohols + $(NH_4)_2SO_4$-based ABS were abandoned due to poor enantioselectivity or lack of stability to form an ATPF. The optimal conditions (40 wt% of PEG + 20 wt% of $(NH_4)_2SO_4$ + [HP-β-CD] = 0.015 mol.L^{-1}, with a PEG of molecular weight of 2000 g.mol^{-1} at pH = 2.5, air flow rate = 20 mL.min^{-1} and flotation time = 1 h) lead to a maximum α of 1.99. The recognition mechanism was based on the formation of "HP-β-CD-PSA" inclusion complexes, more significant for R-PSA. The enantioseparation process was also promoted by the partition of the complexes and free PSA between the two phases. It was also possible to make this type of ethanol/salt-based ABS more efficient in the enantioseparation of PSA by adopting the biphasic recognition concept.[67] Besides HP-β-CD, also L-(+)-tartaric acid diisopropyl ester (L-IPTA) as chiral selector was used. While the HP-β-CD is mainly located in the salt-rich phase, L-IPTA partitions for the ethanol-rich layer. Under the optimized conditions selected (31.47 wt% of ethanol + 15.41 wt% of $(NH_4)_2SO_4$ + [l-IPTA] = 0.12 mol.L^{-1} + [HP-β-CD] = 0.06 mol.L^{-1}, with [PSA] = 1.0 mmol.L^{-1}, at pH = 2.5 and T=10ºC), a separation factor of 4.06 was achieved,

much higher than that of 1.42 obtained by the monophasic recognition ABS.[44] The same optimization parameters (pH, chiral selectors concentration, PSA initial amount and temperature) have a similar influence to that observed for the process based on monophasic recognition (ethanol +$(NH_4)_2SO_4$ + HP-β-CD).[44] Like HP-β-CD, also L-IPTA is more able to recognize molecular PSA, making pH > 2.5 bad for enantioseparation. Moreover, the possibility of L-IPTA molecules interacting with HP-β-CD appears for high concentrations of the chiral selector. Finally, it was proposed a less technologically complex alternative by using ABS composed of β-CD derivatives (sulfobutyl ether, SBE-β-CD, and carboxymethyl, CM-β-CD), acting both as phase former and chiral selector, and acetone. With the help of 3D response surface, it was possible to identify the optimized conditions (with 66.86 wt% acetone + 6.63 wt% of SBE-β-CD with [PSA] = 2.0 mmol.L^{-1} at T = 15 ºC and pH = 3.0) that yielded a separation factor of *circa* 3.1 (experimentally confirmed).[68] Although less efficient than the ABS operating in the biphasic recognition mode, this approach is better than that using monophasic recognition with the extra addition of HP-β-CD.[44,67] Moreover, with the exception of ethanol + $(NH_4)_2SO_4$ + HP-β-CD,[44] ethanol + $(NH_4)_2SO_4$ + HP-β-CD + L-IPTA and acetone + SBE-β-CD-based ABS are more efficient than traditional biphasic recognition ELLE (octanol + water + L-iso-butyl tartrate + HP-β-CD with $\alpha = 2.86$)[113] and aqueous two-phase flotation system (PEG + $(NH_4)_2SO_4$ + HP-β-CD with $\alpha = 1.99$)[66].

Ofloxacin (OFLX) is a large-spectrum antibiotic, whose S-enantiomer is 8 to 128 times and twice more effective at inhibiting *Gram positive* or *Gram negative* bacteria than the R-enantiomer and racemate, respectively.[114] It is thus of relevance to obtain OFLX in its enantiopure state as attempted by Arai and Kuroda[70] in the early 90s. ABS composed of two polymers, 40.7 wt% PEG 6000 + 8 wt% dextran T40, operating in counter-current mode were studied. Bovine serum albumin (BSA) at 6 wt% was used in this work as chiral selector and it was defined to be present in the dextran-rich phase. Proteins, since they are inherently chiral, highly stable and biocompatible can be useful chiral selectors to implement in bio-inspired enantiseparation processes.[115] The counter-current mode allowed improving the *e.e.%* from 1% up to 62% for the R-OFLX after 8 fractions collected. By extracting with methanol and followed by thin-layer chromatography, the authors were able to obtain optically enriched OFLX from the dextran-rich phase with a recovery of 71%. The applicability of the proposed process was

investigated with the resolution of racemates of the hypoglycemic agent midaglizole (DG-5128) and the β-blocker carvedilol using another chiral discriminator, the protein ovomucoid with no success. Shinomiya et al (1998) also employed BSA as chiral selector in ABS operating in counter-current chromatographic mode for the enatioseparation of D,L-KYN. The system selected was composed of 10 wt% of PEG 8000, 5 wt% Na_2HPO_4 and 6 wt% of BSA and yielded a peak resolution of 0.94.[73] The authors have demonstrated that the BSA partitioned more significantly with the mobile phase, while the enantiomers mainly interacted with the column. The L-KYN has higher affinity for BSA, thus eluting before the D isomer.

As mentioned above, the combined use of chiral selectors (the so-called biphasic recognition – Figure 4) may be beneficial to improve enantioseparation processes.[69] Within the domain of chiral ABS, the first report on biphasic recognition used L-tartaric acid (L-TA) and HP-β-CD in systems composed of PEG + $(NH_4)_2SO_4$. HP-β-CD has a stronger affinity for the salt-rich phase due to its enhanced hydrophilicity, while L-tartaric acid remains in the polymer-rich layer. The authors proved that the mixture of L-tartaric acid and HP-β-CD was improving the enantioseparation. The best system selected was composed of 40 wt% of PEG 2000, 25 wt% of $(NH_4)_2SO_4$, [HP-β-CD] = 0.02 mol.L^{-1}, [L-tartaric acid] = 0.05 molL^{-1} at pH = 4,) and yielded a maximum α of 1.32, in one step of extraction.[69] At acidic conditions, especially of pH 4, the amount of protonated OFLX increased and thus, the enantiomers and the chiral selectors interacted more strongly. A careful balance between the chiral selectors content must be achieved, since opposite patterns are obtained for HP-β-CD and L-tartaric acid. Higher concentration of the former (0 – 0.04 mol.L^{-1}, with a maximum α at 0.02 mol.L^{-1}) precludes enantioseparation due to its hydrophilicity, not only forcing the partition of OFLX enantiomers to the salt-rich phase, but also promoting the occurrence of interactions with the L-tartaric acid that will hinder the *"OFLX-HP-β-CD"* complexation. Higher amounts of the later (0 – 0.05 mol.L^{-1}, with a maximum α at 0.05 mol.L^{-1}) induce favourable interactions between OFLX enantiomers and L-tartaric acid, hence partitioning to the PEG-rich phase.

Flurbiprofen (FLU) belongs to the non-steroidal anti-inflammatory drugs and has analgesic and antipyretic activities. It is widely used to manage rheumatoid arthritis.[116] It is still marketed in its racemic form, although there are evidences for the distinct activities of the enantiomers.[117] ABS composed of ethanol and $(NH_4)_2SO_4$, coupled to

biphasic recognition with L-dioctyl tartrate, (L-DOT) and L-tryptophan (L-Trp) were used to resolve racemic FLU. These two chiral selectors were chosen among amino acids, *β*-CD derivatives, and L-tartrate esters. The maximum α attained for FLU enantiomers was 2.34 (on a system composed of 35 wt% of ethanol + 18 wt% of $(NH_4)_2SO_4$ with [L-DOT] = 80 mg, [L-Trp] = 40 mg, [FLU]=0.10 mmol.L^{-1}, at pH = 4.0 and T = 25 °C).[71] L-DOT and L-Trp enantioselectively recognized R- FLU and S- FLU in ethanol-rich and $(NH_4)_2SO_4$-rich phases, respectively. The L-DOT concentration enhanced the separation factor for the R-enantiomer, while the L-Trp showed no significant enantiomeric recognition for any of the enantiomers. The best enantioselectivity achieved was under acidic conditions at pH 4, where both neutral and anionic FLU forms were present in an equimolar ratio. The authors showed that for this specific case, temperature had no significant impact on the enantioselectivity. Moreover, it was proved that the FLU concentration was limited by the amount of chiral selector, revealing that the enantiomeric recognition mechanism was based on a complexation phenomenon.

Wang et al. focused on the hypnotic agent zopiclone (ZPC). They have studied three *β*-CD derivatives, namely CM-*β*-CD, SBE-*β*-CD and HP-*β*-CD, both as chiral selectors and phase forming components in a ABS with hydrophilic organic solvents (alcohols and acetonitrile).[72] The desired opposite partitioning behaviour of ZPC enantiomers was more significantly attained using the ABS composed of 1-propanol and CM-*β*-CD, which was further selected as the optimal system. Under the optimal conditions for S-ZPC (single step process using the system composed of 78.35 wt% of 1-propanol + 2.17 wt% of CM-*β*-CD with [ZPC] = 0.05 mmol.L^{-1}, at T = 30 ºC and pH 8), the parameter α achieved was around 2.58 and the *e.e.*% was 32.66%. Contrarily to what had been widely described before, [68,72] the biphasic recognition, through the addition of L-tartaric acid derivatives was shown to be deleterious to enantioseparation of racemic ZPC. pH 8 led to the best enantioselectivity for S-ZPC, for which more than 50% of ZPC was present in its neutral form. Above and below this pH, the majority of the ZPC species in solution were charged (negative or positively charged, respectively). In these works, it was shown that the CM-*β*-CD molecules mainly showed chiral recognition ability and affinity for molecular ZPC.

Finally, Ni et al. reported the enantioselective biotransformation of the antiallergic drug betahistine intermediate (S)-(4-Chlorophenyl)-(pyridin-2-yl)methanol, (S)-CPMA,

on ABS.[74] This reactive extraction method was based on the enantioselective metabolism of some specific microorganisms. *Kluyveromyces sp. CCTCC M2011385* was isolated for the stereoselective reduction of (4-chlorophenyl)-(pyridin-2-yl)methanone (CPMK) to (S)-CPMA after testing other strains of carbonyl reductase-producing microorganisms. This polymer/salt-based ABS reached 86.7% of *e.e.*% and 92.1% of product yield, after optimization. The optimal conditions found were defined for the system composed of 20 wt% of PEG 4000 + 14 wt% of Na_2HPO_4, with 2g wet cells, 3% (w/v) of glucose, [CPMK] = 6 $g.L^{-1}$ operating under T = 30 ºC for 48 h. In this work, both processes of biotransformation and enantioseletive extraction using ABS were conjugated. Their conjugation showed some advantages, since both hydrophobic substrate and product were accumulated in the PEG-rich phase, and with this, the inhibitory effect of the product and substrate over the microbial cells (located in the salt-rich phase) was minimized.

Table 5. *Summary of the best results of e.e.% and α obtained considering the use of different ABS applied in the extraction of drugs. n.d.- not determined*

Racemate	ABS Phase Formers		Chiral Selector	Selectivity Parameters		Refs.
	1	2		*e.e.*%	*α*	
MA	PEG 2000	$(NH_4)_2SO_4$	*β*-CD	n.d.	2.46	[60]
	Triton X-114	-	Cu_2-*β*-CD	67.91	n.d.	[61]
	Ethanol	$(NH_4)_2SO_4$	Sf-*β*-CD	16.3	1.69	[62]
	Poly(MAH-*β*-CD-co-NIPAAm)	Dextran T40	Poly(MAH-*β*-CD-co-NIPAAm)	n.d.	1.27	[63]
α-CHMA	PEG 6000	$Na_3C_6H_5O_7$	Cu_2-*β*-CD	n.d.	1.36	[64]
	$[C_4mim][BF_4]$	$(NH_4)_2SO_4$	HP-*β*-CD	n.d.	1.59	[65]
PSA	PEG2000	$(NH_4)_2SO_4$	HP-*β*-CD	23.49	1.99	[66]
	Ethanol	$(NH_4)_2SO_4$	HP-*β*-CD	n.d.	1.42	[44]
	Ethanol	$(NH_4)_2SO_4$	L-IPTA + HP-*β*-CD	57.86	4.06	[67]
	Acetone	SBE-*β*-CD	SBE-*β*-CD	31.7	2.1	[68]
OFLX	PEG 2000	$(NH_4)_2SO_4$	L-TA + HP-*β*-CD	n.d.	1.32	[69]
	PEG 6000	Dextran T40	BSA	62	n.d.	[70]
FLU	Ethanol	$(NH_4)_2SO_4$	L-DOT + L-Trp	n.d.	2.34	[71]
ZPC	1-propanol	CM-*β*-CD	CM-*β*-CD	32.66	2.58	[72]
KYN	PEG 8000	Na_2HPO_4	BSA	n.d.	n.d.	[73]
(S)-CPMA	PEG 4000	Na_2HPO_4	microbial cells	86.7	n.d.	[74]

2.1.2.2.2. Amino acids

There is an industrial interest for natural amino acids in the food industry for animal feed, flavour agents and food supplements.[118] In the pharmaceutical industry, unnatural amino acids are used to produce medicines, such as the antagonist cetrorelix acetate.[119] The studied amino acids are mostly tryptophan[78–80] and phenylalanine, [75–77] in ABS containing two polymers,[78] polymer + salt,[75,79] polar organic solvents + salt,[80] and, finally chiral ILs + salt.[76,77] As summarized in Table 6, the chiral selectors used were proteins,[78,79] *β*-CD derivatives[75,80] and chiral ILs (in this last case working as chiral selector and phase former).[76,77] Chen et al.[75] proposed an ABS for the resolution of the racemic phenylalanine and established the optimal chiral separation conditions. The system selected was composed of PEG 2000 and $(NH_4)_2SO_4$ containing combined chiral selectors, namely *β*-CD and HP-*β*-CD. The biggest *α* and *e.e.%* achieved were 1.53 and 12.83% (*β*-CD:HP-*β*-CD ratio of 2:3 at pH = 5.5), respectively. The ABS showed an extractive ability, but no resolution ability in the absence of chiral selectors. Then, an improvement in *α* and *e.e.%* was observed using two selectors instead of a single one, in particular for *β*-CD:HP-*β*-CD ratio of 2:3 and increasing the total concentration of chiral selectors. At pH 5.5 (optimal pH and isoelectric point of Phe) the amino acid is present in its neutral form. HP-*β*-CD has worse recognition for the ionic Phe species, what justifies the improved enantioselectivity at this pH value.

With IL-based ABS appears a good alternative to enantioseparation of racemic Phe with polymeric ABS. Wu et al. proposed the use of newly synthesized chiral modified imizadolium-based ILs ([ChiralFunct^{1}C$_1$im][PF_6] and [ChiralFunct^{2}C$_1$im][PF_6]) and Na_2SO_4 to form ABS. The maximum *e.e.%* obtained was 53%, with the optimal system operating in the conditions: [ChiralFunct^{1}C$_1$im][PF_6]:water volume ratio of 0.66 at 20 ºC for 6 h of IL-Phe contact.[76] Nuclear magnetic resonance (NMR) and discrete Fourier transform results showed that [ChiralFunct^{1}C$_1$im][PF_6] interacts more and forms more stable complexes with D-Phe than with L-Phe. The wide applicability of this ABS was shown for other amino acids, but with lower *e.e.*% values (21 – 38%). In the end, the [ChiralFunct^{1}C$_1$im][PF_6] was recovered by a simple methodology. Dissolving the [ChiralFunct^{1}C$_1$im][PF_6] in acetonitrile, where amino acids are insoluble, the IL was regenerated and further applied keeping good enantioseletivity during at least 6 cycles. However, $[PF_6]^-$ is an hydrophobic and poorly stable anion in water. So, other ILs with

tropine as the cation, [C_nTropine], and proline, [L-Pro], as the anion have been proposed. The ABS was formed in combination with the salting out agent K_2HPO_4. Under the most appropriate conditions (13 $g.g^{-1}$ of [C_8Tropine][Pro] + 30 $g.g^{-1}$ of K_2HPO_4 + 0.51 $g.g^{-1}$ of H_2O + 0.035 $g.g^{-1}$ of $Cu(Ac)_2$ with 0.020 $g.g^{-1}$ of D,L-Phe), the *e.e.*% was 65%.[77] Larger alkyl chain lengths on the cation [$C_n$trop] facilitated the access of D-Phe into the IL-rich phase, which indicated that the [C_8trop][L-Pro] forms more stable ternary complexes with D-Phe, enhancing the *e.e.%*. This system had a particular aspect that is the formation of a third phase, in which the L-Phe was concentrated (at concentration of 0.015 to 0.020 $g.g^{-1}$ of D,L-Phe). Thus, D-Phe is concentrated in the IL-rich phase, and the insoluble interphase was enriched in the L-isomer. NMR studies confirmed that the complex between the IL and D-Phe was more stable than the complex between the IL and L-Phe. Moreover, this analysis led to the hypothesis that [C_8trop][L-Pro] interacts by the three point model, forming a triangle involving $[L\text{-}Pro]^-$, $[C_8trop]^+$ and D-Phe with Cu^{2+} as the central atom. In summary, this system uses more environmentally friendly ILs and guarantees better enantiomeric excess than all the remaining systems used for racemic Phe resolution (65% > 53%[76] > 12.83%[75]) – see Table 6 for comparison.

In 1985, Ekberg et al. developed an enantioselective ABS for separation of D,L-Trp. The system was composed of dextran T40 and PEG 8000 and BSA was the chiral selector operating in counter current chromatography. The separation factor obtained was 3.1, since L-Trp was more retained in the dextran-rich bottom phase, where BSA is present, than D-Trp.[78] A counter-current chromatography application of ABS for the separation of tryptophan enantiomers was proposed by Tong et al.[79] In this case, the system composed of 12 wt% of PEG 8000 + 9 wt% of K_2HPO_4 + 0.1 wt% of NH_3 with BSA (6 wt%) as the chiral selector was applied. The results suggested that BSA was predominantly distributed in the salt-rich phase of the ABS. However, the authors have found many problems developing this process, mainly due to the low mass transfer rate observed and consequent lower resolution of the peaks. However, a relatively high α of 2.605 was achieved. From here and the results reported on Table 6, PEG/dextran/BSA-based system[78] were defined as more efficient than PEG/salt/BSA-based ABS[79].

Chen and his collaborators[80] proposed an ABS composed of ethanol, $(NH_4)_2SO_4$ and *β*-CD as a chiral selector. Under optimized extraction conditions (15.9 wt% of $(NH_4)_2SO_4$ + 7 mL of ethanol + [*β*-CD] = 0.01 $mol.L^{-1}$ at pH = 3 and T = 20 ºC), the highest value

of α obtained was obtained (1.38). The authors defined pH 3 as a parameter favouring the enantioseparation of D,L-Trp, since at this pH this amino acid is in its neutral form, which was facilitating the formation of complexes. The enantioseparation in this ABS was based on the differential solubilities of β-CD and Trp in the two phases. Contrarily to Trp, β-CD is not very soluble in ethanol. By complex formation with β-CD, Trp starts to partition to the salt-rich phase.

Table 6. *Summary of the optimal results obtained for the enantioselective ABS applied in the extraction of amino acids. n.d.- not determined*

Racemate	**Pair of Phase Forming Agents**		**Chiral Selector**	**Selectivity Parameters**		
	1	**2**		***e.e.%***	***α***	
Phe	PEG 2000	$(NH_4)_2SO_4$	*β*-CD+HP-*β*-CD	12.83	1.53	[75]
	[ChiralFunct^{1}C$_1$im][PF_6]	Na_2SO_4	[ChiralFunct^{1}C$_1$im][PF_6]	53	n.d.	[76]
	[C_8tropine][L-Pro]	K_2HPO_4	[C_8tropine][L-Pro]	65	n.d.	[77]
Trp	PEG 8000	Dextran T40	BSA	n.d.	3.1	[78]
	PEG 8000	K_2HPO_4	BSA	n.d.	2.605	[79]
	Ethanol	$(NH_4)_2SO_4$	*β*-CD	n.d.	1.38	[80]
Tyr	[ChiralFunct^{1}C$_1$im][PF_6]	Na_2SO_4	[ChiralFunct^{1}C$_1$im][PF_6]	38	n.d.	[76]
Thr	[ChiralFunct^{1}C$_1$im][PF_6]	Na_2SO_4	[ChiralFunct^{1}C$_1$im][PF_6]	29	n.d.	[76]
Ser	[ChiralFunct^{1}C$_1$im][PF_6]	Na_2SO_4	[ChiralFunct^{1}C$_1$im][PF_6]	21	n.d.	[76]
Asp	[ChiralFunct^{1}C$_1$im][PF_6]	Na_2SO_4	[ChiralFunct^{1}C$_1$im][PF_6]	29	n.d.	[76]
Ile	[ChiralFunct^{1}C$_1$im][PF_6]	Na_2SO_4	[ChiralFunct^{1}C$_1$im][PF_6]	34	n.d.	[76]

2.2. Carbohydrates and amino acids as chiral selectors in IL-based ABS

Most commonly, pairs of polymers or of a polymer and a salt are the choices to form ABS. Nonetheless, multiple other pairs of compounds were proposed in the last decades, such as those bearing carbohydrates and amino acids.[19] Several authors have reported the use of carbohydrates[68,72,46,81–87] and amino acids[90,47,91,92] as phase forming components in ABS, as overviewed in ***section 2.1.2.1.1.*** However, very few[68,72] took advantage of carbohydrates or amino acids as chiral phase formers able to act as chiral selectors for the resolution of racemates, as highlighted in ***section 2.1.2.2.***

Given the ready availability of the two enantiomeric forms of amino acids and sugars alongside with the low price of their natural form, ABS composed of these can be considered an inexpensive chiral pool for resolution studies. Therefore, this chapter evaluates the potential of carbohydrates and amino acids as ABS simultaneously phase forming agents and chiral selectors in the resolution of MA enantiomers. The role of six carbohydrates was studied using ABS composed of $[C_4mim][CF_3SO_3]$ reported in literature. Also, two different amino acids (L-lysine and L-proline) were investigated in ABS composed of $[C_4mim][CF_3SO_3]$ and $[P_{4444}]Br$. Additionally, amino acids-based ABS were used to assess the effect of distinct ILs on the partitioning of MA enantiomers.

2.2.1. Experimental section

2.2.1.1. Chemicals/Materials

The carbohydrates used in this work were D-glucose purchased from AnalaR, D-fructose (purity > 98%) from Panreac, D-maltose (purity > 98%) and D-xylose (purity > 99%) both purchased from Sigma-Aldrich, D-sucrose (purity > 98%) from Prolabo and D-sorbitol (purity = 91.0% - 100.5%) from Fisher Bioreagents. Two amino acids were used, namely L-lysine (purity > 98%) and L-proline (purity > 99%) both acquired from Acros Organics. The ILs used were 1-butyl-3-methylimidazolium trifluoromethanesulfonate, $[C_4mim][CF_3SO_3]$ (purity > 99%), 1-butyl-3-methylimidazolium tetrafluoroborate, $[C_4mim][BF_4]$ (purity > 99%) and 1-butyl-3-methylimidazolium dicyanamide, $[C_4mim][N(CN)_2]$ (purity > 98%) supplied from Iolitec

and tetrabutylphosphonium, bromide [P_{4444}]Br (purity > 96%) from Cytec. The chemical structures of the carbohydrates, amino acids and ILs used in the preparation of the ABS are shown in Figure 13.

The enantiomers used to carry out the partition studies were (R)-(-)-mandelic acid, *R*-MA (purity = 99%), and (S)-(+)-mandelic acid, *S*-MA (purity = 99%), both supplied by Acros Organics. Their chemical structure is represented in Figure 14.

For the HPLC-DAD analysis of the enantiomers, copper (II) sulphate pentahydrate, $CuSO_4 \cdot 5H_2O$ (purity > 98%), L-Phenylalanine, L-Phe (purity > 98%), purchased from AnalaR and Sigma-Aldrich, respectively, and methanol (HPLC grade), acquired from CHEM-LAB, were used for the mobile phase. The water used for the HPLC analysis was ultra-pure water, double distilled and then treated with a Milli-Q plus 185 water purification apparatus. Syringe filters (0.45 μm) and regenerated cellulose membrane filters (0.45 μm), acquired at Specanalitica and Sartorius, respectively, were using during filtration steps.

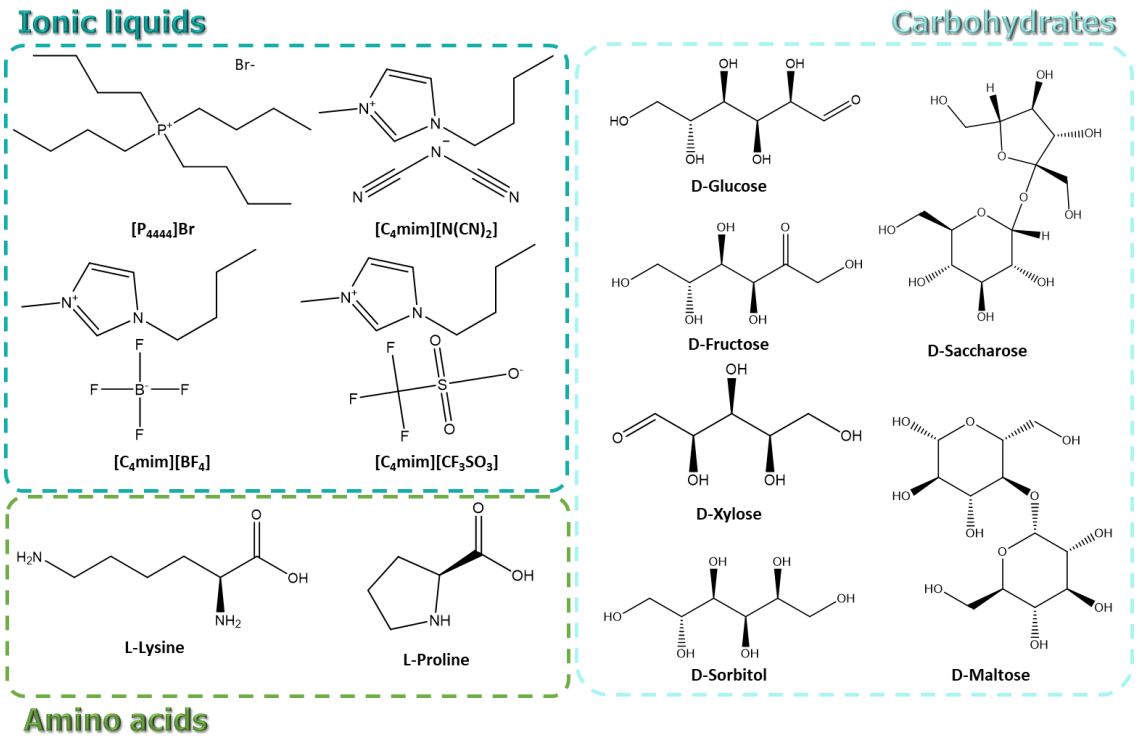

Figure 13. *Name, abbreviation and chemical structure of the ILs, amino acids and carbohydrates evaluated in this section.*

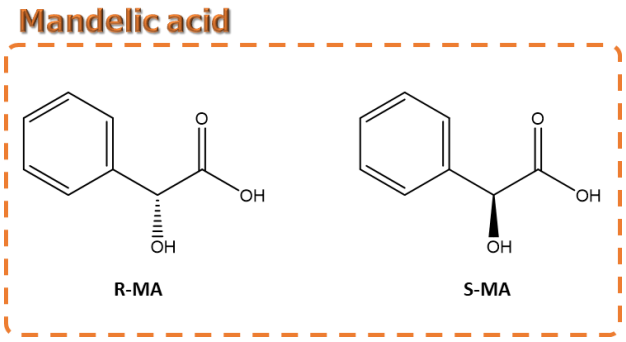

Figure 14. *Chemical structure of MA enantiomers.*

2.2.1.2. Experimental methods

2.2.1.2.1. Partition of MA enantiomers in ABS composed of IL/carbohydrates and IL/amino acids

To evaluate the partition behaviour of MA enantiomers between the coexisting phases of the ABS, mixture points were selected in the biphasic region of phase diagrams previously reported in literature.[46,47] The extraction points selected for the amino acid-based ABS are reported in Tables 7 and 8 and the appropriate amounts of each phase forming agent were added. *R*-MA and *S*-MA aqueous solutions (0.05 g.mL^{-1}) were added in equal amounts at a final mass fraction in the ABS of ca. 0.8 wt% of each enantiomer. To promote the contact between the enantiomers and the ABS chiral phase formers (amino acids or carbohydrates), racemic mixture + amino acid/carbohydrate solutions were left overnight as recommended by Wu et al.[76] The remaining phase forming components were then added and all mixtures were stirred vigorously and placed for at least 18h at 25 (±1)ºC to reach the thermodynamic equilibrium between the two phases and to ensure the mandelic acid complete partitioning. The two phases were then separated, collected to weight measurement (within an uncertainty of ±10^{-4} g), and then filtered with syringe filters for HPLC-DAD quantification.

Table 7. *Conditions studied, approximate mass fraction compositions (in percentage) and phases' identification for the carbohydrate-based partition systems investigated.*

ABS		Top phase	Bottom phase	mass fraction composition (wt%)		Ref
Carbohydrate	**IL**			**Amino acid**	**IL**	
D-Fructose	$[C_4mim][CF_3SO_3]$	CH-rich	IL-rich	25	40	[46]
D-Glucose		CH-rich	IL-rich			
D-Sorbitol		CH-rich	IL-rich			
D-Xylose		CH-rich	IL-rich			
D-Maltose		CH-rich	IL-rich			
D-Sucrose		IL-rich	CH-rich			

Table 8. *Conditions studied, approximate mass fraction compositions (in percentage) and phases' identification for the amino acid-based partition systems investigated.*

ABS		Top phase	Bottom phase	mass fraction composition (wt%)		Ref
Amino acid	**IL**			**Amino acid**	**IL**	
L-Lysine	$[C_4mim][CF_3SO_3]$	AA-rich	IL-rich	15	30	
L-Lysine	$[C_4mim][BF_4]$	AA-rich	IL-rich	15	30	[47]
L-Lysine	$[C_4mim][N(CN)_2]$	IL-rich	AA-rich	15	45	
L-Lysine	$[P_{4444}]Br$	IL-rich	AA-rich	15	45	[120]
L-Proline	$[C_4mim][CF_3SO_3]$	AA-rich	IL-rich	25	40	[47]
L-Proline	$[P_{4444}]Br$	IL-rich	AA-rich	15	60	[120]

2.2.1.2.2 Mandelic acid enantiomers quantification by HPLC-DAD

The quantification of MA enantiomers was done by HPLC-DAD using an analytical method previously developed and validated in our research group, adapted from Yue et al.[121] The liquid chromatograph HPLC Elite LaChrom (VWR Hitachi) used was composed of a diode array detector (DAD) l-2455, column oven l-2300, auto-sampler l-2200 and pump l-2130. The analytical column used was purchased from Merck and was constituted by a sorbent LiChrospher 100 RP-18 (5μm) and cartridge LiChroCART 250-4 HPLC-Cartridge, connected to a 5 μm, 4 mm × 4 mm guard column containing the same stationary phase. The mobile phase composition for the column was the following:

methanol:water (15:85) containing 2 mM of L-Phe and 1 mM of $CuSO_4$. The pH of mobile phase was adjusted to 4.00 (±0.01) by adding ammonia aqueous solution at 5 wt%. The mobile phase was then filtered under vacuum using regenerated cellulose membrane filters (0.45 μm) and degassed in an ultrasound bath. In here, the stationary phase is achiral and is the mobile phase, due to the presence of L-Phe and Cu^{2+}, which promotes the chiral separation within the chromatographic column.

The chromatographic separation was carried out under an isocratic elution with a flow-rate of 0.8 $mL.min^{-1}$. The injection volume was 20 μL and the DAD detector was set to measure at 270 nm. 22 °C and 25 °C were the temperatures at which the column oven and the autosampler operated. The HPLC-DAD quantification was based on a calibration curve (Appendix A) for each of the enantiomers determined with standard solutions of known concentration (10 – 500 $\mu g.mL^{-1}$) prepared in methanol:water (15:85) using the respective peak areas. Retention times of both enantiomers differ, with *R*-MA eluting first at 11 min followed by *S*-MA at 13 min. MA standard solutions were routinely injected to guarantee a correct quantification.

To evaluate the extraction performance, two parameters were calculated, the enantiomeric excess value (*e.e.*%) (Eq. 3,5) and the extraction efficiency (EE) defined by Eq. 4,6.

Amino acid/IL-based ABS: $e.e.\% = \frac{m_{R-MA}^{AA-rich} - m_{S-MA}^{AA-rich}}{m_{R-MA}^{AA-rich} + m_{S-MA}^{AA-rich}} \times 100$ (Eq. 3)

Amino acid/IL-based ABS: $EE_{MA,aa-rich}(\%) = \frac{m_{R/S-MA}^{AA-rich}}{m_{R/S-MA}^{0}} \times 100$ (Eq. 4)

Carbohydrate/IL-based ABS: $e.e.\% = \frac{m_{R-MA}^{CH-rich} - m_{S-MA}^{CH-rich}}{m_{R-MA}^{CH-rich} + m_{S-MA}^{CH-rich}} \times 100$ (Eq. 5)

Carbohydrate/IL-based ABS: $EE_{MA,CH-rich}(\%) = \frac{m_{R/S-MA}^{CH-rich}}{m_{R/S-MA}^{0}} \times 100$ (Eq. 6)

$m_{R/S-MA}^{AA-rich}$ is the mass of the MA enantiomer on the amino acid-rich phase, $m_{R/S-MA}^{CH-rich}$ is the mass of the MA enantiomer on the carbohydrate-rich phase and $m_{R/S-MA}^{0}$ is the initial mass of the MA enantiomer added to the system. For the IL/carbohydrate ABS used, the top phase is carbohydrate-rich and the lower phase is IL-rich, aside from

the sucrose system as reported in Freire et al.[46] work and confirmed by conductivity measurements. For the IL/amino acid ABS,[47] this condition changed depending on the system. Only the chiral selector-rich phases were considered in data interpretation.

2.2.1.2.3. Identification of the phases

Conductivities to identify the top and bottom layers as being CH/AA-rich or IL-rich were determined using a Crison GLP 31 EC meter with a conductivity cell + pt 1000. The identification of the IL-rich phase in IL/amino acid-based ABS containing imidazolium-based ILs was done by UV spectroscopy at *circa* 210 nm using a SHIMADZU UV-1700 Pharma-Spec spectrometer. Non-aromatic IL rich phases were identified by conductivity/RMN.

2.2.1.2.4. pH determination

The pH (± 0.02) of the ABS coexisting phases and the HPLD-DAD mobile phase was determined using a Metrohm 827 pH meter.

2.2.2. Results and discussion

2.2.2.1. Partition studies of MA enantiomers

A screening of chiral ABS composed of carbohydrate + IL + H_2O[46] and amino acid + IL + H_2O[47] was performed for the extraction of MA enantiomers. Only the chiral selector-enriched phases (*i.e.* carbohydrate-rich or amino acid-rich) were considered. The detailed data obtained for the enantiomeric excess and extraction efficiencies is available in Appendix B and C for carbohydrates and amino acids, respectively.

In the carbohydrate/[C_4mim][CF_3SO_3]-based ABS, with the exception of the system containing D-Maltose, MA displays a higher affinity for the IL-rich phase, the most hydrophobic phase. In general, it seems that the MA preferentially partitions to the IL-rich phase, independently of the sugar structure. The higher affinity of MA for the most hydrophobic phase could actually be explained by the higher hydrophobicity of MA suggested by its octanol-water partition coefficient of around 6.31 (log P = 0.80)[122] more than by the possibility of salting-out effects normally ruling the partition of biomolecules between aqueous phases. Actually, D-Maltose with its unexpected behaviour proves this

theory, because despite its strongest salting-out nature[46] it drives the MA to preferentially partition to the D-Maltose-rich phase. This fact underpins that the partition is possibly caused by specific interactions between the MA and the main phase formers, and deserves further study in the future. Figure 15 displays the extraction and enantiomeric separation results of the carbohydrate based-ABS evaluated. It is possible to rank their aptitude to separate *R*-MA and *S*-MA as following (based on the *e.e.%* results): D-Fructose > D-Glucose > D-Sorbitol > D-Sucrose > D-Maltose > D-Xylose. Positive values of enantiomeric excess indicate a preferential interaction with *R*-MA, while negative values indicate a favourable interaction with *S*-MA. This type of system produced a diversified scenario, although enantiomeric excess did not surpass 10% in any case. Excepting for D-Xylose, monosacharides (D-Fructose and D-glucose) seem to be more efficient for MA enantioseparation than polyols (D-Sorbitol) and disaccharides (D-Sucrose and D-Maltose). The best system was D-Fructose + $[C_4mim][CF_3SO_3]$ with an *e.e.*% of 9.3 ± 1.7% and the biggest difference between the $EE_{MA,CH\text{-}rich}$ for *R*-MA and *S*-MA (36.4 ± 0.5% vs. 29.9 ± 1.2%, respectively). This result indicates the preferential interaction of D-fructose with the *R*-MA enantiomer. However, at the pH of this system (at ca. 5.3, Appendix D), fructose is present in its neutral form and MA in its anionic form.[123] It would be worth in the future to study the effect of the pH of the medium upon the separation in order to have molecular MA and thus enhance the interactions between neutral D-fructose and *R*-MA.

In what regards the amino acid/IL-based ABS, the MA enantiomers partition patterns depend on both the amino acid and IL employed as shown in Figure 16. For the L-lysine + imidazolium based-IL systems, MA displays a higher affinity for the AA-rich phase. For the L-Proline + imidazolium based-IL the opposite trend was observed. L-Lysine is more polar than L-Proline, since it has an additional $–NH_2$ group in its side chain.[47] MA is present in its anionic[123] (Appendix E) form (which is more polar than the molecular MA)[123] at the pH of the ABS (Appendix B), being the partition dictated by the polarity of the amino acid. For the $[P_{4444}]Br$ based-ABS the partition was slightly higher for the AA-rich phase, in a similar manner, independently of the amino acid.

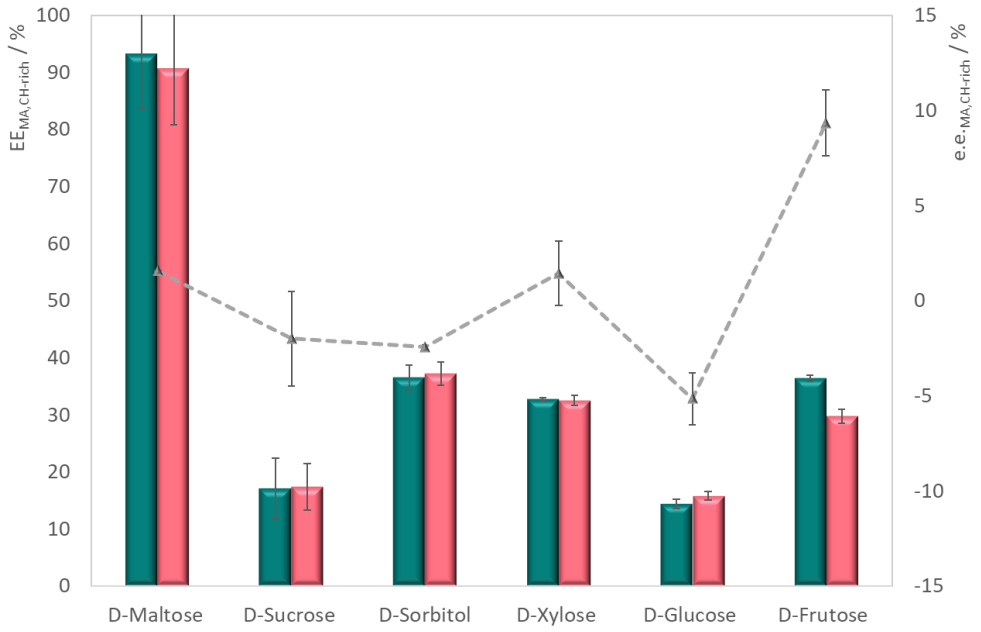

Figure 15. *Extraction efficiencies (primary scale, bars, $EE_{MA,CH\text{-}rich}$) obtained for R-MA (■) and S-MA (■) and the enantiomeric excess (secondary scale, ▲, $e.e._{MA,CH\text{-}rich}$%) reached with the studied carbohydrate/[C_4mim][CF_3SO_3]-based ABS.*

For the amino acid/IL-based ABS, the following trend for enantiomeric excess is observed: L-lysine + [C_4mim][CF_3SO_3] > L-lysine + [C_4mim][BF_4] > L-proline + [C_4mim][CF_3SO_3] > L-lysine + [C_4mim][$N(CN)_2$] > L-lysine + [P_{4444}]Br > L-proline + [P_{4444}]Br (*cf.* Figure 16 A). Imidazolium-based ILs seem to be the best pairs to both amino acids, rather than [P_{4444}]Br, for the enantioselective partition of racemic MA. In one hand, L-lysine is shown to be more efficient than L-proline for the [C_4mim][CF_3SO_3]-based ABS. On the other hand, no difference was noted in the ABS containing [P_{4444}]Br (*cf.* Figure 16AB).

Figure 16A displays the effect of the IL with fixed amino acid. For L-lysine-based systems, MA enantiomers were preferentially extracted to the amino acid-rich phase, more notoriously when [C_4mim][CF_3SO_3] was used. The L-lysine + [C_4mim][CF_3SO_3] system possesses the highest *e.e.*% (5.8 ± 1.9%) as well as the most notorious difference between $EE_{MA,aa\text{-}rich}$ for *R*-MA and *S*-MA (75.2 ± 3.3% and 66.5 ± 4.8%, respectively). This result indicates the preferential interaction of L-lysine with *R*-MA enantiomer. Within the pH of these systems (around 10.3), MA is in its ionic form (Appendix E), while lysine is either zwitterionic or anionic. Neutralizing the pH of the system should favour the interaction between the molecules since lysine would have a global positive

charge, that could lead to a better recognition of anionic MA.[123] For the L-proline-based systems, MA enantiomers display similar affinities for both phases, revealing a poor ability to separate the enantiomers.

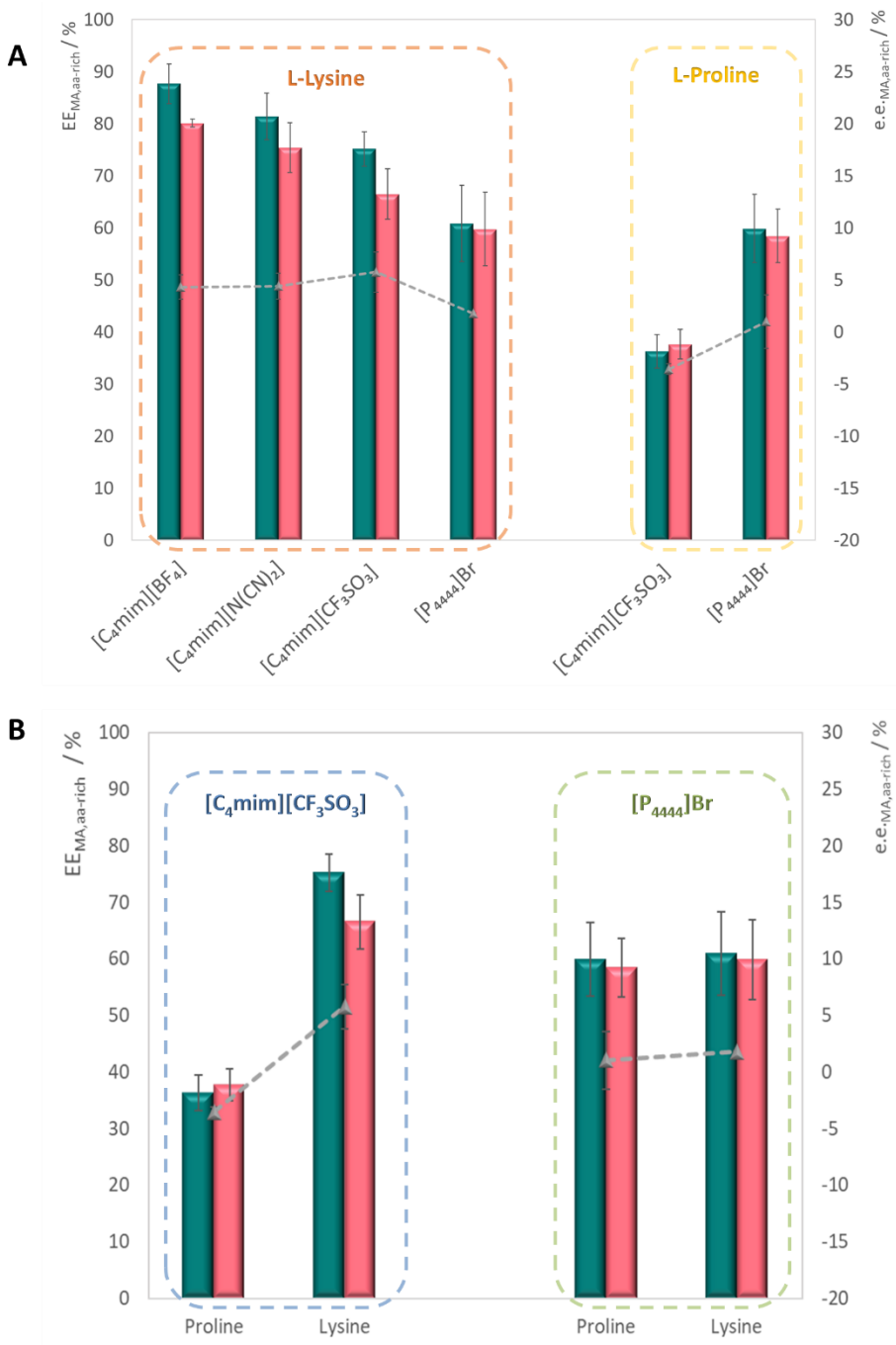

Figure 16. *Extraction efficiencies (primary scale, bars, $EE_{MA,aa\text{-}rich}$) obtained for R-MA (■) and S-MA (■) and the enantiomeric excess (secondary scale, ▲, $e.e._{MA,aa.rich}$%) reached with the studied amino acids/IL-based ABS:* ***A****, effect of the IL,* ***B****, effect of the amino acid.*

2.3. Development of cationic CIL-based ABS

Ionic liquids (ILs) are salts with low melting temperatures, by definition below 100 ºC, that are composed of organic cations and inorganic or organic anions. They present several advantages of non-volatility, non-flammability, and thermal stability.[19,100] Commonly referred to as "*designer solvents*",[101] ILs can be tailored to specific functions, thus expanding their applicability in the field of separation. By using chiral cations, anions or both, CILs can be developed to act as chiral selectors in many chiral applications,[102][102,108] such as for chiral ABS.[19]

Previously, anionic CIL-based ABS have been studied for the enantioselective resolution of MA enantiomers, with limited success (maximum *e.e.%* of 12.4 ± 2.0%).[124] MA's net charge within the pH range studied is mostly negative, being likely repelled from the chiral centres of anionic CILs. Taking this into account, the present chapter is dedicated at the development of enantioselective cationic CIL-based ABS for chiral resolution. Cationic CILs based on the quininium, proline and valinolium cations were synthesized and used in ABS simultaneously as phase forming components and chiral selectors for the resolution of MA. First, the phase diagrams of the ABS composed of distinct CILs + salts were determined and the partition of *R*-MA and *S*-MA further evaluated. The ABS developed allowed to infer on the CIL structure and role of the salt type on both phase formation and MA partition behaviour.

2.3.1. Experimental section

2.3.1.1.Chemicals/Materials

Six cationic CILs were synthesized in this work: 1-methyl quininium methylsulfate, [C_1Qui][C_1SO_4]; *N*,*N*-dimethyl-L-proline methyl ester iodide, [$C_1C_1C_1$Pro]I; *N*,*N*-dimethyl-L-proline methyl ester methylsulfate, [$C_1C_1C_1$Pro][C_1SO_4]; *N*,*N*-diethyl-L-proline ethyl ester bromide, [$C_2C_2C_2$Pro]Br; *N*,*N*,*N*-trimethyl-L-valinolium iodide, [$C_1C_1C_1$Val]I; and *N*,*N*,*N*-trimethyl-L-valinolium methylsulfate, [$C_1C_1C_1$Val][C_1SO_4]. These ILs were synthesized in our laboratory, according to well-established protocols described by Sintra et al.[125] Their chemical structures and abbreviation names are shown in Figure 17. For the synthesis of the CILs, the reagents used were quinine (purity = 98%), iodomethane (purity = 99%), dimethyl sulfate (purity

= 99%), dichloromethane anhydrous (purity = 99.8%), ethanol (purity = 99.8%), acetone (HPLC grade), potassium carbonate (purity = 99%), L-proline (purity = 99%), bromoethane (purity = 98%), acetonitrile (purity = 99.8%), chloroform (purity = 99%), L-valine (purity = 98%), sodium borohydride (purity = 99%), sulfuric acid (purity = 99.9%), methanol (purity = 99%), ethyl acetate (purity = 99.8%), potassium hydroxide (purity = 90%), formic acid (purity = 98%), formaldehyde (37 wt % in water solution) and hydrochloric acid (37 wt% in water solution) acquired from Sigma-Aldrich.

The salts used in this work were potassium phosphate tribasic, K_3PO_4, obtained from Acros Organics, di-potassium hydrogen phosphate tri-hydrated, $K_2HPO_4 \cdot 3H_2O$, purchased from Panreac and potassium carbonate, K_2CO_3 (purity > 99 wt%), acquired from Sigma-Aldrich. All the chemicals and materials used for HPLC-DAD as well as the model MA enantiomers chosen to carry out the partitioning studies are already described in ***section 2.2.2.1***.

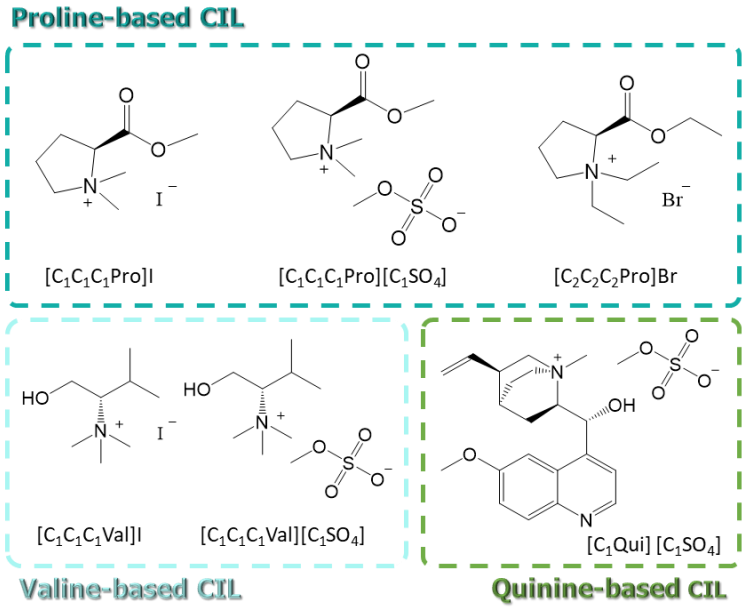

Figure 17. *Chemical structure of the CILs used in this section.*

2.3.1.2.Experimental methods

2.3.1.2.1. Synthesis of CILs

The synthesis of chiral ILs based on the quininium, proline and valinolium cations was performed as reported by Sintra et al.[125] The neutralization reaction occurred by

reacting the respective precursor with iodomethane, dimethyl sulfate or bromoethane. The characterization of the synthesized ILs is described in Appendix F.

2.3.1.2.2. Phase diagrams and TLs

The ternary phase diagrams of ABS composed of CIL + salts were determined using the cloud point titration method at 25 (±1) ºC and atmospheric pressure. The experimental procedure adopted has been validated in previous reports.[47,126] Summing up, aqueous solutions of the different salts at ≈ 35-50 (wt%) were prepared and repetitively added dropwise to the CILs aqueous solutions at ≈ 6-70 (wt%) until the detection of a cloudy solution (biphasic region). This step was followed by the addition of water until the solution turns clear (monophasic region). This procedure was repeated alternately, under constant stirring. Each mixture composition was determined by the weight quantification of all components added within an uncertainty of ± 10^{-4} g. It should be stressed that the amount of water present in hydrated salts was discounted in the calculation of the mass fraction of the salts.

The experimental binodal curves were correlated using Eq. 7, proposed by Merchuk et al.,[127]

$$[CIL] = \mathrm{A}\exp[(\mathrm{B}[\mathrm{salt}]^{0,5}) - (\mathrm{C}[\mathrm{salt}]^{3})] \qquad \text{(Eq. 7)}$$

where [CIL] and [Salt] are the CIL and salt weight fractions percentages, respectively, and A, B and C are constants obtained by the regression of the experimental binodal data.

The tie-lines (TLs) were determined through a well-established gravimetric method originally proposed by Merchuk et al.[127] and widely used by our research group in IL-based ABS. Two mixture points for each ABS, at the biphasic region, were prepared by weighing the appropriate amounts of IL + salt + water and further vigorously stirred and allowed to reach the thermodynamic equilibrium by the complete separation of phases for at least 18 h at 25 (±1) ºC. After this period, each phase was carefully separated and weighted within ±10^{-4} g. The top phase is CIL-rich and the bottom phase is salt-rich.

Each individual TL was determined by a weight balance approach through the relationship between the top weight phase composition and the overall system composition. For the determination of TLs the following system (Eq. 8 to 11) of four

equations and four unknown values ($[CIL]_{CIL}$, $[CIL]_{Salt}$, $[Salt]_{Salt}$ and $[Salt]_{CIL}$) was solved to estimate the concentration of CIL and salt in each phase), the result mandatorily meeting a set of premises (Eq. 12 to 14):[127]

$$[\mathrm{CIL}]_{\mathrm{CIL}} = \mathrm{A}\exp\left(\mathrm{B}[\mathrm{salt}]_{\mathrm{CIL}}^{0.5} - \mathrm{C}[\mathrm{salt}]_{\mathrm{CIL}}^{3}\right) \quad \text{(Eq. 8)}$$

$$[\mathrm{CIL}]_{\mathrm{salt}} = \mathrm{A}\exp\left(\mathrm{B}[\mathrm{salt}]_{\mathrm{salt}}^{0.5} - \mathrm{C}[\mathrm{salt}]_{\mathrm{salt}}^{3}\right) \quad \text{(Eq. 9)}$$

$$[\mathrm{CIL}]_{\mathrm{CIL}} = \frac{[\mathrm{CIL}]_{\mathrm{M}}}{\alpha} - \left(\frac{1-\alpha}{\alpha}\right)[\mathrm{CIL}]_{\mathrm{salt}} \quad \text{(Eq. 10)}$$

$$[\mathrm{Salt}]_{\mathrm{CIL}} = \frac{[\mathrm{salt}]_{\mathrm{M}}}{\alpha} - \left(\frac{1-\alpha}{\alpha}\right)[\mathrm{salt}]_{\mathrm{salt}} \quad \text{(Eq. 11)}$$

$$m_{CIL,M} = \frac{m_{CIL}\times[CIL]_{CIL}}{100} + \frac{m_{salt}\times[CIL]_{salt}}{100} \quad \text{(Eq.12)}$$

$$m_{salt,M} = \frac{m_{CIL}\times[salt]_{CIL}}{100} + \frac{m_{salt}\times[salt]_{salt}}{100} \quad \text{(Eq.13)}$$

$$\frac{[salt]_{salt}-[salt]_{M}}{[salt]_{M}-[salt]_{CIL}} = \frac{m_{CIL}}{m_{salt}} \quad \text{(Eq.14)}$$

where the subscripts salt and CIL designate the salt-rich and CIL-rich phases, respectively, and M is the initial mixture composition. The parameter α is the ratio between the CIL-rich phase weight and the total weight of the mixture. $m_{IL,M}$, $m_{salt,M}$ correspond to the amounts of IL and salt weighed to prepare the mixture point, whilst m_{IL} and m_{salt} are the masses of IL-rich and salt-rich phases, respectively. For the calculation of the tie-line length (TLL), which is the Euclidean distance between the CIL-rich phase and the salt-rich phase compositions, Eq. 15 was applied.[127]

$$\mathrm{TLL} = \sqrt{([\mathrm{salt}]_{\mathrm{CIL}} - [\mathrm{salt}]_{\mathrm{salt}})^2 + ([\mathrm{CIL}]_{\mathrm{CIL}} - [\mathrm{CIL}]_{\mathrm{salt}})^2} \quad \text{(Eq. 15)}$$

2.3.1.2.3. Partition studies of MA enantiomers in ABS composed of CILs/salts

To evaluate the partitionof MA enantiomers between the coexisting phases in each type of chiral ABS tested, mixture points were selected in the biphasic region of phase diagrams. The extraction points selected for the cationic CIL-K_3PO_4 ABS are reported in Table 9 and appropriate amounts of each phase forming agent were added. *R*-MA and *S*-MA aqueous solutions (0.05 $g.mL^{-1}$) were added in equal amounts at a final mass fraction in the ABS of ca. 0.8 wt% of each enantiomer. To promote the contact between the enantiomers and the CIL, these were left overnight as recommended by Wu et al.[76] The

remaining phase forming components were then added and all mixtures were stirred vigorously and placed for at least 18 h at 25 (±1)ºC to reach the thermodynamic equilibrium between the phases, and to ensure the mandelic acid complete partitioning. The two phases were then separated, collected to weight measurement (within an uncertainty o $\pm 10^{-4}$ g), and then filtered with syringe filters for HPLC-DAD quantification (***section 2.2.2.2.***).

Table 9. *Conditions studied, approximate mass fraction compositions (in percentage) and phases' identification for the CIL-based partition systems investigated.*

ABS		Top phase	Bottom phase	pH	mass fraction composition (wt%)	
CIL	**Salt**				**CIL**	**Salt**
$[C_1Qui][C_1SO_4]$	K_3PO_4	IL-rich	Salt-rich	≈ 13	2.5	18
$[C_2C_2C_2Pro]Br$		IL-rich	Salt-rich		10	35
$[C_1C_1C_1Val]I$		IL-rich	Salt-rich		10	35
$[C_1C_1C_1Pro]I$		IL-rich	Salt-rich		10	35
$[C_1C_1C_1Val]$ $[C_1SO_4]$		IL-rich	Salt-rich		10	25
$[C_2C_2C_2Pro]Br$	K_2CO_3	IL-rich	Salt-rich		20	25
$[C_2C_2C_2Pro]Br$	K_2HPO_4	IL-rich	Salt-rich	≈ 9	20	25

To evaluate the extraction performance, two parameters were calculated, the enantiomeric excess value (*e.e.* %) (Eq. 16) and the extraction efficiency (EE) defined by Eq. 17, which gives the direct comparison between the partition behaviour of the two enantiomers.

CIL/Salt-based ABS: $e.e.\% = \frac{m_{R-MA}^{CIL-rich} - m_{S-MA}^{CIL-rich}}{m_{R-MA}^{CIL-rich} + m_{S-MA}^{CIL-rich}} \times 100$ (Eq.16)

CIL/Salt-based ABS: $EE_{MA,CIL-rich}(\%) = \frac{m_{R/S-MA}^{CIL-rich}}{m_{R/S-MA}^{0}} \times 100$ (Eq. 17)

$m_{R/S-MA}^{CIL-rich}$ is the mass of the MA enantiomer on the CIL-rich phase and $m_{R/S-MA}^{0}$ the initial mass of the MA enantiomer.

2.3.2. Results and discussion

The ability of the CILs to form ABS firstly with K_3PO_4 and further on with other salts of weaker salting out power was carefully screened in order to create a versatile platform for enantiomeric resolution.

The phase diagrams determination and characterization was performed as it is essential to develop an extraction process. The phase diagrams are shown in weight fraction to allow a direct screening of the mixture compositions required to obtain a biphasic system and in molality units for a better notion of the CILs/salt structure effect on the phase diagrams behaviour with no differences coming from the distinct molecular weights of the CILs/salts. In all CIL-based ABS the biphasic region is positioned above the binodal curve and the monophasic region below. Phase diagrams with the larger biphasic areas have CILs that are more easily salted-out by the salt.

The detailed experimental data for the ternary phase diagrams and the corresponding constants (A, B and C) and standard deviations (σ) obtained considering Eq. 7 are presented in Appendix G (Tables G1-G9). The TLs, TLLs and the values for α for all the systems determined by Eq. 8-11 are presented in Table F1 in Appendix H. Moreover, a representative example of the graphical representation of a binodal curve, fitting of the experimental data by the Merchuk equation and TLs is given in Figure 18.

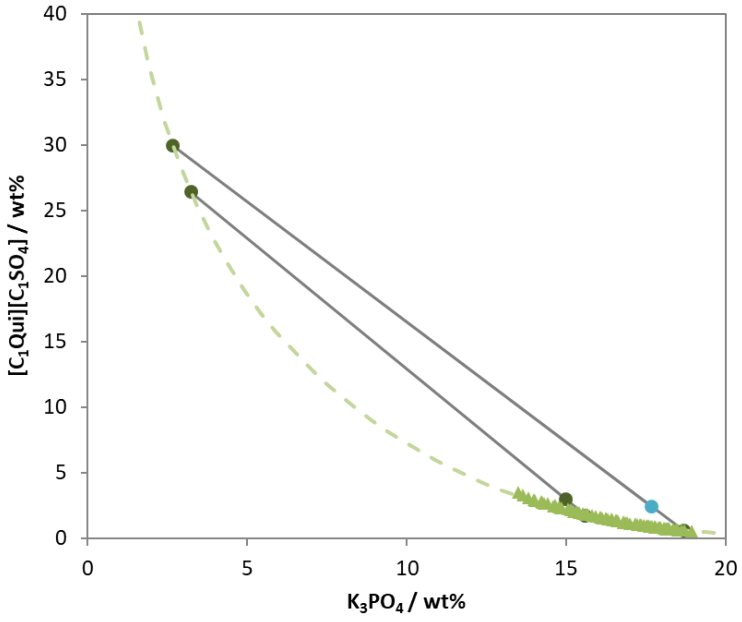

Figure 18. *Representative example of a phase diagram for the ABS composed of $[C_1Qui][C_1SO_4]$ + K_3PO_4 + H_2O at 25 (±1)°C: binodal curve data (▲), TL data (●), extraction point (●) and fitting of the experimental data by Merchuk equation (Eq.7).*

2.3.2.1.Phase diagrams and partition of MA enantiomers in CIL-based ABS: CIL structure effect

In a first approach, the ability of the CILs to induce the formation of ABS was investigated using K_3PO_4. According to Freire et al.,[19] who has thoroughly reviewed IL + salt ABS formation mechanisms, these are shown to be based on the hydrophobicity/hydrophilicity of the IL and the salting-out aptitude of the salt. K_3PO_4 is composed of a trivalent anion and is found to be a strong salting-out agent according to the Hofmeister series.[128] It contains a high charge density and a high hydration energy (ΔG_{hyd}) which results on an enhanced phase separation aptitude as it promotes the partition of the water from the IL to the salt through the creation of ion-water hydration complexes.[129] The K_3PO_4 is a good option to start studying the role of CIL structure on the ABS formation as it will induce phase separation for a wider range of CILs.

The ternary phase diagrams of the ABS composed of K_3PO_4 and CILs, namely $[C_1Qui][C_1SO_4]$, $[C_1C_1C_1Pro]I$, $[C_2C_2C_2Pro]Br$, $[C_1C_1C_1Val]I$ and $[C_1C_1C_1Val][C_1SO_4]$ are graphically represented in Figure 19. $[C_1C_1C_1Pro][C_1SO_4]$ did not form ABS in the presence of K_3PO_4 aqueous solution, being thus disregarded for any further study. The binodal curves depicted in Figure 19 allow the evaluation of the CIL structure effect on the K_3PO_4-based ABS formation.

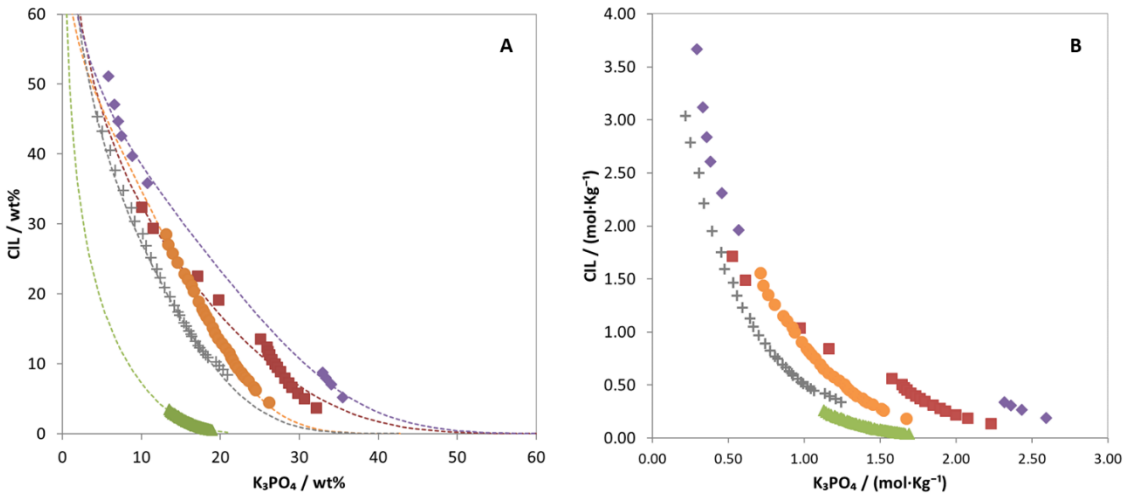

Figure 19. *Phase diagrams of the ternary systems composed of CILs+ K_3PO_4 + H_2O at 25 (±1)ºC and atmospheric pressure in weight percentage (A) and molality units (B): (●) $[C_1C_1C_1Val][C_1SO_4]$, (■) $[C_2C_2C_2Pro]Br$, (✚) $[C_1C_1C_1Val]I$, (▲) $[C_1Qui][C_1SO_4]$, (◆) $[C_1C_1C_1Pro]I$.*

The ability of CILs to create ABS follows the order: $[C_1Qui][C_1SO_4]$ > $[C_1C_1C_1Val]I$ > $[C_1C_1C_1Val][C_1SO_4]$ > $[C_2C_2C_2Pro]Br$ > $[C_1C_1C_1Pro]I$. $[C_1Qui][C_1SO_4]$ shows the greatest capacity to for ABS, since this is one of the most hydrophobic CILs considered in this set. The CILs studied allow to infer on the role of the cation in ABS formation ($[C_1Qui][C_1SO_4]$ vs. $[C_1C_1C_1Val][C_1SO_4]$ vs. $[C_1C_1C_1Pro][C_1SO_4]$). Taking into account the hydrophobicity of the core structure of each cation, it is possible to conclude that the higher the hydrophobicity, the higher the ability to phase separation. The hydrophobicity in ABS studies is often derived from the solvatochromic parameters but since they are not available for the novel ILs here studied we can alternatively express them in terms of the octanol-water partition coefficients (log K_{ow}), where compounds of log $K_{ow} > 0$ are more hydrophobic and compounds of log $K_{ow} < 0$ are more hydrophilic. According to the log K_{ow} values for their core structures, the most hydrophobic compound is $[C_1Qui][C_1SO_4]$ (log K_{ow} = 3.44 for quinine), followed by $[C_1C_1C_1Val][C_1SO_4]$ (log K_{ow} = -0.08 for valinol) and $[C_1C_1C_1Pro][C_1SO_4]$ (log K_{ow} = -0.10 for proline methyl ester).[123] A similar hydrophilicity of $[C_1C_1C_1Val][C_1SO_4]$ and $[C_1C_1C_1Pro][C_1SO_4]$ is noticed, but the later completely failed to form ABS in the presence of K_3PO_4. This may be justified by the extra degree of hydrophobicity provided by the addition of a higher number methyl groups to valinol than to proline methyl ester (3 vs. 2 methyl groups). The IL's cation hydrophobicity-hydrophilicity role in ABS formation is well-studied in literature and closely agrees to the findings of this work.[19]

The impact of the anion on the CIL-based ABS can also be studied by fixing the $[C_1C_1C_1Val]^+$ cation for the anions $[C_1SO_4]^-$ and I^-. According to literature,[130] the influence of the IL anions upon ABS formation closely correlates with their hydrogen bonding accepting ability, and thus with the anions' hydrogen-bonding basicity (β). So, anions with lower capacity to establish hydrogen bonds (lower β) are better candidates for ABS formation. Using the scale of hydrogen bond basicity of ILs proposed by Cláudio et al.,[131] the I^- is positioned below $[C_1SO_4]^-$ what is in agreement with their relative aptitude to form ABS.

Having the CIL + K_3PO_4 ABS determined and characterized, it is important to assess on the CIL structure influence on the partition of MA enantiomers. Given the distinct extensions of the phase diagrams represented in Figure 19A, different mixture points at the biphasic region were selected (2.5 wt% $[C_1Qui][C_1SO_4]$ + 18 wt% K_3PO_4,

10 wt% $[C_2C_2C_2Pro]Br$ + 35 wt% K_3PO_4, 10 wt% $[C_1C_1C_1Val]I$ + 35 wt% K_3PO_4, 10 wt% $[C_1C_1C_1Pro]I$ + 35 wt% K_3PO_4 and 10 wt% $[C_1C_1C_1Val][C_1SO_4]$ + 25 wt% K_3PO_4).

For most CIL/salt-based ABS studied, MA displays a higher affinity for the salt-rich phase (Figure 20). Given the alkaline nature of K_3PO_4[132,133] and the pKa = 3.75 of MA,[123] MA is negatively charged within the range of pH, due to the deprotonation of one of its hydroxyl groups. Although MA has low polarity (log K_{ow} = 0.90),[123] its anionic conjugate is more polar and will partition to the salt-rich phase (more hydrophilic). Also, a similar phenomenon was observed for the partition of gallic acid in several IL-based ABS. By changing the salt and its inherent pH, the authors were able to tune the partition of gallic acid to opposite phases.[132] The proline-based CILs are an exception to this behaviour, since they induce a similar partition of MA between the two phases. This phenomenon can be attributed to their higher hydrophilicity.

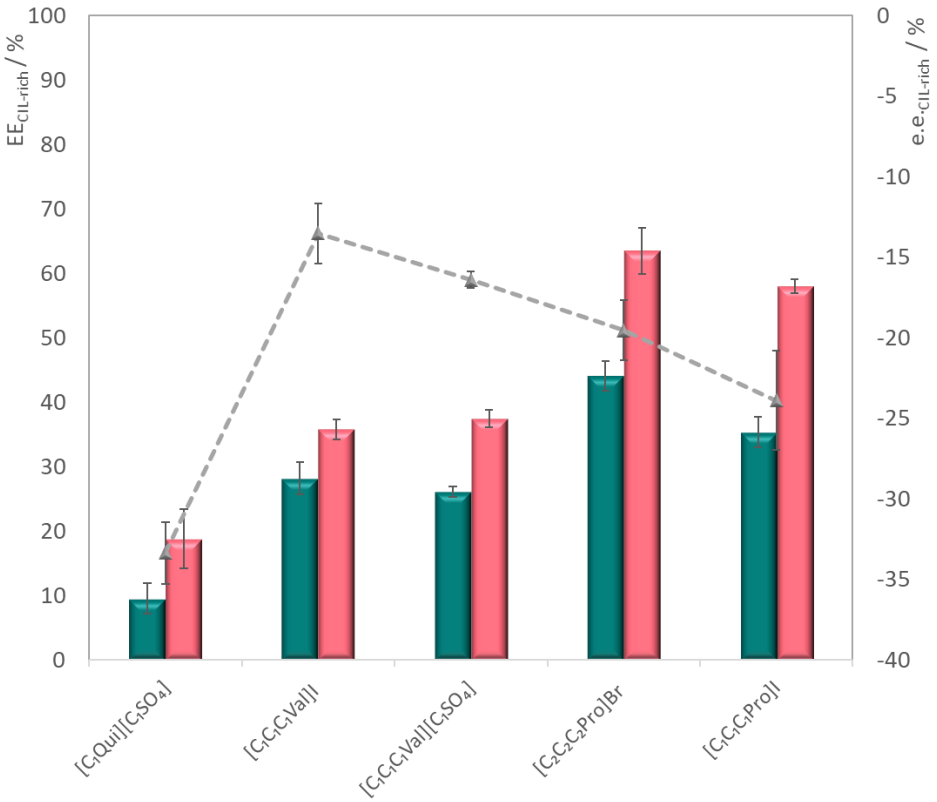

Figure 20 *Extraction efficiencies (primary scale, bars, $EE_{MA,CIL\text{-}rich}$) obtained for R-MA (■) and S-MA (■) and the enantiomeric excess (secondary scale, ▲, $e.e._{MA,CILrich}$%) reached with the studied CIL + K_3PO_4 -based ABS.*

Also, as MA is present in its anionic form, there is the possibility of some specific interactions being promoted between MA target enantiomers and CIL cations. Figure 20

displays the enantiomeric excess results of the CIL-based ABS developed. The following enantiomeric excess tendency was achieved for the CIL + K_3PO_4 systems: $[C_1Qui][C_1SO_4]$ > $[C_1C_1C_1Pro]I$ > $[C_2C_2C_2Pro]Br$ > $[C_1C_1C_1Val][C_1SO_4]$ > $[C_1C_1C_1Val]I$. $[C_1Qui][C_1SO_4]$ + K_3PO_4 presents the highest *e.e.%* of -33.4 ± 1.9%, thus revealing the greatest aptitude to separate these enantiomers. The negative value of *e.e.%* indicates the preferential interaction of $[C_1Qui][C_1SO_4]$ with the *S*-MA enantiomer. Additionally, it is demonstrated that this extraction system is of simpler nature, since the *S*-MA can form a stable complexes with the CIL than the *R*-MA without the mediation of additives (such as Cu^{2+}) as used in the work reported by Wu et al.[77] The detailed data obtained for the enantiomeric excess and extraction efficiencies is available in Appendix I.

2.3.2.2. Phase diagrams and partition studies of MA enantiomers in CIL-based ABS: salt effect

In order to understand the impact of the salt on the enantioseparation ability of CIL-based ABS, further studies were performed with salts carefully chosen from the Hofmeister series.[128] The use of weaker salting-out agents and the introduction of different ionic species in solution could be beneficial to prevent the partition of both enantiomers toward the CIL-rich phase due to the salt action rather than the CIL effect.[134] Besides K_3PO_4 (the strongest salting out agent of the Hofmeister series),[135] K_2HPO_4 and K_2CO_3 were here tested. The most efficient CIL tested so far, $[C_1Qui][C_1SO_4]$, was inapt to form ABS with K_2HPO_4 and K_2CO_3 due to its poor water solubility. Because of its enhanced ability to separate both enantiomers (*e.e.%* = -19.5 ± 1.9%), $[C_2C_2C_2Pro]Br$ was selected for this study.

The ternary phase diagrams of the systems composed of $[C_2C_2C_2Pro]Br$ and the three salts the are graphically represented in Figure 21 allowing the evaluation of the effect of the salt type on the ABS formation.

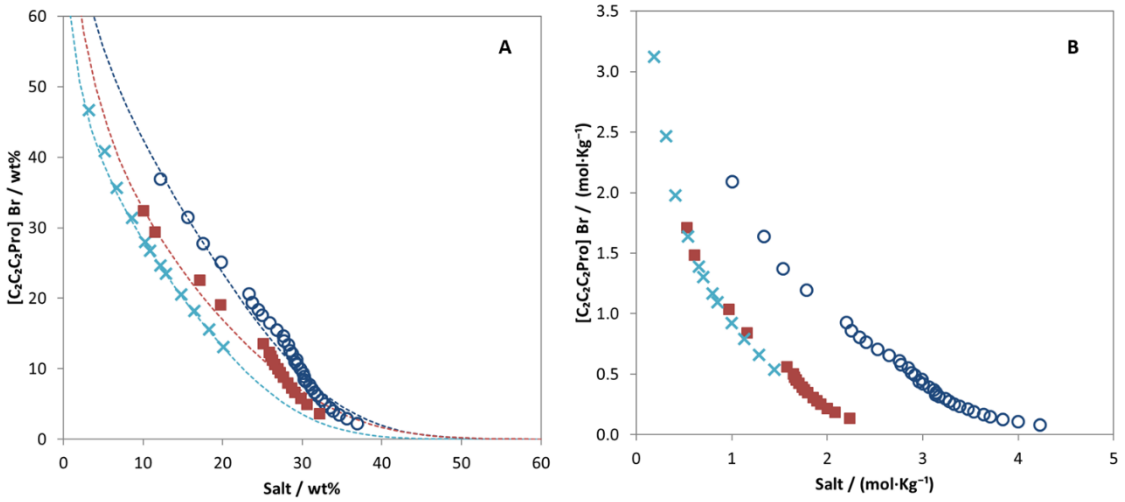

Figure 21. *Phase diagrams of the ternary systems composed of $[C_2C_2C_2Pro]Br$ + Salt + H_2O at 25 (±1)ºC and atmospheric pressure in weight percentage (A) and molality units (B): (○)K_2CO_3, (■)K_3PO_4 and (✖)K_2HPO_4.*

The ABS formation ability follows the order K_3PO_4 ≈ K_2HPO_4 > K_2CO_3. This follows the Hofmeister series and is in good agreement with other studies where the salt effect was evaluated in IL-based ABS.[128,135] The salting-out of salts to form ABS can be related to the Gibbs free energy of hydration ($\Delta_{hyd}G$) of the salt ions, as the salting-out ability seems to increase with the $\Delta_{hyd}G$. Accordingly, the results show that CO_3^{2-} ($\Delta_{hyd}G$= -1315) presents a lower energy when compared to the other anions, HPO_4^{2-} and PO_4^{3-} ($\Delta_{hyd}G$= -1789 and $\Delta_{hyd}G$= -2765, respectively).[135]

Having the biphasic regions well defined for these three CIL-based ABS, it was possible to select the mixture points to carry out the enantioseparation studies.

The equivalent partition of MA between the two phases is similar for the three salts and it is in accordance with the previous results for the screened CILs-based ABS. For the system composed of $[C_2C_2C_2Pro]Br$ + K_3PO_4 the following values were attained: *e.e.%* of -19.5 ± 1.9% and EE_{MA} for *R*-MA and *S*-MA of 44.1 ± 2.3 and 63.5 ± 3.6, respectively. This indicates the preferential interaction of $[C_2C_2C_2Pro]Br$ with the *S*-MA enantiomer. The enantiomeric separation results of the $[C_2C_2C_2Pro]Br$ + salt systems tested has the following enantiomeric excess tendency: $[C_2C_2C_2Pro]Br$ + K_3PO_4 > $[C_2C_2C_2Pro]Br$ + K_2CO_3 > $[C_2C_2C_2Pro]Br$ + K_2HPO_4. $[C_2C_2C_2Pro]Br$ + K_3PO_4 performed with the highest *e.e.%* value, yet the salts with lesser salting out ability did not favour the enantioselective partition of the MA enantiomers.

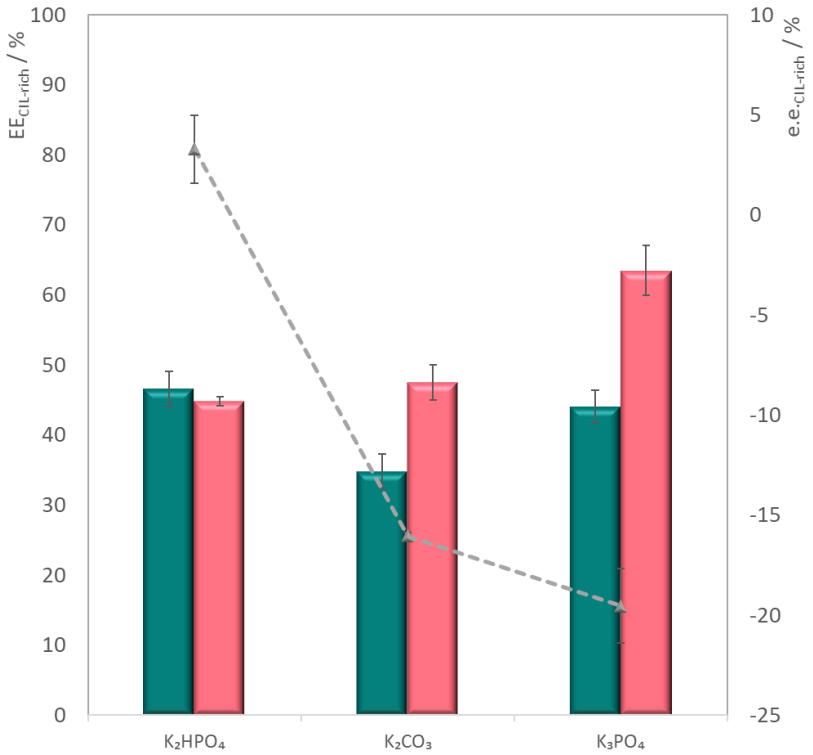

Figure 22. *Extraction efficiencies (primary scale, bars, $EE_{MA,CIL\text{-}rich}$) obtained for R-MA (■) and S-MA (■) and the enantiomeric excess (secondary scale, ▲, $e.e._{MA,CILrich}$%) reached with the studied $[C_2C_2C_2Pro]Br$ + salt -based ABS.*

2.4. Critical comparison of several chiral ABS used for MA chiral resolution

The performance of the most promising ABS studied in this thesis for each type of system is here further compared with results from other studies. The reported enantiomeric excesses/enantioselectivities are depicted in Table 10. $[C_1Qui][C_1SO_4]$ + K_3PO_4 presents an *e.e.%* of -33.4 ± 1.9%, thus revealing the greatest aptitude to separate these enantiomers achieved in this thesis. Only two other authors reported the use of the chiral selector as a phase forming component in the ABS.[63,124] The quinine-based ABS here developed provided a higher *e.e.%* when compared to both other works reported, namely by Rocha et. al[124] with the use of anionic CILs/salt and by Tan et al.[63] with the use of a chiral *β*-CD derived polymer. Still, the systems where an extra chiral selector was added performed better, in general. In those works[60–62] the chiral selectors used were *β*-CD or its derivatives and these were added as an extra fourth element to the system. This feature bring an extra degree of complexity to the system. The highest value of

selectivity was attained by Xing et al.[61], where the use of surfactants was explored as phase formers in ABS. This system, however, had to be induced by temperature to allow phase split, which implies higher energetic costs. It should be stressed, however, that no optimization other than CIL structure and salt type was conducted. In future, conditions such as pH, TLLs and racemate concentrations deserve further evaluation.

Table 10. *Comparative summary of the different ABS explored in this thesis and in the literature for the resolution of MA enantiomers. The α values reported for the systems developed in this thesis were estimated as the mass ratio of enantiomers present in the chiral phase.*

System type	ABS Phase Formers		Chiral Selector	Selectivity Parameters		Refs.
	1	2		*e.e.*%	*α*	
Chiral polymer	Poly(MAH-*β*-CD-co-NIPAAm)	Dextran T40	Poly(MAH-*β*-CD-co-NIPAAm)	n.d.	1.27	[63]
Carbohydrate	D-Fructose	$[C_4mim][CF_3SO_4]$	D-Fructose	9.33	1.21	Present thesis
	PEG 2000	$(NH_4)_2SO_4$	*β*-CD	n.d.	2.46	[60]
	Triton X-114	-	Cu_2-*β*-CD	67.91	n.d.	[61]
	Ethanol	$(NH_4)_2SO_4$	Sf-*β*-CD	16.3	1.69	[62]
Amino acid	L-Lysine	$[C_4mim][CF_3SO_4]$	L-Lysine	5.76	1.11	Present thesis
CIL	$[C_1Qui][C_1SO_4]$	K_3PO_4	$[C_1Qui][C_1SO_4]$	-33.41	1.91	Present thesis
	$[N_{4444}]_2$[L-Glu]	Na_2SO_4	$[N_{4444}]_2$[L-Glu]	12.40	1.28	

3. Separation of enantiomers using solid-liquid biphasic systems

3.1. Literature review

Recently, a solid-liquid biphasic approach for the resolution of enantiomers was proposed by Song's group.[136] This approach was aimed at resolving racemic amino acids using CILs aqueous solutions in a simpler and quicker way. Moreover, it allows the simultaneous separation and recovery of the target enantiomer, having enhanced cost-effectiveness and simplicity.

Using aqueous solutions composed of dicationic imidazolium-based CILs and cooper acetate, the authors reported L-Phe preferential precipitation. By 2D NMR and infrared spectroscopy, it was possible to attribute this phenomenon to the stronger cooperative interactions of the L-Phe with the CIL and the copper ion. In the precipitate, the maximum *e.e.%* value was of 99.2%. D-Phe remained in solution at an *e.e.%* value of 67.8%.

The same group proposed another solid-liquid system for the resolution of racemic phenylalanine, instead based on tropin-proline CILs.[137] The *e.e.%* value in the solid phase was 98%, with preferential interaction with the L-Phe. The resolution was attributed to the formation of complexes between the L-proline anion, the L-phenylalanine and the copper ion. The possibility to recycle the CIL was also successfully demonstrated. The very high resolution efficiency attained for racemic phenylalanine is patent in both works, revealing its promising status although yet poorly explored.

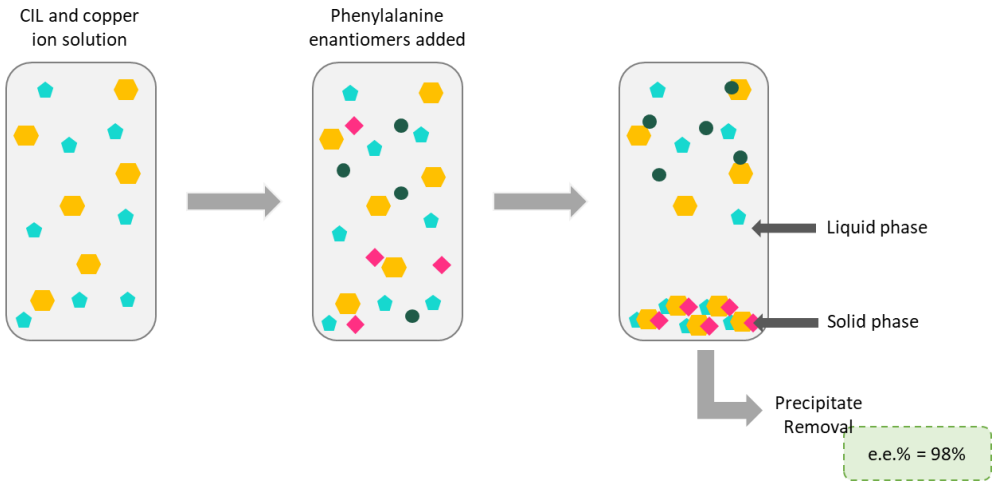

Figure 23. *Schematic representation of a chiral separation of phenylalanine enantiomers using an IL-based solid-liquid two-phase system. Copper ion( ), CIL( ), L-phenylalanine ( ), D-phenylalanine ( ). Adapted from.* [137]

3.2. Development of anionic CILs-based SLBS

Given the limited number of CILs and target racemic compounds reported in SLBS, it is of great interest to explore the ILs structural versatility and expand the type of target racemic compounds covered.

In this chapter, anionic CILs were used to develop a new SLBS. The CILs were formed by quaternary ammonium or cholinium cations paired with amino acids as anions. These CILs are of low toxicity as revealed in a study[124] and economically appealing.[138] The precipitation studies were performed using six CILs' aqueous solutions, where the impacts of the cation core, amino acid structure and chirality were investigated.

3.2.1. Experimental section

3.2.1.1.Chemicals/Materials

The anionic ILs used in this chapter were: tetrabutylammonium L-phenylalaninate, [N_{4444}][L-Phe]; tetrabutylammonium D-phenylalaninate, [N_{4444}][D-Phe]; (2-hydroxyethyl)trimethylammonium L-phenylalaninate, [Ch][L-Phe]; (2-hydroxyethyl)trimethylammonium D-phenylalaninate, [Ch][D-Phe]; (2-hydroxyethyl)trimethylammonium L-alaninate, [Ch][L-Ala]; and

di(tetrabutylammonium) L-glutamate, $[N_{4444}]_2$[L-Glu]. For the synthesis of these ILs, the reagents used were tetrabutylammonium hydroxide, $[N_{4444}]$[OH] (40 wt% in water), choline hydroxide, [Ch][OH] (45 wt% in methanol), L-phenylalanine (purity = 99.0%) and D-phenylalanine (purity > 98%), which were acquired from Sigma-Aldrich, L-glutamic acid (purity = 99%), purchased from Riedel-de-Haën, and L-alanine (purity = 99%) acquired from Acros Organics. The CILs structures are represented in Figure 24. The cationic CILs tested in this chapter were: $[C_1Qui][C_1SO_4]$, $[C_1C_1C_1Pro]I$, $[C_2C_2C_2Pro]Br$, $[C_1C_1C_1Pro][C_1SO_4]$, $[C_1C_1C_1Val]I$, $[C_1C_1C_1Val][C_1SO_4]$. The chemicals used to synthesize these ILs are detailed in ***section 2.3.1.1.***.

The solvents used were acetonitrile and methanol, both with HPLC gradient grade, supplied by Fisher Chemical and CHEM-LAB, respectively.

All the chemicals and materials for HPLC-DAD quantification, as well as the model MA enantiomers chosen to carry out the partitioning studies are already reported in ***section 2.2.2.1.***.

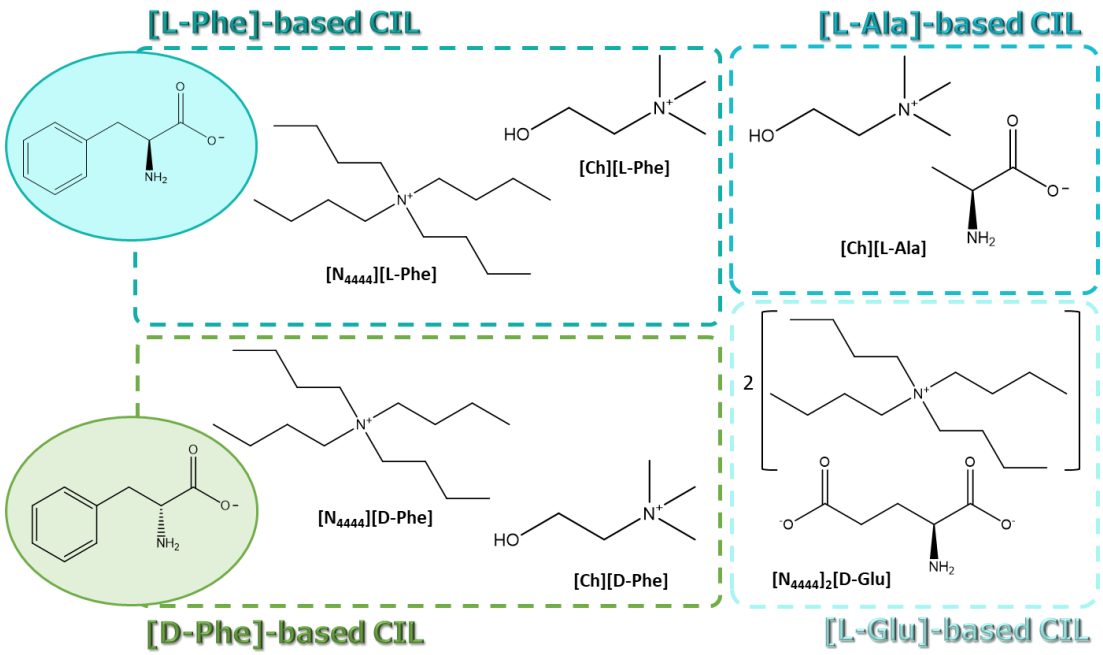

Figure 24. *Name, abbreviation and chemical structures of the CILs used in this section.*

3.2.1.2.Experimental

3.2.1.2.1. Synthesis of CILs

The synthesis of chiral ILs based on the quininium, proline and valinolium cations was performed as reported by Sintra et al. [125] The neutralization reaction occurred by reacting [Ch][OH] or [N_{4444}][OH] with the respective precursor. The characterization of the synthesized cationic ILs is described in Appendix F and of the anionic in Appendix J. For the synthesis of the cholinium-based IL with L-Alanine a similar approach was performed with the change of the amino acid being the only difference.

3.2.1.2.2. Resolution procedure

An aqueous solution of CILs was prepared and the equimolar equivalent amount of each MA enantiomer was dissolved in the solution (0.154 mol.L^{-1}). The mixture was stirred overnight at low speed (5 rpm) to promote the contact between the CILs and the MA enantiomers. After this period, for the systems where a precipitate was formed, this was separated from the liquid phase. The solid and liquid phases were analysed by HPLC-DAD as previously described (see ***section 2.2.1.2.2.***). The enantiomeric excess was calculated for both phases.

CIL-based SLBS: $e.e.\% = \frac{[R-MA]^{in\ solid\ (in\ liquid)} - [S-MA]^{in\ solid\ (in\ liquid)}}{[R-MA]^{in\ solid\ (in\ liquid)} + [S-MA]^{in\ solid\ (in\ liquid)}} \times 100$ (Eq.18)

$[R-MA]^{in\ solid\ (in\ liquid)}$ is the R-enantiomer concentration present either in the solid or in the liquid phase. $[S-MA]^{in\ solid\ (in\ liquid)}$ is the S-enantiomer concentration present either in the solid or in the liquid phase. The same process was performed and conditions maintained for the samples using L/D-phenylalanine.

3.2.1.2.3. Characterization of the precipitates by single crystal X-ray diffraction

Single crystal X-ray diffraction of the precipitates was done following the procedure described by Maximo et al.,[139] at 180 K with monochromated Mo−Kα radiation (λ = 0.71073 Å) on a Bruker SMART Apex II diffractometer (Bruker, Billerica, USA) equipped with a CCD area detector. Data reduction was carried out using a SAINT-

NT software (Bruker, Billerica, USA), and multiscan absorption corrections were applied to all raw intensity data using the SADABS program (Bruker, Billerica, USA). The structures were solved by a combination of direct methods with subsequent difference Fourier syntheses and refined by full matrix least-squares on F2 using the SHELX-97.24. The single cell unit parameters detailed in Appendix K.

3.2.2. Results and discussion

The ability of CILs to promote the enantioselective precipitation of MA enantiomers was initially screened by using cationic CILs ([C_1Qui][C_1SO_4], [$C_1C_1C_1$Pro]I, [$C_2C_2C_2$Pro]Br, [$C_1C_1C_1$Pro][C_1SO_4], [$C_1C_1C_1$Val]I, and [$C_1C_1C_1$Val][C_1SO_4]) and anionic CILs ([N_{4444}][L-Phe], [N_{4444}][D-Phe], [Ch][L-Phe], [Ch][D-Phe], [Ch][L-Ala] and [N_{4444}]$_2$[L-Glu]).

All cationic CILs failed to promote precipitation. Considering the anionic CILs, only the Phe-based ones were able to promote the enantioselective precipitation of the MA enantiomers. Taking these results into account, both phenylalanine enantiomers were also tested, individually, for their aptitude to precipitate selectively MA enantiomers. The data is presented in Table 11. The results indicate that L-Phe is more prone to precipitate *S*-MA, while *R*-MA is more easily precipitated by the D-Phe, being in accordance with the literature.[140,141] The same behaviour was noted for the phenylalanine-based ILs, independently of the cation. The IL-based systems showed higher enantioselectivities for the solid phase, when compared with the isolated amino acid systems. Additionally, the SLBS developed do not require an additive (e.g. copper anion) as previously reported in other works,[137,136] what further enhances even more the simplicity of this technology.

To better understand the interactions established between the MA enantiomers and the CILs that induced such precipitation patterns, X-Ray diffraction analysis of the solids was done. Only the CILs bearing the $[Ch]^+$ cation were able to form mono-crystals and thus, to be analysed by single crystal X-ray diffraction. Figure 25 corresponds to the results attained from the analysis of an L-Phe/*S*-MA crystal coming from the [Ch][L-Phe]-based SLBS. The X-ray structure data allowed to confirm that [L-Phe] and *S*-MA were present in the solid state. Accordingly, L-Phe favourably interacts with the *S*-MA

enantiomer, explaining the precipitation results. Following the same line of thinking, D-Phe will form more stable complexes with the *R*-MA enantiomer.

Table 11. *Enantiomeric excess values attained with the SLBS.*

ABS	**e.e. $_{solid\text{-}phase}$%**	**e.e. $_{liquid\text{-}phase}$%**
L-Phe	-35.08	30.10
D-Phe	33.57	-28.97
$[N_{4444}]$[L-Phe]	-45.60	20.08
$[N_{4444}]$[D-Phe]	48.96	-16.98
[Ch][L-Phe]	-38.78	22.66
[Ch][D-Phe]	42.79	-16.23

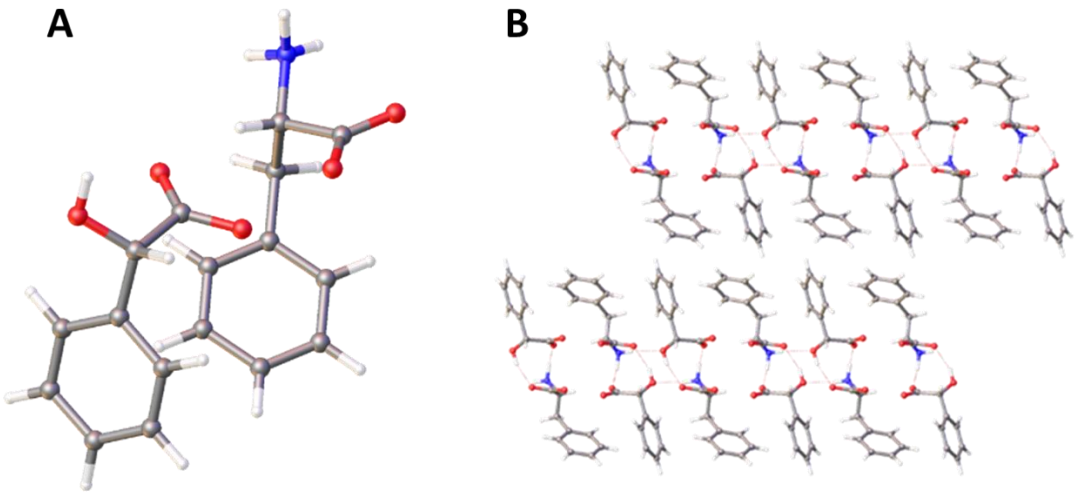

Figure 25. *The structures retrieved from the X-ray diffraction data: (a) the crystal unit, a binary complex L-Phe+S-MA; (b) the crystal structure by stacking of crystal units.*

The results attained for the complex formed are in agreement with Guo et al. and can be justified by the solubility of the complexes.[142] The solubility of [L-Phe]:[*S*-MA] is lower than that of [L-Phe]:[*R*-MA], implicitly indicating the stronger interaction between the first complex.[142] Crystallographic studies of diastereomeric crystals performed by Okamura et al.[140] indicate that a common characteristic hydrogen-bond network is formed in [L-Phe]:[*S*-MA] crystals. The binding forces for this complex are

much stronger. Each unit has hydrogen bonds with translational neighboring units, resulting in the formation of a columnar structure which is stable and favorable from the viewpoint of hydrogen bonding interaction (Figure 25B). Meanwhile, [L-Phe]:[*R*-MA], is less stable, since the hydrogen bond pattern by carboxylate and ammonium was not found. Okamura describes six kinds of hydrogen bonds but two out of them were bifurcated, thus reducing the interaction force of its hydrogen bond.[140] The lattice energy and the interaction forces of [L-Phe]:[*R*-MA] are lower than those of [L-Phe]:[*S*-MA] which results in the higher solubility.

It can be further assumed that the cation of the IL will help promote the precipitation of the complex. Based on that assumption, in aqueous solution, the $[MA]^-$ enantiomers would compete with the $[L\text{-}Phe]^-$, thus freeing this molecule to interact with [*S*-MA]. Simultaneously, the $[Ch]^+$ would interact with the [*R*-MA], coexisting in the liquid phase. Figure 26 describes the possible outcome of the interactions established.

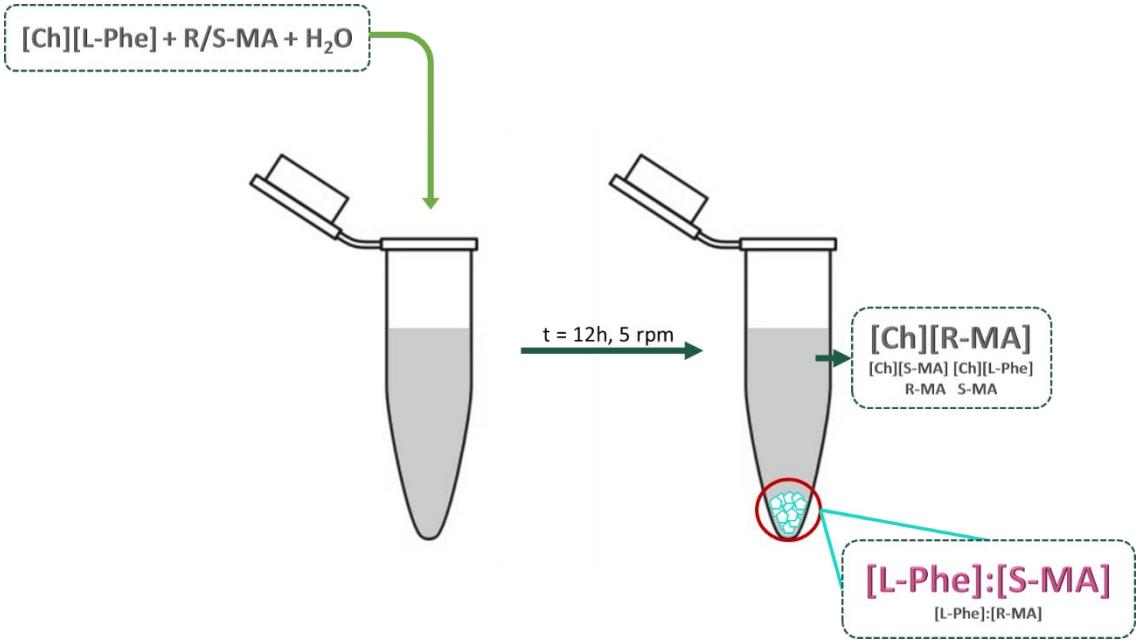

Figure 26. *Schematic representation of the SLBS technology and the possible outputs.*

Comparing the opposite capacity of [Ch][L-Phe] and [Ch][L-Ala] in creating SLBS, it is possible to infer about the amino acid structure importance. Particularly for these two amino acids, the role of the interactions established due to the presence of the aromatic rings can be asserted. L-Ala shows a similar structure to L-Phe, sharing the same chiral centre. However, the first lacks the presence of an aromatic ring. This indicates that the aromatic ring interaction favours the positioning of the chiral centres, promoting their

interaction, thus allowing enantiospecific recognition. Interaction between the positive electrostatic potential of one ring with the negative electrostatic potential of the neighbour ring should stabilise and contribute to the molecular stacking. It is then possible to infer that a similar reason is behind the inability of $[N_{4444}]_2$[L-Glu] to form a precipitate, since [L-Glu] also lacks the presence of an aromatic ring. Moreover, the higher amount of cations present, since two exist per anion, could lead to a sort of steric hindrances.

The cationic CILs did not promote the enantioselective precipitation of MA. It is possible that interactions are established between the cation and the negatively charged enantiomer in a selective manner; however, impediments on a structural level may occur. Both for the valine and proline-based CILs the lack of aromatic rings must influence the lack of stability for a macromolecular arrangement. Quinine, has a very low solubility in water, and thus could facilitate the precipitation of a complex. However, it can be assumed that the complex structure of the molecule does not promote a stable arrangement with the MA enantiomer, or that the solubility of the complex is not low enough to induce precipitation and so, no solid complex is noted.

4. Conclusions

Considering the wide range of compounds that can be used to form ABS, those of chiral nature were identified and used in this thesis to create a versatile enantioseparation platform for racemic MA (here used as model compound). Briefly, carbohydrates, amino acids and chiral ILs were used as chiral selectors and solvents in ABS. Since most of the ABS reported in literature use an additional chiral selector, these systems can be foreseen as simpler alternatives.

In a first approach, a chiral separation platform based on ABS composed of carbohydrates and amino acids with ILs was developed in order to separate MA enantiomers. However, these systems did not show great aptitude for the task proposed with maximum enantiomeric excess values of *e.e.%* 9.3 ± 1.7%.

Owing to the "*designer solvent*" status of ILs, these can be composed of chiral anions, cations or both and used for chiral separation purposes. In this ambit, ABS composed of cationic CILs and salts were studied. The phase diagrams were determined and further used to study the partition of MA enantiomers. The role of the CIL structure was the main influencer in both phase diagrams formation (with the hydrophobicity of the cation playing the major role) and enantioseparation ability. Some of these systems displayed good enantioselectivities, with the $[C_1Qui][C_1SO_4]$ + K_3PO_4 ABS presenting the best performance (*e.e.%* = -33.4 ± 1.9%).

In order to fulfil the goal of creating simple techniques for racemates resolution, CIL-based SLBS were also developed. IL-based SLBS offer an extra degree of simplicity when compared to ABS, since less chemicals are used and one of the enantiomers can be directly isolated. This technique is recent and poorly explored in literature, but it was the one attaining the highest enantiosselectivities of this thesis (*e.e.%* of 49.0% with $[N_{4444}]$[D-Phe]), without further additives. X-Ray diffraction was additionally used to attempt understanding the molecular mechanisms behind the enantioseparation. The choice of the chiral anion structure was shown to be crucial for MA chiral resolution.

5. Future work

To achieve our goal of creating a simple and highly efficient platform for the enantioseparation of chiral drugs, further optimization studies must be performed. Conditions other than the structure of the ILs, salts, amino acids and carbohydrates should be explored, namely pH, temperature, TLLs, racemate concentration, and racemate structure. Given the lack of understanding of the interactions behind the enantioseparation in ABS, molecular-level studies should also be conducted. NMR can be a useful technique as revealed in other studies of the same type.[77,136] Meanwhile, liquid-liquid chromatographic techniques, namely the use of centrifugal partition chromatography (CPC), should be investigated aiming at to develop the continuous purification of the racemates by the utilization of several equilibrium units.

After reaching more significant *e.e.%* values, further purification steps should be carried. The enantiomers can be isolated from the ABS phases, for instance, by crystallization induced by antisolvents, pH or temperature. With the isolation of the enantiomers achieved, the ultimate step of this approach - the recycling and reuse of the phases - should be exploited. By guaranteeing a high recovery yield of the phases, there is an increase in the cost-effectiveness and sustainability of this technology. For the SLBS, operational conditions like temperature, pH, enantiomers' concentration, should also be optimized aiming at increasing the enantiomeric excess as much as possible. Again, and following the same line of thinking for ABS, the recycling and reuse of the liquid phase should be considered.

6. References

1. Lin GQ, Zhang JG, Cheng JF. Overview of Chirality and Chiral Drugs. Chiral Drugs: Chemistry and Biological Action. Hoboken, NJ, USA: John Wiley & Sons, Inc.; 2011. 3-28 .

2. Núñez MC, García-Rubiño ME, Conejo-García A, Cruz-López O, Kimatrai M, Gallo M a, et al. Homochiral drugs: a demanding tendency of the pharmaceutical industry. Curr Med Chem. 2009;16(16):2064–74.

3. Nguyen LA, He H, Pham-Huy C. Chiral drugs: an overview. Int J Biomed Sci. 2006;2(2):85–100.

4. Piutti A. Sur une nouvelle espèce d'asparagine. Cristallogr Chim. 1886;103:134.

5. Miller MT, Strömland K. The study of malformations "by the company they keep". Trans Am Ophthalmol Soc. 1992;90:247–63.

6. Chhabra N, Aseri ML, Padmanabhan D. A review of drug isomerism and its significance. Int J Appl basic Med Res. 2013;3(1):16–8.

7. Islam MR, Mahdi JG, Bowen ID. Pharmacological Importance of Stereochemical Resolution of Enantiomeric Drugs. Drug Saf. 1997;17(3):149–65.

8. U.S. Food and Drug Administration. Guidances (Drugs) - Development of New Stereoisomeric Drugs. Center for Drug Evaluation and Research. 2014.

9. European Medicines Agency Veterinary Medicines and Inspections. Guideline on test procedures and acceptance criteria for new veterinary drug substances and new medicinal product: chemical substances. 2005.1–20.

10. The Nobel Prize in Chemistry. 2001.

11. Schuur B, Verkuijl BJ V, Minnaard AJ, de Vries JG, Heeres HJ, Feringa BL. Chiral separation by enantioselective liquid-liquid extraction. Org Biomol Chem. 2011;9(1):36–51.

12. Lorenz H, Seidel-Morgenstern A. Processes to separate enantiomers. Angew Chemie - Int Ed. 2014;53(5):1218–50.

13. Subramanian G, editor. Chiral Separation Techniques: A Practical Approach. 3rd ed. Weinheim, Germany: Wiley-VCH Verlag GmbH & Co. KGaA; 2006.

14. Köllges T, Vetter T. Model-Based Analysis of Continuous Crystallization/Reaction Processes Separating Conglomerate Forming Enantiomers. Cryst Growth Des. 2017;17:233–47.

15. Wang Y, Chen A. Crystallization-based separation of enantiomers. Stereoselective Synthesis of Drugs and Natural Products. 1st ed. JohnWiley & Sons, Inc; 2013. 1663–82.

16. Snyder LR, Kirkland JJ, Dolan JW. Introduction to Moderns Liquid Chromatography. 3rd ed. John Wiley & Sons, Inc.; 2010.

17. Wang T, Yang H, Qiu R, Huang S. Synthesis of novel chiral imidazolium stationary phases and their enantioseparation evaluation by high-performance liquid chromatography. Anal Chim Acta. 2016;944:70–7.

18. Francotte E, Lindner W, editors. Chirality in Drug Research. Combinatorial Chemistry. Weinheim, FRG: Wiley-VCH Verlag GmbH & Co. KGaA; 2006.

19. Freire MG, Cláudio AFM, Araújo JMM, Coutinho J a. P, Marrucho IM, Lopes JNC, et al. Aqueous biphasic systems: a boost brought about by using ionic liquids. Chem Soc Rev. 2012;41(14):4966.

20. Kowacz M, Groves P, Esperança JMSS, Rebelo LPN. On the use of ionic liquids to tune crystallization. Cryst Growth Des. 2011;11(3):684–91.

21. Judge RA, Takahashi S, Longenecker KL, Fry EH, Abad-Zapatero C, Chiu ML. The Effect of Ionic Liquids on Protein Crystallization and X-ray Diffraction Resolution. Cryst Growth Des. 2009;9(8):3463–9.

22. Swatloski RP, Spear SK, Holbrey JD, Rogers RD. Dissolution of cellose with ionic liquids. J Am Chem Soc. 2002;124(18):4974–5.

23. Weber CC, Kunov-Kruse a J, Rogers RD, Myerson a S. Manipulation of ionic liquid anion-solute-antisolvent interactions for the purification of acetaminophen. Chem Commun (Camb). 2015;51(20):4294–7.

24. Ventura SPM, e Silva FA, Quental M V., Mondal D, Freire MG, Coutinho JAP. Ionic-Liquid-Mediated Extraction and Separation Processes for Bioactive Compounds: Past, Present, and Future Trends. Chem Rev. 2017;117(10):6984–7052.

25. Tang K, Yi J, Huang K, Zhang G. Biphasic Recognition Chiral Extraction: A Novel Method for Separation of Mandelic Acid Enantiomers. Chirality. 2009;21:390–395.

26. Yu RJ, Van Scott EJ. Alpha-hydroxyacids and carboxylic acids. J Cosmet Dermatol. 2004;3(2):76–87.

27. Mills J, Schmiegel KK, Shaw WN. Phenethanolamines, compositions containing the same, and method for effecting weight control. US Patent 4391826 A, 1979.

28. Galan A, Andreu D, Echavarren AM, Prados P, De MJ. A receptor for the enantioselective recognition of phenylalanine and tryptophan under neutral conditions. J Am Chem Soc. 1992;114(8):1511–2.

29. Steensma M, Kuipers NJM, de Haan AB, Kwant G. Influence of process parameters on extraction equilibria for the chiral separation of amines and amino-alcohols with a chiral crown ether. J Chem Technol Biotechnol. 2006;81(4):588–97.

30. Tsukube H, Yonemitsub O. Enantioselective binding and extraction of zwitterionic amino acids by chiral lanthanide complexes. Chem Commun. 1996;(4):477–8.

31. Konishi K, Yabara K, Toshishige H, Aida T, Inoue S, Soc PJC, et al. A Novel Anion-Binding Chiral Receptor Based on a Metalloporphyrin with Molecular Asymmetry . Highly Enantioselective Recognition of Amino Acid Derivatives. J Am Chem Soc. 1994;116(4):1337–44.

32. Reeve TB, Cros JP, Gennari C, Piarulli U, De Vries JG. A practical approach to the resolution of racemic N-benzyl α-amino acids by liquid-liquid extraction with a lipophilic chiral salen-cobalt(III) complex. Angew Chemie - Int Ed. 2006;45(15):2449–53.

33. Tang K, Wang Y, Zhang P, Huang Y, Dai G. Process optimization of continuous liquid-liquid extraction in centrifugal contactor separators for separation of oxybutynin enantiomers. Sep Purif Technol. 2015;150:170–8.

34. Tang K, Zhang P, Pan C, Li H. Equilibrium Studies on Enantioselective Extraction of Oxybutynin Enantiomers by Hydrophilic b-Cyclodextrin Derivatives. AIChE J. 2011;57(11):3027–36.

35. Ren Z, Zeng Y, Hua Y, Cheng Y, Guo Z. Enantioselective liquid-liquid extraction of racemic ibuprofen by L-tartaric acid derivatives. J Chem Eng Data. 2014;59(8):2517–22.

36. Jiao FP, Chen XQ, Hu WG, Ning FR, Huang KL. Enantioselective extraction of mandelic acid enantiomers by L-dipentyl tartrate and β-cyclodextrin as binary chiral selectors. Chem Pap. 2007;61(4):326–8.

37. Liu J-J, Liu C, Tang K-W, Zhang P-L. Biphasic recognition chiral extraction — novel way of separating pantoprazole enantiomers. Chem Pap. 2014;68(5):599–607.

38. Jiao FP, Chen XQ, Yang L, Hu YH. Enantioselective extraction of mandelic acid enantiomers using ester alcohol l-tartarate as chiral selector. Lat Am Appl Res. 2008;38(3):249–52.

39. Tang K, Song L, Liu Y, Pan Y, Jiang X. Separation of flurbiprofen enantiomers by biphasic recognition chiral extraction. Chem Eng J. 2010;158(3):411–7.

40. Davankov VA. The nature of chiral recognition: Is it a three-point interaction? Chirality. 1997;9(2):99–102.

41. Martínez-Aragón M, Burghoff S, Goetheer ELV, de Haan AB. Guidelines for solvent selection for carrier mediated extraction of proteins. Sep Purif Technol. 2009. 65(1):65–72.

42. Anastas PT, Warner JC. Green Chemistry: Theory and Practice. Oxford University Press. 1998.

43. Albertsson P-Å. Partition of cell particles and macromolecules. Arch Biochem Biophys. 1963;100(2):341–2.

44. Wang J, Chen X, Jiao F. Enantioseparation of phenylsuccinic acid enantiomers based on aqueous two-phase system with ethanol/ammonium sulfate: Phase diagrams optimization and partitioning experiments. J Incl Phenom Macrocycl Chem. 2015;81(3–4):475–84.

45. Reis IAO, Santos SB, Pereira FDS, Sobral CRS, Freire MG, Freitas LS, et al. Extraction and Recovery of Rutin from Acerola Waste using Alcohol-Salt-Based Aqueous Two-Phase Systems. Sep Sci Technol. 2014;49(5):656–63.

46. Freire MG, Louros CLS, Rebelo LPN, Coutinho JAP. Aqueous biphasic systems composed of a water-stable ionic liquid + carbohydrates and their applications. Green Chem. 2011;13(6):1536.

47. Domínguez-Pérez M, Tomé LIN, Freire MG, Marrucho IM, Cabeza O, Coutinho JAP. (Extraction of biomolecules using) aqueous biphasic systems formed by ionic liquids and aminoacids. Sep Purif Technol. 2010;72(1):85–91.

48. Aguilar O, Albiter V, Serrano-Carreón L, Rito-Palomares M. Direct comparison between ion-exchange chromatography and aqueous two-phase processes for the partial purification of penicillin acylase produced by E. coli. J Chromatogr B Anal Technol Biomed Life Sci. 2006;835(1–2):77–83.

49. Rosa PAJ, Azevedo AM, Sommerfeld S, Bäcker W, Aires-Barros MR. Aqueous two-phase extraction as a platform in the biomanufacturing industry: Economical and environmental sustainability. Biotechnol Adv. 2011;29(6):559–67.

50. Freire MG, Neves CMSS, Marrucho IM, Canongia Lopes JN, Rebelo LPN, Coutinho J a. P. High-performance extraction of alkaloids using aqueous two-phase systems with ionic liquids. Green Chem. 2010;12(10):1715.

51. Cláudio AFM, Ferreira AM, Freire CSR, Silvestre AJD, Freire MG, Coutinho JAP. Optimization of the gallic acid extraction using ionic-liquid-based aqueous two-phase systems. Sep Purif Technol. 2012;97:142–9.

52. Shang QK, Li W, Jia Q, Li DQ. Partitioning behavior of amino acids in aqueous two-phase systems containing polyethylene glycol and phosphate buffer. Fluid Phase Equilib. 2004;219(2):195–203.

53. Asenjo JA, Andrews BA. Aqueous two-phase systems for protein separation: A perspective. J Chromatogr A. 2011;1218(49):8826–35.

54. Ventura SPM, de Barros RLF, de Pinho Barbosa JM, Soares CMF, Lima ÁS, Coutinho JAP, et al. Production and purification of an extracellular lipolytic enzyme using ionic liquid-based aqueous two-phase systems. Green Chem. 2012;14(3):734.

55. Ferreira AM, Faustino VFM, Mondal D, Coutinho JAP, Freire MG. Improving the extraction and purification of immunoglobulin G by the use of ionic liquids as adjuvants in aqueous biphasic systems. J Biotechnol. 2016;236:166–75.

56. Silva MFF, Fernandes-Platzgummer A, Aires-Barros MR, Azevedo AM.

Integrated purification of monoclonal antibodies directly from cell culture medium with aqueous two-phase systems. Sep Purif Technol. 2014;132:330–5.

57. Luechau F, Ling TC, Lyddiatt A. Primary capture of high molecular weight nucleic acids using aqueous two-phase systems. Sep Purif Technol. 2009;66(1):202–7.

58. Zawadzki M, e Silva FA, Domańska U, Coutinho JAP, Ventura SPM, Kümmerer K, et al. Recovery of an antidepressant from pharmaceutical wastes using ionic liquid-based aqueous biphasic systems. Green Chem. 2016;18(12):3527–36.

59. Silva FA, Sintra T, Ventura SPM, Coutinho JAP. Recovery of paracetamol from pharmaceutical wastes. Sep Purif Technol. 2014;122:315–22.

60. Tan L, Long Y, Jiao F, Che XQ. Enantioselective Extraction of Mandelic Acid Enantiomers by Aqueous Two-Phase Systems of Polyethylene Glycol and Ammonium Sulfate Containing β -Cyclodextrin as Chiral Selector. Iran Chem Soc. 2011;8(4):889–96.

61. Xing J min, Li F fang. Chiral separation of mandelic acid by temperature-induced aqueous two-phase system. J Chem Technol Biotechnol. 2012;87(3):346–50.

62. Li F-F, Tan Z-J, Guo Z-F. Enantioseparation of mandelic acid and α-cyclohexylmandelic acid using an alcohol/salt-based aqueous two-phase system. Chem Pap. 2014;68(11):1539–45.

63. Tan Z, Li F, Zhao C, Teng Y, Liu Y. Chiral separation of mandelic acid enantiomers using an aqueous two-phase system based on a thermo-sensitive polymer and dextran. Sep Purif Technol. 2017;172:382–7.

64. Li LH, Li FF. Chiral separation of α-cyclohexyl-mandelic-acid by aqueous two phase system combined with Cu2-β-cyclodextrin complex. Chem Eng J. 2012;211–212:240–5.

65. Chen L-L, Li F-F, Tan Z-J. Chiral separation of α-cyclohexylmandelic acid enantiomers using ionic liquid/salt aqueous two-phase system. Chem Pap. 2015;69(11):1465–1472.

66. Zhuang J, Yang W, Chen X, Jiao F. Enantioseparation of phenylsuccinic acid enantiomers using aqueous two-phase flotation and their determination by HPLC and UV detection. Chromatographia. 2014;77(9–10):679–85.

67. Chen X, Wang J, Jiao F. Efficient enantioseparation of phenylsuccinic acid enantiomers by aqueous two-phase system-based biphasic recognition chiral extraction : Phase behaviors and distribution experiments. Process Biochem. 2015;50:1468–78.

68. Wang J, Liu Q, Rong L, Yang H, Jiao F, Chen X. Enantioselective extraction of phenylsuccinic acid in aqueous two-phase systems based on acetone and β -cyclodextrin derivative : Modeling and optimization through response surface methodology. J Chromatogr A. 2016;1467:490–6.

69. Jiao F, Wang J, Jiang X, Yang H, Shi S, Chen X, et al. Biphasic recognition

enantioseparation of ofloxacin enantiomers by an aqueous two-phase system. J Chem Technol Biotechnol. 2015;90(12):2234–9.

70. Arai T, Kuroda H. Distribution behavior of some drug enantiomers in an aqueous two-phase system using counter-current extraction with protein. Chromatographia. 1991;32(1–2):56–60.

71. Chen Z, Zhang W, Wang L, Fan H, Wan Q, Wu X. Enantioseparation of Racemic Flurbiprofen by Aqueous Two-Phase Extraction With Binary Chiral Selectors of L-dioctyl Tartrate and L-tryptophan. Chirality. 2015;27:650–7.

72. Wang J, Yang H, Yu J, Chen X, Jiao F. Macrocyclic β-cyclodextrin derivative-based aqueous-two phase systems: Phase behaviors and applications in enantioseparation. Chem Eng Sci. 2016;143:1–11.

73. Shinomiya K, Kabasawa Y, Ito Y. Enantiomeric Separation of Commercial D , L-Kynurenine with an Aqueous Two-Phase Solvent System by Cross-Axis Coil Planet Centrifuge. J Liq Chromatogr Relat Technol. 1998;21(1–2):135–41.

74. Ni Y, Zhou J, Sun Z. Production of a key chiral intermediate of Betahistine with a newly isolated Kluyveromyces sp. in an aqueous two-phase system. Process Biochem. 2012;47:1042–8.

75. Chen X, Liu L, Jiao F, Wang Z. Extraction of Phenylalanine Enantiomers by Aqueous Two Phase Systems Containing Combinatorial Chiral Selector. Chinese J Chem. 2012;30(4):965–9.

76. Wu D, Zhou Y, Cai P, Shen S, Pan Y. Specific cooperative effect for the enantiomeric separation of amino acids using aqueous two-phase systems with task-specific ionic liquids. J Chromatogr A. 2015;1395:65–72.

77. Wu H, Yao S, Qian G, Yao T, Song H. A resolution approach of racemic phenylalanine with aqueous two-phase systems of chiral tropine ionic liquids. J Chromatogr A. 2015;1418:150–7.

78. Ekberg B. Direct chiral resolution in an aqueous two-phase counter-current distribution principle. J Chromatogr. 1985;333:211–4.

79. Tong S, Ito Y, Ma Y. Enantioseparation of DL-tryptophan by spiral tube assembly counter-current chromatography and evaluation of mass transfer rate for enantiomers. J Chromatogr A. 2014;1374:77–84.

80. Chen X, Dong Q, Yu J, Jiao F. Extraction of Tryptophan enantiomers by aqueous two-phase systems of ethanol and $(NH_4)_2SO_4$. J Chem Technol Biotechnol. 2012;88(8):1545–50.

81. Sadeghi R, Ebrahimi N, Tehrani MD. Investigation of carbohydrates as non-charged, non-toxic and renewable soluting-out agent for polymer based aqueous biphasic systems implementation. Polym (United Kingdom). 2016;98:365–77.

82. Sousa KM, Maciel GELO, Buarque FS, Santos AJ, Marques MN, Cavalcanti EB, et al. Novel phase diagrams of aqueous two-phase systems based on

tetrahydrofuran + carbohydrates + water: Equilibrium data and partitioning experiments. Fluid Phase Equilibria. 2017. 1-9.

83. De Brito Cardoso G, Mourão T, Pereira FM, Freire MG, Fricks AT, Soares CMF, et al. Aqueous two-phase systems based on acetonitrile and carbohydrates and their application to the extraction of vanillin. Sep Purif Technol. 2013;104:106–13.

84. De Brito Cardoso G, Souza IN, Mourão T, Freire MG, Soares CMF, Lima ÁS. Novel aqueous two-phase systems composed of acetonitrile and polyols: Phase diagrams and extractive performance. Sep Purif Technol. 2014;124:54–60.

85. Sousa KM, Merlo LHZ, Marques MN, Cavalcanti EB, Souza RL, Soares CMF, et al. Partitioning of diuron in a novel aqueous two-phase system based on polyols and tetrahydrofuran. Fluid Phase Equilib. 2016;429:325–30.

86. Wu B, Zhang YM, Wang HP. Phase behavior for ternary systems composed of ionic liquid plus saccharides plus water. J Phys Chem B. 2008;112(20):6426–9.

87. Ferreira AM, Esteves PDO, Boal-Palheiros I, Pereiro AB, Rebelo LPN, Freire MG. Enhanced tunability afforded by aqueous biphasic systems formed by fluorinated ionic liquids and carbohydrates. Green Chem. 2016;18(4):1070–9.

88. Freire MG, Neves CMSS, Marrucho IM, Coutinho AP. Hydrolysis of Tetrafluoroborate and Hexafluorophosphate Counter Ions in Imidazolium-Based Ionic Liquids. 2010;2:3744–9.

89. Bhushan R, Dixit S. Amino acids as chiral selectors in enantioresolution by liquid chromatography. Biomed Chromatogr. 2012;26(8):962–71.

90. Sadeghi R, Hamidi B, Ebrahimi N. Investigation of Amino Acid − Polymer Aqueous Biphasic Systems. J Phys Chem B 2014,. 2014;118:10285−10296.

91. Chakraborty A, Sen K. L -proline based aqueous biphasic system: Design and application to isolate the alkaline earths. J Chem Eng Data. 2014;59(4):1288–94.

92. Zhang J, Zhang Y, Chen Y, Zhang S. Mutual Coexistence Curve Measurement of Aqueous Biphasic Systems Composed of [bmim][BF_4] and Glycine, l -Serine, and l -Proline, Respectively. J Chem Eng Data. 2007;52(6):2488–90.

93. Chakraborty A, Sen K. Comparison of Salt Cations in the Design of Nonionic Surfactant Based Aqueous Biphasic Systems: Application in Polyphenol Separations. J Chem Eng Data. 2016;61(11):3710–3717.

94. Álvarez MS, Rivas M, Deive FJ, Sanrom MA. Ionic liquids and non-ionic surfactants: a new marriage for aqueous segregation. RSC Adv. 2014;4:32698–700.

95. Lu X, Cao Q, Yu J, Lei Q, Xie H, Fang W. Formation of Novel Aqueous Two-Phase Systems with Piperazinium- Based Ionic Liquids and Anionic Surfactants : Phase Behavior and Microstructure. J Phys Chem B. 2015;119(35):11798–11806.

96. Dalton DD, Taylor DR, Waters DG. Synthesis and Use of a Novel Chiral

Surfactant Based on (R,R) -Tartaric Acid and Its Application to Chiral Separations in Micellar Electrokinetic Capillary Chromatography (MECC). 1995;7:513–20.

97. Danino D, Mancini G, Sabadini E. Generation of a Chiral Giant Micelle. Langmuir. 2016;32(33):8461–8466.

98. Davidson TA, Mondal K, Yang X. Use of a chiral surfactant for enantioselective reduction of a ketone. J Colloid Interface Sci. 2004;276:498–502.

99. Lee C, O'Rear EA, Harwell JH, Sheffield JA. Synthesis and Characterization of a Simple Chiral Surfactant, Sodium S-(-)-fl-Citronellyl Sulfate. J Colloid Interface Sci. 1990;137(1):296–9.

100. Rogers RD, Seddon KR. Chemistry. Ionic liquids--solvents of the future? Science. 2003;302(5646):792–3.

101. Freemantle M. Designer Solvents: Ionic liquids may boost clean technology development. Chem Eng News. 1998;76(13):32–7.

102. Baudequin C, Baudoux J, Levillain J, Cahard D, Gaumont AC, Plaquevent JC. Ionic liquids and chirality: Opportunities and challenges. Tetrahedron Asymmetry. 2003;14(20):3081–93.

103. Bwambok DK, Marwani HM, Fernand VE, Fakayode SO, Lowry M, Negulescu I, et al. Synthesis and Characterization of Novel Chiral Ionic Liquids and Investigation of their Enantiomeric Recognition Properties. Natl Inst Heal. 2009;20(2):151–8.

104. Singh A, Chopra HK. New benzimidazolium-based chiral ionic liquids: Synthesis and application in enantioselective sodium borohydride reductions in water. Tetrahedron Asymmetry. 2016;27(11–12):448–53.

105. Vasiloiu M, Cervenka I, Gaertner P, Weil M, Schröder C, Bica K. Amino alcohol-derived chiral ionic liquids: structural investigations toward chiral recognition. Tetrahedron Asymmetry. 2015;26(18–19):1069–82.

106. Heckel T, Winkel A, Wilhelm R. Chiral ionic liquids based on nicotine for the chiral recognition of carboxylic acids. Tetrahedron Asymmetry. 2013;24(18):1127–33.

107. Kumar V, Pei C, Olsen CE, Schäffer SJC, Parmar VS, Malhotra S V. Novel carbohydrate-based chiral ammonium ionic liquids derived from isomannide. Tetrahedron Asymmetry. 2008;19(6):664–71.

108. Ding J, Armstrong DW. Chiral ionic liquids: Synthesis and applications. Chirality. 2005;17(5):281–92.

109. Wang R, Chang Y, Tan Z, Li F. Phase behavior of aqueous biphasic systems composed of novel choline amino acid ionic liquids and salts. J Mol Liq. 2016;222:836–44.

110. Song CP, Ramanan RN, Vijayaraghavan R, Douglas RM, Chan E-S, Ooi C-W.

Green, Aqueous Two-Phase Systems Based on Cholinium Aminoate Ionic Liquids with Tunable Hydrophobicity and Charge Density. ACS Sustain Chem Eng. 2015;3:3291−3298.

111. Mondal D, Sharma M, Quental M V, Tavares APM. Suitability of bio-based ionic liquids for the extraction and puri fi cation of IgG antibodies †. Royal Society of Chemistry; 2016;6071–81.

112. Bi P yu, Dong H ru, Dong J. The recent progress of solvent sublation. J Chromatogr A. 2010;1217(16):2716–25.

113. Tang K, Yi J, Liu Y, Jiang X, Pan Y. Enantioselective separation of R,S-phenylsuccinic acid by biphasic recognition chiral extraction. Chem Eng Sci. 2009;64(18):4081–8.

114. Hayakawa I, Atarashi S, Yokohama S, Imamura M, Sakano K, Furukawa M. Synthesis and antibacterial activities of optically active ofloxacin. Antimicrob Agents Chemother. 1986;29(1):163–4.

115. Fu Y, Yang J, Zhang J, Li W. Bio-inspired enantioseparation for chiral compounds. Chinese J Chem Eng. 2016;24(1):31–8.

116. Richy F, Rabenda V, Mawet A, Reginster JY. Flurbiprofen in the symptomatic management of rheumatoid arthritis: A valuable alternative. Int J Clin Pract. 2007;61(8):1396–406.

117. Collins AN, Sheldrake GN, Crosby J. Chirality in industry II developments in the commercial manufacture and applications of optically active compounds. J. Wiley; 1997. 418 p.

118. Leuchtenberger W, Huthmacher K, Drauz K. Biotechnological production of amino acids and derivatives: Current status and prospects. Appl Microbiol Biotechnol. 2005;69(1):1–8.

119. Bommarius AS, Schwarm M, Drauz K. Biocatalysis to amino acid-based chiral pharmaceuticals - Examples and perspectives. J Mol Catal - B Enzym. 1998;5(1–4):1–11.

120. Capela E V., Quental M V., Domingues P, Coutinho JAP, Freire MG. Effective separation of aromatic and aliphatic amino acid mixtures using ionic-liquid-based aqueous biphasic systems. Green Chem. 2017;19(8):1850–4.

121. Yue Y, Jiang X-Y, Yu J-G, Tang K-W. Enantioseparation of mandelic acid enantiomers in ionic liquid aqueous two-phase extraction systems. Chem Pap. 2013;68(4):465–71.

122. Cheméo - Chemical & Physical Properties by Cheméo. 2017. https://www.chemeo.com/

123. ChemSpider | Search and share chemistry. 2017. https://www.chemspider.com/.

124. Rocha SN. Synthesis and characterization of chiral ionic liquids and their

application in the development of aqueous biphasic systems. University of Aveiro; 2016.

125. Sintra TE. Synthesis of more benign ionic liquids for specific applications. 2017.

126. Passos H, Ferreira AR, Cláudio AFM, Coutinho JAP, Freire MG. Characterization of aqueous biphasic systems composed of ionic liquids and a citrate-based biodegradable salt. Biochem Eng J. 2012;67:68–76.

127. Merchuk JC, Andrews BA, Asenjo JA. Aqueous two-phase systems for protein separation. J Chromatogr B Biomed Sci Appl. 1998;711(1–2):285–93.

128. Hofmeister F. Zur Lehre von der Wirkung der Salze : zweite Mittheilung. Arch für Pathol Anat und Physiol und für Klin Med. 1888;25(4–5):247–60.

129. Kurnia KA, Freire MG, Coutinho JAP. Effect of polyvalent ions in the formation of ionic-liquid-based aqueous biphasic systems. J Phys Chem B. 2014;118(1):297–308.

130. Ventura SPM, Neves CMSS, Freire MG, Marrucho IM, Oliveira J, Coutinho JAP. Evaluation of anion influence on the formation and extraction capacity of ionic-liquid-based aqueous biphasic systems. J Phys Chem B. 2009;113(27):9304–10.

131. Cláudio AFM, Swift L, Hallett JP, Welton T, Coutinho JAP, Freire MG. Extended scale for the hydrogen-bond basicity of ionic liquids. Phys Chem Chem Phys. 2014;16(14):6593.

132. Cláudio AFM, Ferreira AM, Freire CSR, Silvestre AJD, Freire MG, Coutinho JAP. Optimization of the gallic acid extraction using ionic-liquid-based aqueous two-phase systems. Sep Purif Technol. 2012;97:142–9.

133. Mourão T, Cláudio AFM, Boal-Palheiros I, Freire MG, Coutinho JAP. Evaluation of the impact of phosphate salts on the formation of ionic-liquid-based aqueous biphasic systems. J Chem Thermodyn. 2012;54:398–405.

134. Louros CLS, Cláudio AFM, Neves CMSS, Freire MG, Marrucho IM, Pauly J, et al. Extraction of Biomolecules Using Phosphonium-Based Ionic Liquids + K_3PO_4 Aqueous Biphasic Systems. Int J Mol Sci. 2010;11(4):1777–91.

135. Shahriari S, Neves CMSS, Freire MG, Coutinho JAP. Role of the Hofmeister series in the formation of ionic-liquid-based aqueous biphasic systems. J Phys Chem B. 2012;116(24):7252–8.

136. Huang X, Wu H, Wang Z, Luo Y, Song H. High resolution of racemic phenylalanine with dication imidazolium-based chiral ionic liquids in a solid-liquid two-phase system. J Chromatogr A. 2017;1479:48–54.

137. Zhixia Wang, Zhenbo Hou, Shun Yao, Min Lin, Hang Song. A new and recyclable system based on tropin ionic liquids for resolution of several racemic amino acids. Anal Chim Acta. 2017;960:81–9.

138. Passos H, Freire MG, Coutinho JAP. Ionic liquid solutions as extractive solvents

for value-added compounds from biomass. Green Chem. 2014;16(12):4786–815.

139. Maximo GJ, Santos RJBN, Brandão P, Esperança JMSS, Costa MC, Meirelles AJA, et al. Generating ionic liquids from ionic solids: An investigation of the melting behavior of binary mixtures of ionic liquids. Cryst Growth Des. 2014;14(9):4270–7.

140. Okamura K, Hiramatsu H, Nishimura N. Instrumental Achievements Crystal Structures of Diastereomeric 1 : 1 Complexes of (R) - and (S) -Phenylalanine (S) - Mandelic Acid. Analytical Sciences. 1997;13(2):315-317.

141. Pham X-H, Kim J-M, Chang S-M, Kim I, Kim W-S. Enantioseparation of D/L-mandelic acid with L-phenylalanine in diastereomeric crystallization. J Mol Catal B Enzym. 2009;60(1–2):87–92.

142. Guo HS, Kim JM, Pham XH, Chang SM, Kim WS. Predicting the enantioseparation efficiency of chiral mandelic acid in diastereomeric crystallization using a quartz crystal microbalance. Cryst Growth Des. 2011;11(1):53–8.

Appendix

A. Calibration curves for mandelic acid enantiomers

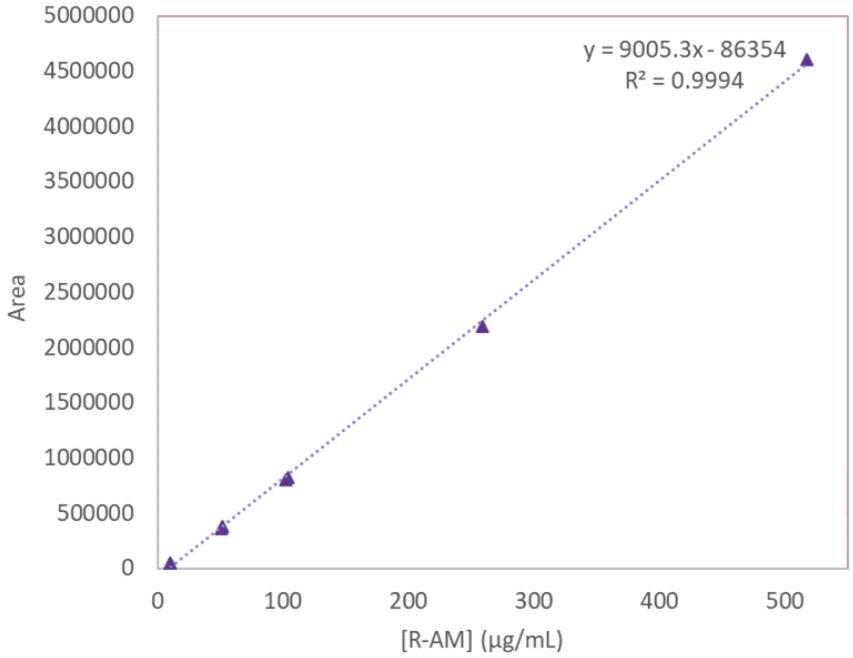

Figure A1. *Calibration curve of R-MA.*

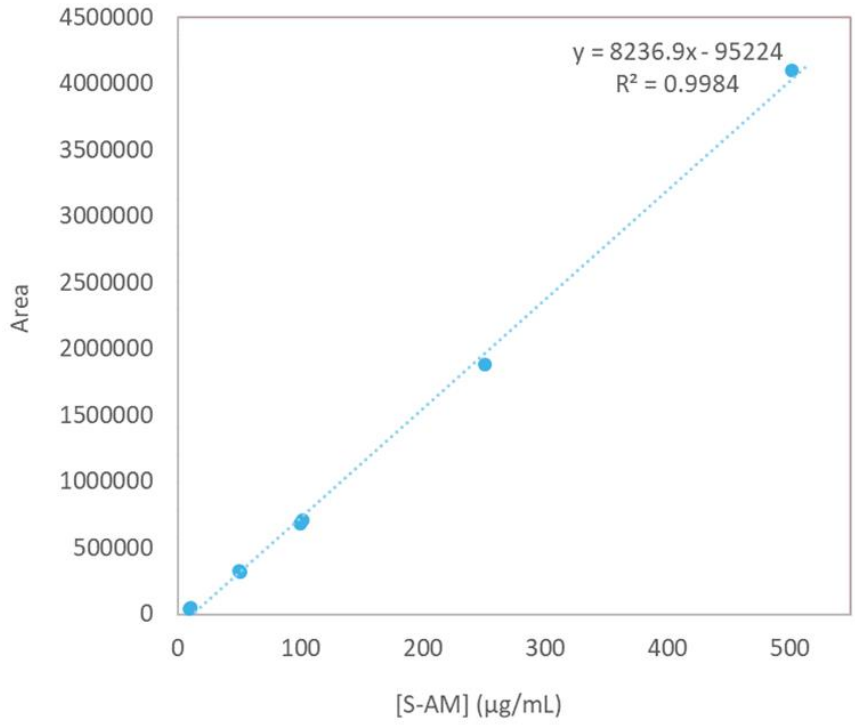

Figure A2. *Calibration curve of S-MA.*

B. Partitioning studies of mandelic acid enantiomers for carbohydrate ABS

Figure B1. *Average of the experimental weight fraction compositions (wt%), enantiomeric excess (e.e. %), extraction efficiencies of the enantiomers ($EE_{R\text{-}MA}$ and $EE_{S\text{-}MA}$) and respective standard deviations (σ) for the carbohydrate-based partition systems investigated.*

ABS	**100 × Mass fraction composition / (wt%)**		***e.e.%***	**$EE_{R\text{-}MA}$ / (%)**	**$EE_{S\text{-}MA}$ / (%)**
	$[QS]_M$	$[IL]_M$			
Carbohydrates + [C₄mim][CF₃SO₃] + water					
D-Maltose	25.79	39.09	1.6 ± 0.0	93.1 ± 9.5	90.5 ± 9.7
D-Sucrose	24.94	39.96	-2.0 ± 2.5	17.1 ± 5.3	17.3 ± 4.1
D-Sorbitol	24.73	39.81	-2.4 ± 0.1	36.5 ± 2.2	37.2 ± 2.1
D-Xylose	24.87	39.89	1.4 ± 1.7	32.7 ± 0.3	32.5 ± 0.9
D-Glucose	24.80	39.86	-5.2 ± 1.4	14.4 ± 0.8	15.8 ± 0.7
D-Fructose	24.85	39.73	9.3 ± 1.7	36.4 ± 0.5	29.7 ± 1.2

C. Partitioning studies of mandelic acid enantiomers for aminoacid-based ABS

Table D1. *Average of the experimental weight fraction compositions (wt%), enantiomeric excess (e.e. %), extraction efficiencies of the enantiomers ($EE_{R\text{-}MA}$ and $EE_{S\text{-}MA}$) and respective standard deviations (σ) for the amino acid-based partition systems investigated.*

ABS	100 × Mass fraction composition / (wt%)		*e.e.%*	$EE_{R\text{-}MA}$ / (%)	$EE_{S\text{-}MA}$ / (%)
	$[QS]_M$	$[IL]_M$			
Amino acids + IL+ water					
L-Lysine + [C4mim][CF3SO3]	16.66	29.86	5.8 ± 1.9	75.1 ± 3.3	66.5 ± 4.8
L-Lysine + [C4mim][BF4]	16.79	29.91	4.3 ± 1.2	87.7 ± 3.8	80.2 ± 0.8
L-Lysine + [C4mim][N(CN)2]	16.05	46.52	4.4 ± 1.3	81.4 ± 4.4	75.4 ± 4.8
L-Lysine + [P4444]Br	16.79	44.53	1.8 ± 0.1	60.9 ± 7.3	59.8 ± 7.1
L-Proline + [C4mim][CF3SO3]	16.94	58.75	-3.6 ± 0.5	36.3 ± 3.2	37.7 ± 2.9
L-Proline + [P4444]Br	24.83	40.31	1.0 ± 2.6	59.9 ± 6.6	58.5 ± 5.2

D. Characterization of the phases

Table C1. *pH values of the IL/carbohydrate-based ABS phases.*

ABS	$pH_{IL\text{-}rich\ phase}$	$pH_{carbohydrate\text{-}rich\ Phase}$
D-Frutose + $[C_4mim][CF_3SO_3]$	5.31	5.27
D-Glucose + $[C_4mim][CF_3SO_3]$	5.24	5.33
D-Sorbitol + $[C_4mim][CF_3SO_3]$	5.31	5.40
D-Xylose + $[C_4mim][CF_3SO_3]$	5.14	5.15
D-Maltose + $[C_4mim][CF_3SO_3]$	5.15	5.29
D-Sucrose + $[C_4mim][CF_3SO_3]$	5.50	5.39

Table C2. *pH values of the IL/amino acid-based ABS phases.*

ABS	$pH_{IL\text{-}rich\ phase}$	$pH_{amino\ acid\text{-}rich\ phase}$
L-Lysine + $[C_4mim][CF_3SO_3]$	10.36	10.32
L-Lysine + $[C_4mim][BF_4]$	10.33	9.87
L-Lysine + $[P_{4444}]Br$	10.28	10.75
L-Lysine + $[C_4mim][N(CN)_2]$	10.60	10.67
L-Proline + $[C_4mim][CF_3SO_3]$	6.29	6.45
L-Proline + $[P_{4444}]Br$	4.57	4.53

E. Representation of the madelic acid's chemical structures present in solution at distinct pH values

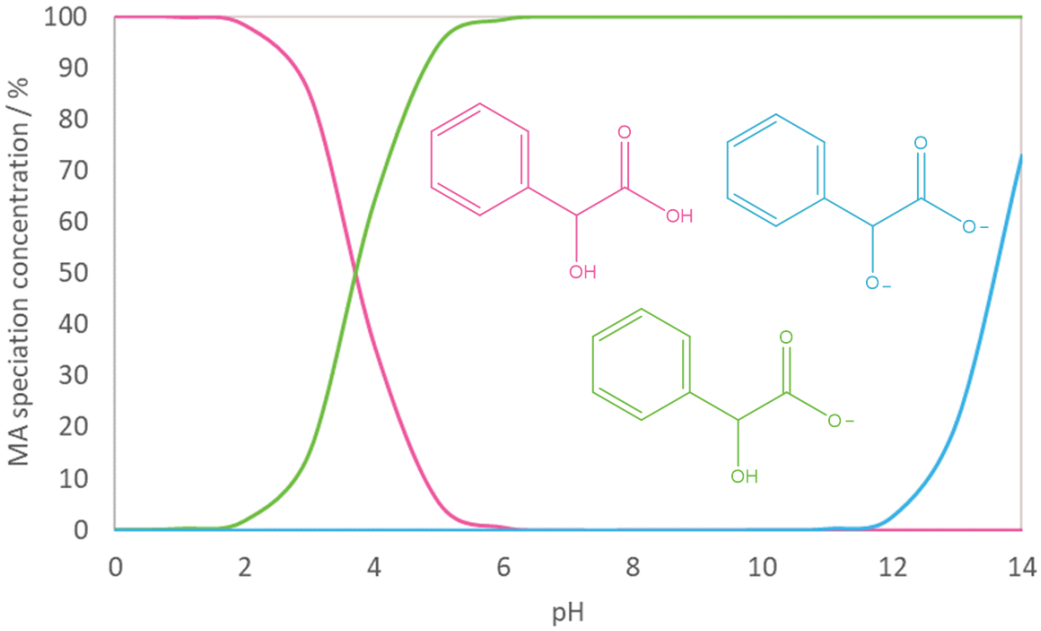

Figure E1: Mandelic acid speciation at distinct pH values. This information was adapted from the Chemspider database (www.chemspider.com).[123]

F. Characterization of chiral cationic ILs

Three cation precursors were considered to prepare the six CILs: ***i)*** quinine, ***ii)*** L-proline and ***iii)*** L-valine. The chemical structures and acronym of all CILs synthesized are depicted in Figure 17. The structure of all compounds synthesized was confirmed by ^{1}H and ^{13}C NMR spectroscopy, showing a high purity level of the ionic structures after their synthesis.

i) Quinine-based CILs

- ***1-Methyl quininium methylsulfate,*** **[C_1Qui][C_1SO_4]**

[C_1Qui][C_1SO_4] was obtained as a white solid (66% yield). ^{1}H NMR (d_6-DMSO, 300 MHz, [ppm]): δ 8.75 (d, 1H, J_{HH} = 4.5 Hz, CNC<u>H</u>CH), 7.95 (d, 1H, J_{HH} = 9.2 Hz, OCCHC<u>H</u>), 7.66 (d, 1H, J_{HH} = 4.5 Hz, CNCHC<u>H</u>), 7.43 (dd, 1H, J_{HH} = 9.2 Hz and J_{HH} = 2.5 Hz, OCC<u>H</u>CH), 7.16 (d, 1H, J_{HH} = 2.5 Hz, OCC<u>H</u>C), 6.51 (d, 1H, J_{HH} = 3.3 Hz, NCHC<u>H</u>OH), 6.18 (s, br, 1H, O<u>H</u>), 5.81 – 5.59 (m, 1H, CHC<u>H</u>CHH), 5.08 (d, 1H, J_{HH} = 17.3 Hz, CHCHC<u>H</u>H), 4.97 (d, 1H, J_{HH} = 10.5 Hz, CHCHCH<u>H</u>), 4.07 (s, br, 4H, NC<u>H</u>CHOH and OC<u>H</u>$_3$), 3.71 – 3.52 (m, 3H, NC<u>H</u>$_2$CH and NCH<u>H</u>CH$_2$), 3.39 (s, br, 4H, NCHC<u>H</u>H and C<u>H</u>$_3SO_4$), 3.32(s, 3H, NCH$_3$), 2.82 – 2.70 (m, 1H, C<u>H</u>CHCHH), 2.17 – 2.03 (m, 2H, NC<u>H</u>HCH$_2$ and NCH$_2$CH$_2$C<u>H</u>), 2.03 – 1.96 (m, 1H, NCH$_2$C<u>H</u>H), 1.94 – 1.81 (m, 1H, , NCHCH<u>H</u>), 1.37 – 1.23 (m, 1H, NCH$_2$CH<u>H</u>). ^{13}C NMR (d_6-DMSO, 75 MHz, [ppm]): δ 157.90 (CHOCH$_3$), 148.01, 144.42, 144.15, 138.56, 131.99, 125.66, 122.14, 120.47, 117.06, 102.05, 67.30, 64.40, 64.35, 56.02 (O<u>C</u>H$_3$), 54.69, 53.33 (<u>C</u>H$_3SO_4$), 49.25 (N<u>C</u>H$_3$), 38.11, 26.42, 25.13, 19.83.

ii) L-Proline-based CILs

- ***N,N-Dimethyl-L-proline methyl ester iodide,*** **[$C_1C_1C_1$Pro]I**

[$C_1C_1C_1$Pro]I was obtained as a white solid (15% yield). ^{1}H NMR (d_6-DMSO, 300 MHz, [ppm]): δ 4.62 (t, 1H, J_{HH} = 10.0 Hz, C<u>H</u>COOCH$_3$), 3.74 (s, br, 4H, CHCOOC<u>H</u>$_3$ and C<u>H</u>HN(CH$_3$)$_2$), 3.64 – 3.54 (m, 1H, CH<u>H</u>N(CH$_3$)$_2$), 3.26 (s, 3H, N(C<u>H</u>$_3$)(CH$_3$)), 3.02 (s,

3H, N(CH_3)($C\underline{H}_3$)), 2.43 – 2.24 (m, 2H, $C\underline{H}_2CHCOOCH_3$), 2.10 – 2.00 (m, 2H, $C\underline{H}_2CH_2CHCOOCH_3$). ^{13}C NMR ($d_6$-DMSO, 75 MHz, [ppm]): δ 166.71 ($\underline{C}OOCH_3$), 73.10 ($\underline{C}HCOOCH_3$), 67.51 ($\underline{C}H_2N(CH_3)_2$), 53.83 ($COO\underline{C}H_3$), 52.14 (N($\underline{C}H_3$)($CH_3$)), 46.77 (N($CH_3$)($\underline{C}H_3$)), 24.66 ($\underline{C}H_2CHCOOCH_3$), 19.14 ($\underline{C}H_2CH_2CHCOOCH_3$).

- ***N,N-Dimethyl-L-proline methyl ester methylsulfate,* [$C_1C_1C_1$Pro][C_1SO_4]**

[$C_1C_1C_1$Pro][C_1SO_4] was obtained as a slight yellow liquid (76% yield). ^{1}H NMR (d_6-DMSO, 300 MHz, [ppm]): δ 4.58 (t, 1H, J_{HH} = 9.9 Hz, $C\underline{H}COOCH_3$), 3.74 (s, br, 4H, CH_3SO_4 and $C\underline{H}HN(CH_3)_2$), 3.61 – 3.50 (m, 1H, $CH\underline{H}N(CH_3)_2$), 3.34 (s, 3H, $CHCOOC\underline{H}_3$), 3.25 (s, 3H, N($C\underline{H}_3$)(CH_3)), 3.01 (s, 3H, N(CH_3)($C\underline{H}_3$)), 2.42 – 2.22 (m, 2H, $C\underline{H}_2CHCOOCH_3$), 2.12 – 1.99 (m, 2H, $C\underline{H}_2CH_2CHCOOCH_3$). ^{13}C NMR ($d_6$-DMSO, 75 MHz, [ppm]): δ 166.76 ($\underline{C}OOCH_3$), 73.01 ($\underline{C}HCOOCH_3$), 67.49 ($\underline{C}H_2N(CH_3)_2$), 53.73 ($\underline{C}H_3SO_4$), 53.41 ($COO\underline{C}H_3$), 52.07 (N($\underline{C}H_3$)($CH_3$)), 46.53 (N($CH_3$)($\underline{C}H_3$)), 24.65 ($\underline{C}H_2CHCOOCH_3$), 19.08 ($\underline{C}H_2CH_2CHCOOCH_3$).

- ***N,N-Diethyl-L-proline ethyl ester bromide,* [$C_2C_2C_2$Pro]Br**

[$C_2C_2C_2$Pro]Br was obtained as a white solid (34% yield). ^{1}H NMR (d_6-DMSO, 300 MHz, [ppm]): δ 4.62 (t, 1H, J_{HH} = 8.1 Hz, $C\underline{H}COOCH_2CH_3$), 4.26 – 4.12 (m, 2H, $CHCOOC\underline{H}_2CH_3$), 3.66 – 3.29 (m, 6H, $C\underline{H}_2N(C\underline{H}_2CH_3)_2$), 2.43 – 2.18 (m, 2H, $C\underline{H}_2CHCOOCH_2CH_3$), 2.04 (p, 2H, J_{HH} = 7.7 Hz, $C\underline{H}_2CH_2CHCOOCH_2CH_3$), 1.32 – 1.08 (m, 9H, $COOCH_2C\underline{H}_3$ and $N(CH_2C\underline{H}_3)_2$). ^{13}C NMR ($d_6$-DMSO, 75 MHz, [ppm]): δ 166.79 ($\underline{C}OOCH_2CH_3$), 70.99 ($\underline{C}HCOOCH_2CH_3$), 63.01 ($CHCOO\underline{C}H_2CH_3$), 60.33 ($\underline{C}H_2N(CH_2CH_3)_2$), 55.01 ($CH_2N(CH_2\underline{C}H_3)_2$), 52.19 ($CH_2N(CH_2\underline{C}H_3)_2$), 25.65 ($\underline{C}H_2CHCOOCH_2CH_3$), 19.83 ($\underline{C}H_2CH_2CHCOOCH_2CH_3$), 14.20 ($COOCH_2\underline{C}H_3$), 9.16 ($N(CH_2\underline{C}H_3)_2$), 8.77 ($N(CH_2\underline{C}H_3)_2$).

iii) L-Valine-based CILs

- ***N,N,N-Trimethyl-L-valinolium iodide,* [$C_1C_1C_1$Val]I**

[$C_1C_1C_1$Val]I was obtained as a white solid (90% yield). ^{1}H NMR (d_6-DMSO, 300 MHz, [ppm]): δ 5.20 (t, 1H, J_{HH} = 4.6 Hz, OH), 3.87 – 3.70 (m, 2H, OHCH_2), 3.21 – 3.16 (m, 1H, N(CH_3)$_3$CH), 3.09 (s, 9H, N(CH_3)$_3$CH), 2.41 – 2.32 (m, 1H, (CH_3)$_2$CH), 0.97 (d, 3H, J_{HH} = 7.0 Hz, (CH_3)CH(CH_3)), 0.90 (d, 3H, J_{HH} = 6.7 Hz, (CH_3)CH(CH_3)). ^{13}C NMR (d_6-DMSO, 75 MHz, [ppm]): δ 79.49 (N(CH_3)$_3$CH), 55.98 (OHCH2), 52.53 (N(CH_3)$_3$), 25.95 ((CH_3)$_2$CH), 23.55 ((CH_3)CH(CH_3)), 18.10 ((CH_3)CH(CH_3)).

- ***N,N,N-Trimethyl-L-valinolium methylsulfate,* [$C_1C_1C_1$Val][C_1SO_4]**

[$C_1C_1C_1$Val][C_1SO_4] was obtained as a colourless liquid (88% yield). ^{1}H NMR (d_6-DMSO, 300 MHz, [ppm]): δ 5.25 (t, 1H, J_{HH} = 4.5 Hz, OH), 3.87 – 3.70 (m, 2H, OHCH_2), 3.34 (s, 3H, CH_3SO_4), 3.18 – 3.13 (m, 1H, N(CH_3)$_3$CH), 3.07 (s, 9H, N(CH_3)$_3$CH), 2.43 – 2.32 (m, 1H, (CH_3)$_2$CH), 0.98 (d, 3H, J_{HH} = 7.0 Hz, (CH_3)CH(CH_3)), 0.92 (d, 3H, J_{HH} = 6.7 Hz, (CH_3)CH(CH_3)). ^{13}C NMR (d_6-DMSO, 75 MHz, [ppm]): δ 79.49 (N(CH_3)$_3$CH), 56.01 (OHCH_2), 53.42 (CH_3SO_4), 52.39 (N(CH_3)$_3$), 25.94 ((CH_3)$_2$CH), 23.52 ((CH_3)CH(CH_3)), 18.01 ((CH_3)CH(CH_3)).

G. Experimental weight fraction binodal data

Table G1. *Experimental weight fraction data for the ternary system composed of $[C_1Qui][C_1SO_4]$ (1) + K_3PO_4 (2) + H_2O (3) at 25 (±1) °C and atmospheric pressure.*

$[C_1Qui][C_1SO_4]$					
100 w_1	100 w_2	100 w_1	100 w_2	100 w_1	100 w_2
3.4797	13.4833	2.2910	14.8513	1.5938	16.0788
3.3512	12.9854	2.2601	14.6509	1.5784	15.9235
3.2739	13.6274	2.2250	15.0564	1.5647	16.1400
3.1658	13.1774	2.1810	14.7585	1.5457	15.9443
3.0937	13.8071	2.1481	15.1518	1.5273	16.2407
3.0105	13.4358	2.0941	14.7708	1.5050	16.0031
2.9514	13.9729	2.0568	15.2343	1.4870	16.2988
2.9110	13.7813	2.0310	15.0434	1.4623	16.0276
2.8871	14.0025	2.0096	15.3158	1.4397	16.4101
2.8673	13.9063	1.9867	15.1415	1.4223	16.2117
2.8346	14.2131	1.9661	15.4075	1.4082	16.4558
2.7687	13.8824	1.9325	15.1442	1.3956	16.3086
2.7304	14.2545	1.9050	15.5102	1.3819	16.5486
2.7078	14.1362	1.8740	15.2584	1.3572	16.2524
2.6898	14.3131	1.8481	15.6119	1.3378	16.6027
2.6548	14.1269	1.8275	15.4376	1.3112	16.2716
2.6265	14.4116	1.8123	15.6488	1.2926	16.6195
2.5870	14.1950	1.7939	15.4902	1.2760	16.4062
2.5429	14.6490	1.7814	15.6662	1.2551	16.8048
2.4953	14.3750	1.7547	15.4308	1.2304	16.474
2.4752	14.5886	1.7281	15.8156	1.2140	16.7993
2.4446	14.4081	1.7106	15.6555	1.1996	16.600
2.4105	14.7759	1.6931	15.9131	1.1879	16.8357
2.3663	14.5048	1.6597	15.5992	1.1692	16.5712
2.3377	14.8221	1.6293	16.0608	1.1526	16.9167
2.3094	14.6424	1.6083	15.8541	1.1425	16.7686

Table G1. *Experimental weight fraction data for the ternary system composed of $[C_1Qui][C_1SO_4]$ (1) + K_3PO_4 (2) + H_2O (3) at 25 (±1) °C and atmospheric pressure. (Continuation)*

$[C_1Qui][C_1SO_4]$					
100 w_1	100 w_2	100 w_1	100 w_2	100 w_1	100 w_2
1.1316	16.9983	0.8502	17.7836	0.6673	18.3609
1.1197	16.8192	0.8424	17.6205	0.6619	18.2126
1.1038	17.1588	0.8353	17.8163	0.6552	18.4439
1.0818	16.8158	0.8287	17.6750	0.6487	18.2635
1.0628	17.2368	0.8212	17.8840	0.6417	18.5080
1.0505	17.0378	0.8144	17.7367	0.6337	18.2759
1.0385	17.3106	0.8071	17.9449	0.6242	18.6111
1.0257	17.0981	0.8007	17.8020	0.6117	18.2373
1.0153	17.3381	0.7957	17.9458	0.5991	18.7020
1.0055	17.1701	0.7894	17.8049	0.5850	18.2615
0.9943	17.4340	0.7810	18.0496	0.56728	18.9455
0.9843	17.2598	0.7745	17.8983	0.5524	18.4480
0.9773	17.4284	0.7684	18.0772	0.6673	18.3609
0.9681	17.2648	0.7609	17.9015	0.6619	18.2126
0.9580	17.5113	0.7511	18.1964	0.6552	18.4439
0.9489	17.3466	0.7418	17.9701	0.6488	18.2635
0.9395	17.5807	0.7351	18.1784	0.6417	18.5080
0.9291	17.3854	0.7273	17.9856	0.6337	18.2759
0.9209	17.5913	0.7233	18.1092	0.6242	18.6111
0.9109	17.3997	0.7183	17.9815		
0.9012	17.6482	0.7136	18.1270		
0.8911	17.4509	0.7082	17.9877		
0.8824	17.6788	0.7003	18.2411		
0.8751	17.5312	0.6932	18.0556		
0.8664	17.7631	0.6841	18.3548		
0.8576	17.5837	0.6749	18.1078		

Table G2. *Experimental weight fraction data for the ternary system composed of [$C_1C_1C_1$Val]I (1) + K_3PO_4 (2) + H_2O (3) at 25 (±1) °C and atmospheric pressure.*

[$C_1C_1C_1$Val]I					
100 w_1	100 w_2	100 w_1	100 w_2		
45.3499	4.39335	22.3253	12.3498	13.1836	16.8733
44.146	4.27672	21.6587	11.9811	12.949	16.5730
43.2232	5.02528	20.9142	12.9473	12.614	17.1813
41.9877	4.88164	20.3398	12.5917	12.5166	17.0486
40.5556	6.08241	19.5693	13.6333	12.3151	17.4196
38.6886	5.80241	18.9911	13.2305	12.0983	17.1129
37.6817	6.69469	18.3448	14.1445	11.7233	17.8249
36.1497	6.42251	17.9374	13.8303	11.5626	17.5806
34.7802	7.69781	17.3936	14.6264	11.2791	18.1325
33.6708	7.45226	17.2026	14.4658	11.1427	17.9133
32.3426	8.73961	16.921	14.8851	10.8803	18.4354
31.0863	8.40015	16.4832	14.4999	10.8355	18.3595
30.3412	9.15963	15.8953	15.4124	10.2978	19.4377
29.7009	8.96633	15.6779	15.2017	10.0994	19.0633
28.5662	10.1553	15.3677	15.6941	9.70651	19.8811
27.5462	9.79265	15.073	15.3932	9.5445	19.5493
26.8395	10.5699	14.6743	16.0464	9.16131	20.3738
25.9945	10.2371	14.4963	15.8517	8.90356	19.8007
25.1651	11.1895	14.2419	16.2771	8.42564	20.8896
24.4326	10.8638	14.0823	16.0947	8.27398	20.5135
23.5065	11.9715	13.9087	16.3905		
22.8847	11.6548	13.6386	16.0722		

Table G3. *Experimental weight fraction data for the ternary system composed of $[C_1C_1C_1Val][C_1SO_4]$ (1) + K_3PO_4 (2) + H_2O (3) at 25 (±1) °C and atmospheric pressure.*

$[C_1C_1C_1Val][C_1SO_4]$					
100 w_1	100 w_2	100 w_1	100 w_2	100 w_1	100 w_2
38.1059	10.2622	16.617	17.9523	8.04053	23.1032
34.6445	9.33002	16.1979	18.5109	7.92517	22.7717
32.146	11.5496	15.8562	18.1204	7.58508	23.5156
30.7425	11.0453	15.2351	18.9817	7.30408	22.6444
28.5762	13.0931	14.9272	18.5981	6.62942	24.2573
27.7231	12.7022	14.4508	19.2845	6.52229	23.8654
27.0444	13.3731	14.1673	18.906	6.29792	24.4241
26.5871	13.147	13.6185	19.7273	5.76499	22.3573
25.8341	13.9106	13.4231	19.4442	4.52451	26.1765
25.3737	13.6627	12.9314	20.201	4.0087	23.1923
24.524	14.5483	12.7506	19.9186		
24.0026	14.239	12.2796	20.6644		
22.8656	15.4644	12.0481	20.2748		
22.6154	15.2952	11.5232	21.1388		
22.1253	15.8328	11.2749	20.6832		
21.8406	15.6291	10.8999	21.3291		
21.2134	16.3321	10.7739	21.0826		
20.8645	16.0635	10.5274	21.5178		
20.4207	16.575	10.2853	21.023		
19.8467	16.1091	9.81804	21.89		
18.9068	17.2456	9.67425	21.5694		
18.5241	16.8966	9.36529	22.1615		
17.8669	17.7202	9.2244	21.8281		
17.6844	17.5392	8.79849	22.672		
17.3904	17.9144	8.65791	22.3098		
17.1967	17.7148	8.38541	22.8699		
16.8342	18.1869	8.28297	22.5905		

Table G4. *Experimental weight fraction data for the ternary system composed of $[C_2C_2C_2Pro]Br$ (1) + K_3PO_4 (2) + H_2O (3) at 25 (±1) °C and atmospheric pressure.*

$[C_2C_2C_2Pro]Br$			
100 w_1	100 w_2	100 w_1	100 w_2
34.5968	9.37142	10.0271	26.8925
33.4794	9.06874	9.92852	26.6281
32.4439	10.0263	9.49909	27.2077
31.2633	9.66146	9.39095	26.8979
29.428	11.4441	8.90251	27.5808
28.4834	11.0768	8.7439	27.0894
22.5748	17.0823	8.01405	28.1694
22.0231	16.6648	7.88582	27.7186
19.1217	19.7426	7.29061	28.6477
18.7694	19.3788	7.1858	28.2359
13.5975	25.0685	6.6904	29.0488
13.3974	24.6996	6.5534	28.454
12.3942	25.8474	5.80702	29.7721
12.2367	25.5188	5.70677	29.2582
11.8094	26.0254	5.001	30.59
11.6787	25.7374	4.84603	29.6421
11.2914	26.2113	3.68433	32.1318
11.1517	25.8869	3.57364	31.1665
10.6608	26.5094		
10.5431	26.2167		

Table G5. *Experimental weight fraction data for the ternary system composed of [$C_1C_1C_1$Pro]I (1) + K_3PO_4 (2) + H_2O (3) at 25 (±1) °C and atmospheric pressure.*

[$C_1C_1C_1$Pro]I	
100 w_1	100 w_2
67.3622	1.37789
56.6758	1.1593
51.5907	4.68355
52.6796	4.78241
51.1111	5.84407
48.4911	5.5445
47.0832	6.55761
45.6124	6.35277
44.7027	7.03258
43.4391	6.83378
42.6184	7.46868
41.6253	7.29464
39.6865	8.83839
38.5053	8.57534
35.8533	10.7699
35.0428	10.5264
8.74177	32.9767
8.69232	32.7902
8.00664	33.3935
7.9628	33.2107
7.02802	34.0592
6.97204	33.7879
5.17576	35.5014
5.10948	35.0468

Table G6. *Correlation constants obtained by the regression of the experimental binodal data from Eq. 16 and Eq. 17 and respective standard deviations, σ, of the CIL + K_3PO_4 + H_2O systems.*

CIL	***A*** ± σ	***B*** ± σ	10^5 (***C*** ± σ)
$[C_1Qui][C_1SO_4]$	99.99 ± 0.17	-0.73 ± 0.01	29.92 ± 1.06
$[C_1C_1C_1Val]I$	103.37 ± 7.64	-0.39 ± 0.03	9.36 ± 1.17
$[C_1C_1C_1Val][C_1SO_4]$	76.10 ± 23.54	-0.21 ± 0.09	10.38 ± 1.53
$[C_2C_2C_2Pro]Br$	99.58 ± 2.75	-0.34 ± 0.01	2.96 ± 0.43
$[C_1C_1C_1Pro]I$	82.00 ± 8.27	-0.23 ± 0.04	2.86 ± 0.83

Table G7. *Experimental weight fraction data for the ternary system composed of $[C_2C_2C_2Pro]Br$ (1) + K_2CO_3 (2) + H_2O (3) at 25 (±1) °C and atmospheric pressure.*

K_2CO_3					
100 w_1	100 w_2	100 w_1	100 w_2	100 w_1	100 w_2
36.9434	12.1862	13.1273	27.594	6.70955	31.4919
34.8731	11.5032	12.6237	28.453	6.56191	30.799
31.1988	15.5578	12.4919	28.1561	6.19639	31.8678
29.975	14.9475	12.1779	28.7049	6.04792	31.1042
27.7851	17.5073	11.9561	28.1821	5.62995	32.4091
27.2579	17.1751	11.3797	29.2332	5.46189	31.4416
25.1224	19.7457	11.1743	28.7056	5.05693	32.8166
24.0897	18.934	11.0003	29.0371	4.9242	31.9553
20.6965	23.3079	10.9053	28.7865	4.51841	33.4411
20.1636	22.7078	10.6422	29.298	4.38629	32.4632
19.4176	23.717	10.4754	28.839	4.03862	33.8521
19.1689	23.4132	10.0275	29.7432	3.9064	32.7438
18.4365	24.4285	9.85148	29.221	3.47906	34.63
18.2293	24.1539	9.44474	30.0784	3.37291	33.5735
17.6694	24.9473	9.26206	29.4966	2.95859	35.5896
17.4426	24.6271	8.92122	30.2506	2.80587	33.7525
16.5755	25.8878	8.74131	29.6405	2.27039	36.8505
16.3704	25.5675	8.50042	30.2012	2.21556	35.9607
15.5675	26.7651	8.43539	29.9701		
15.4054	26.4863	8.23965	30.4346		
14.6846	27.5857	8.14304	30.0777		
14.4003	27.0517	7.81449	30.881		
13.9892	27.7063	7.61587	30.0961		
13.8719	27.474	7.21295	31.1484		
13.4195	28.2082	7.06537	30.5111		

Table G8. *Experimental weight fraction data for the ternary system composed of $[C_2C_2C_2Pro]Br$ (1) + K_2HPO_4 (2) + H_2O (3) at 25 (±1) °C and atmospheric pressure.*

K_2HPO_4	
100 w_1	100 w_2
46.6524	3.19319
44.2525	3.02893
40.868	5.17824
38.3658	4.8612
35.6638	6.71133
34.4575	6.48433
31.4327	8.64796
30.5346	8.40088
28.0267	10.2678
27.7344	10.1607
26.7403	10.9124
26.4561	10.7964
24.6236	12.2049
24.4629	12.1252
23.4818	12.8874
23.1973	12.7312
20.5473	14.8332
20.3517	14.692
18.1942	16.4347
18.0247	16.2817
15.6079	18.2728
15.4769	18.1194
13.0958	20.1213
13.0146	19.9965

Table G9. *Correlation constants obtained by the regression of the experimental binodal data from Eq. 16 and Eq. 17 and respective standard deviations, σ, of the [$C_2C_2C_2$Pro]Br + Salt + H_2O systems.*

Salt	***A*** ± σ	***B*** ± σ	10^5 (***C*** ± σ)
K_2CO_3	99.28 ± 3.20	-0.26 ± 0.01	3.59 ± 0.33
K_2HPO_4	78.10 ± 5.54	-0.30 ± 0.03	5.26 ± 1.41

H.TLs data, the TLLs and α values

Variable	100x Mass fraction composition / wt%						TLL	α
	$[CIL]_{CIL}$	$[Salt]_{CIL}$	$[CIL]_{M}$	$[Salt]_{M}$	$[CIL]_{Salt}$	$[Salt]_{Salt}$		
CIL + K_3PO_4 + water								
[C_1Qui][C_1SO_4]	29.96	2.66	2.43	17.68	0.59	18.68	33.45	0.06
	26.46	3.22	2.99	14.97	1.77	15.59	27.62	0.05
[$C_1C_1C_1$Val]I	50.98	3.23	9.98	34.49	0.01	42.09	64.10	0.20
	52.18	3.03	20.46	19.87	0.89	30.27	58.07	0.38
[$C_1C_1C_1$Val][C_1SO_4]	49.12	4.04	10.02	24.92	1.72	29.35	53.73	0.18
	51.40	3.28	20.46	19.87	1.38	30.11	56.76	0.38
[$C_2C_2C_2$Pro]Br	38.79	7.37	9.92	34.86	0.92	43.43	52.29	0.24
	45.81	5.08	20.76	25.98	1.13	42.35	58.19	0.44
[$C_1C_1C_1$Pro]I	31.02	14.69	10.01	35.00	1.93	42.81	40.46	0.28
	50.74	4.32	25.27	29.65	0.14	54.64	71.36	0.50
[$C_2C_2C_2$Pro]Br + Salt + water								
K_2CO_3	46.74	8.15	20.93	25.75	2.78	38.12	0.41	53.21
K_2HPO_4	40.50	4.57	18.56	24.40	0.30	40.89	54.18	0.45

I. Partitioning studies of mandelic acid enantiomers for CIL-based ABS

Table H1. *Average of the experimental weight fraction compositions (wt%), enantiomeric excess (e.e. %), extraction efficiencies of the enantiomers ($EE_{R\text{-}MA}$ and $EE_{S\text{-}MA}$) and respective standard deviations (σ) for all the CIL-based partition systems investigated.*

ABS	100x Mass fraction composition / wt%		*e.e.%*	$EE_{R\text{-}MA}$ / (%)	$EE_{S\text{-}MA}$ / (%)
	[CIL]	[Salt]			
CIL + K_3PO_4 + water					
[C_1Qui][C_1SO_4] + K_3PO_4	2.46	17.83	-33.4 ± 1.9	9.5 ± 2.3	18.8 ± 4.6
[$C_1C_1C_1$Val]I + K_3PO_4	9.85	34.22	-13.5 ± 1.8	28.2 ± 2.5	35.8 ± 1.5
[$C_1C_1C_1$Val][C_1SO_4]	10.04	24.79	-16.4 ± 0.5	26.1 ± 0.8	37.5 ± 1.3
[$C_2C_2C_2$Pro]Br + K_3PO_4	9.93	34.74	-19.5 ± 1.9	44.1 ± 2.3	63.5 ± 3.6
[$C_1C_1C_1$Pro]I + K_3PO_4	9.99	34.68	-24.9 ± 3.1	35.4 ± 2.4	57.9 ± 1.1
[$C_2C_2C_2$Pro]Br + Salt + water					
[$C_2C_2C_2$Pro]Br + K_2CO_3	20.88	25.82	-16.1 ± 0.2	34.8 ± 2.4	47.5 ± 2.5
[$C_2C_2C_2$Pro]Br + K_2HPO_4	18.78	24.46	3.3 ± 1.7	46.5 ± 2.5	44.8 ± 0.6

J. Characterization of chiral anionic ILs

- ***Tetrabutylammonium L-phenylalaninate,* [N_{4444}][L-Phe]**

[N_{4444}][L-Phe] was obtained as a white solid (93% yield). ^{1}H NMR (D_2O, 300 MHz, [ppm]): δ 0.95 (t, 12H, J_{HH} = 7.3 Hz, $NCH_2CH_2CH_2C\underline{H}_3$), 1.27 – 1.45 (sext, 8H, J_{HH} = 7.3 Hz, $NCH_2CH_2C\underline{H}_2CH_3$), 1.55 – 1.72 (m, 8H, $NCH_2C\underline{H}_2CH_2CH_3$), 2.87 (dd, 1H, $J_{H1H\beta}$ = 7.3 Hz, $J_{H\alpha H\beta}$ = 13.5 Hz, C_6H_5-C$\underline{H}$(β)), 3.01 (dd, 1H, $J_{H1H\alpha}$ = 5.6 Hz, $J_{H\alpha H\beta}$ = 13.5 Hz, C_6H_5-C$\underline{H}$(α)), 3.08 – 3.29 (m, 8H, $NC\underline{H}_2CH_2CH_2CH_3$), 3.53 (dd, 1H, $J_{H1H\alpha}$ = 5.6 Hz, $J_{H1H\beta}$ = 7.3 Hz, O_2C-C$\underline{H}$), 7.23 – 7.45 (m, 5H, $C_6\underline{H}_5$-CH_2). ^{13}C NMR (D_2O, 75.47 MHz, [ppm]): δ 12.77, 19.09, 23.06, 40.39, 57.28, 58.03, 126.65, 128.56, 129.38, 137.99, 181.79.

- ***Tetrabutylammonium D-phenylalaninate,* [N_{4444}][D-Phe]**

[N_{4444}][D-Phe] was obtained as a light yellow solid (97% yield). ^{1}H NMR (D_2O, 300 MHz, [ppm]): δ 0.95 (t, 12H, J_{HH} = 7.3 Hz, $NCH_2CH_2CH_2C\underline{H}_3$), 11.28 – 1.43 (sext, 8H, J_{HH} = 7.3 Hz, $NCH_2CH_2C\underline{H}_2CH_3$), 1.55 – 1.71 (m, 8H, $NCH_2C\underline{H}_2CH_2CH_3$), 2.87 (dd, 1H, $J_{H1H\beta}$ = 7.4 Hz, $J_{H\alpha H\beta}$ = 13.5 Hz, C_6H_5-C$\underline{H}$(β)), 3.02 (dd, 1H, $J_{H1H\alpha}$ = 5.5 Hz, $J_{H\alpha H\beta}$ = 13.5 Hz, C_6H_5-C$\underline{H}$(α)), 3.09 – 3.25 (m, 8H, $NC\underline{H}_2CH_2CH_2CH_3$), 3.53 (dd, 1H, $J_{H1H\alpha}$ = 5.5 Hz, $J_{H1H\beta}$ = 7.3 Hz, O2C-C$\underline{H}$), 7.25 – 7.43 (m, 5H, $C_6\underline{H}_5$-CH_2). ^{13}C NMR (D_2O, 75.47 MHz, [ppm]): δ 12.79, 19.09, 23.05, 40.29, 57.24, 58.02, 126.68, 128.59, 129.39, 137.91, 181.52.

- ***Di(tetrabutylammonium) L-glutamate,* [N_{4444}]$_2$[L-Glu]**

[N_{4444}]$_2$[L-Glu] was obtained as a white solid (99% yield). 1H NMR (D_2O, 300 MHz, [ppm]): δ 0.95 (t, 24H, J_{HH} = 7.3 Hz, $NCH_2CH_2CH_2C\underline{H}_3$), 1.37 (sext, 16H, J_{HH} = 7.3 Hz, $NCH_2CH_2C\underline{H}_2CH_3$), 1.56 – 1.98 (m, 18H, O_2C-C$\underline{H}_2CH_2$ and $NCH_2C\underline{H}_2CH_2CH_3$), 2.15 – 2.27 (m, 2H, O_2C-C$\underline{H}_2CH_2$), 3.11 – 3.33 (m, 17H, O_2C-C$\underline{H}$-NH_2 and $NC\underline{H}_2CH_2CH_2CH_3$). 13C NMR ($D_2O$, 75.47 MHz, [ppm]): δ 12.77, 19.07, 23.06, 31.28, 34.05, 55.75, 58.04, 181.71, 182.08.

- ***(2-Hydroxyethyl)trimethylammonium L-phenylalaninate,* [Ch][L-Phe]**

[Ch][L-Phe] was obtained as a yellow liquid (90% yield). ^{1}H NMR (D_2O, 300 MHz, [ppm]): δ 2.85 (dd, 1H, $J_{H1H\beta}$ = 7.3 Hz, $J_{H\alpha H\beta}$ = 13.5 Hz, C_6H_5-C<u>H</u>(β)), 3.00 (dd, 1H, $J_{H1H\alpha}$ = 5.6 Hz, $J_{H\alpha H\beta}$ = 13.5 Hz, C_6H_5-C<u>H</u>(α)), 3.14 (s, 9H, N(C<u>H</u>$_3$)$_3$), 3.42 – 3.54 (m, 3H, H_2N-C<u>H</u> e HO-CH_2C<u>H</u>$_2$), 3.97 – 4.04 (m, 2H, HO-C<u>H</u>$_2$$CH_2$), 7.26 – 7.41 (m, 5H, C_6<u>H</u>$_5$-CH_2). ^{13}C NMR (D_2O, 75.47 MHz, [ppm]): δ 40.44, 53.76, 55.49, 57.30, 67.31, 126.66, 128.58, 129.39, 138.05, 181.77.

- ***(2-Hydroxyethyl)trimethylammonium D-phenylalaninate,* [Ch][D-Phe]**

[Ch][D-Phe] was obtained as a yellow liquid (89% yield). ^{1}H NMR (D_2O, 300 MHz, [ppm]): δ 2.86 (dd, 1H, $J_{H1H\beta}$ = 7.3 Hz, $J_{H\alpha H\beta}$ = 13.5 Hz, C_6H_5-C<u>H</u>(β)), 3.01 (dd, 1H, $J_{H1H\alpha}$ = 5.6 Hz, $J_{H\alpha H\beta}$ = 13.6 Hz, C_6H_5-C<u>H</u>(α)), 3.15 (s, 9H, N(C<u>H</u>$_3$)$_3$), 3.43 – 3.54 (m, 3H, H_2N-C<u>H</u> e HO-CH_2C<u>H</u>$_2$), 3.98 – 4.05 (m, 2H, HO-C<u>H</u>$_2$$CH_2$), 7.25 – 7.40 (m, 5H, C_6<u>H</u>$_5$-CH_2). ^{13}C NMR (D_2O, 75.47 MHz, [ppm]): δ 40.44, 53.76, 55.49, 57.30, 67.37, 126.66, 128.58, 129.39, 138.05, 181.77.

K. *Crystal data*

Table K1: Single cell unit parameters.

A	19.25750 Å
B	5.71920 Å
C	15.61720 Å
α	90.00000°
β	115.41400°
γ	90.00000°